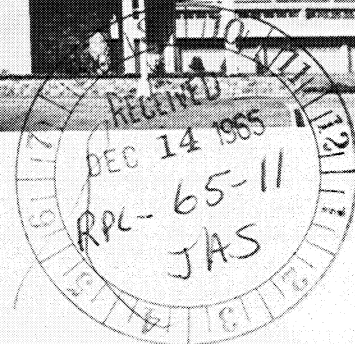




NBS REPORT
8881



CHARACTERISTICS OF LIQUID-SOLID MIXTURES
OF HYDROGEN AT THE TRIPLE POINT

by

D. B. Mann, P. R. Ludtke,
C. F. Sindt, D. B. Chelton,
D. E. Daney and G. L. Pollack



GPO PRICE \$ _____

CFSTI PRICE(S) \$ _____

Hard copy (HC) 5.00

Microfiche (MF) 1.00

ff 653 July 65

N66-14628

(ACCESSION NUMBER)

(THRU)

170

1

(PAGES)

(CODE)

69092

23

(NASA OR OR TMA OR AD NUMBER)

(CATEGORY)

U. S. DEPARTMENT OF COMMERCE
NATIONAL BUREAU OF STANDARDS
BOULDER LABORATORIES
Boulder, Colorado

THE NATIONAL BUREAU OF STANDARDS

The National Bureau of Standards is a principal focal point in the Federal Government for assuring maximum application of the physical and engineering sciences to the advancement of technology in industry and commerce. Its responsibilities include development and maintenance of the national standards of measurement, and the provisions of means for making measurements consistent with those standards; determination of physical constants and properties of materials; development of methods for testing materials, mechanisms, and structures, and making such tests as may be necessary, particularly for government agencies; cooperation in the establishment of standard practices for incorporation in codes and specifications; advisory service to government agencies on scientific and technical problems; invention and development of devices to serve special needs of the Government; assistance to industry, business, and consumers in the development and acceptance of commercial standards and simplified trade practice recommendations; administration of programs in cooperation with United States business groups and standards organizations for the development of international standards of practice; and maintenance of a clearinghouse for the collection and dissemination of scientific, technical, and engineering information. The scope of the Bureau's activities is suggested in the following listing of its four Institutes and their organizational units.

Institute for Basic Standards. Applied Mathematics. Electricity. Metrology. Mechanics. Heat. Atomic Physics. Physical Chemistry. Laboratory Astrophysics.* Radiation Physics. Radio Standards Laboratory.* Radio Standards Physics; Radio Standards Engineering. Office of Standard Reference Data.

Institute for Materials Research. Analytical Chemistry. Polymers. Metallurgy. Inorganic Materials. Reactor Radiations. Cryogenics.* Materials Evaluation Laboratory. Office of Standard Reference Materials.

Institute for Applied Technology. Building Research. Information Technology. Performance Test Development. Electronic Instrumentation. Textile and Apparel Technology Center. Technical Analysis. Office of Weights and Measures. Office of Engineering Standards. Office of Invention and Innovation. Office of Technical Resources. Clearinghouse for Federal Scientific and Technical Information.**

Central Radio Propagation Laboratory.* Ionospheric Telecommunications. Tropospheric Telecommunications. Space Environment Forecasting. Aeronomy.

* Located at Boulder, Colorado 80301.

** Located at 5285 Port Royal Road, Springfield, Virginia 22171.



NATIONAL BUREAU OF STANDARDS REPORT

NBS PROJECT

31505-12-3150452

October 1, 1965

NBS REPORT

8881

CHARACTERISTICS OF LIQUID-SOLID MIXTURES OF HYDROGEN AT THE TRIPLE POINT

by

D. B. Mann, P. R. Ludtke,
C. F. Sindt, D. B. Chelton,
D. E. Daney and G. L. Pollack

Cryogenics Division
NBS Institute for Materials Research
Boulder, Colorado

IMPORTANT NOTICE

NATIONAL BUREAU OF STANDARDS REPORTS are usually preliminary or progress accounting documents intended for use within the Government. Before material in the reports is formally published it is subjected to additional evaluation and review. For this reason, the publication, reprinting, reproduction, or open-literature listing of this Report, either in whole or in part, is not authorized unless permission is obtained in writing from the Office of the Director, National Bureau of Standards, Washington, D.C. 20234. Such permission is not needed, however, by the Government agency for which the Report has been specifically prepared if that agency wishes to reproduce additional copies for its own use.



U.S. DEPARTMENT OF COMMERCE
NATIONAL BUREAU OF STANDARDS

TABLE OF CONTENTS

	<u>Page</u>
LIST OF FIGURES	v
ABSTRACT	ix
INTRODUCTION	1
Liquid-Solid Technology	1
Objectives of Program	2
SUMMARY	3
PART A. PRODUCTION	7
1. Introduction	7
1.1 Activity Summary	7
2. Equipment	8
2.1 Description	9
2.2 Operation	31
3. Results	32
3.1 Photoinstrumentation	32
3.2 Production by Spray Method	33
3.3 Production by Freeze-Thaw Method	36
3.4 Liquid Nitrogen Shielding	41
4. Future Work	41
4.1 Production Apparatus	41
4.2 Photoinstrumentation	44
4.3 Liquid-Solid Mixture Study	45
4.4 Data Analysis	46
PART B. SOLID PARTICLE SIZE AND TERMINAL VELOCITY DETERMINATION	49
1. Introduction	49
1.1 Activity Summary	49
2. Photoinstrumentation	50
3. Heat Leak	53
4. Particle Size and Aging Study	55
4.1 Experimental Apparatus and Modifications	55
4.2 Experimental Procedure	57
4.3 Data Processing	63
4.3.1 Benson-Lehner Film Reader	63
4.3.2 IBM 7090	66
4.3.3 Plotter	66
4.4 Accuracy	70
4.5 Experimental Results	71
5. Terminal Velocity Measurements	71
5.1 Experimental Apparatus	76
5.2 Experimental Procedure	76
5.3 Data Processing	77
5.4 Accuracy	79
5.5 Experimental Results	79

Table of Contents (Cont'd.)	Page
6. Solid Particle Microphotography	80
7. The T-S Diagram	82
8. Conclusions	84
9. Future Work	85
10. Appendix-Provisional Data.	86
PART C. TRANSPORT CHARACTERISTICS	105
1. Introduction	105
1.1 Activity Summary	105
2. Particle Size	107
2.1 Discussion	107
3. Particle Terminal Velocity	114
4. Dewar Pressurization Techniques	118
4.1 Experimental Apparatus Modification and Procedures	118
4.2 Experimental Results and Discussion	120
4.3 Solid Hydrogen Tubes.	121
5. Preliminary Transfer Studies	122
5.1 Flow Apparatus and Procedure	122
5.2 Transfer Characteristics	124
6. Line Pressure Drops From Classical Equations	131
7. Aged Solid Hydrogen-Spraying	134
8. Aged Solid Hydrogen-Continuous Pumping	135
9. Freeze-Thaw Solid Formation	136
10. Quality Determinations	139
10.1 Expansion to the Triple Point	139
10.2 Formation of Solid at the Triple Point	143
10.3 Experimental Determination of Liquid-Solid Quality	146
10.3.1 Volumetric Method	146
10.3.2 Calorimetric Method	148
10.4 Sources of Error	149
10.5 Summary	150
11. Cryogenic Colloids	152
12. Conclusions	155
13. Future Work	156
13.1 Liquid-Solid Flow	156
13.2 Homogeneous Mixtures	156
REFERENCES	158

LIST OF FIGURES

	<u>Page</u>
Figure 1. Pump Specifications	10
Figure 2. Pumping Capacity - Worthington Pumps	11
Figure 3. Three Rough Vacuum Pumps - Liquefier Building	12
Figure 4. 10 HP High Vacuum Pump - Liquefier Building. . .	13
Figure 5. Liquid-Solid Hydrogen System Flow Schematic . . .	15
Figure 6. Vacuum Control Valve and Precisor	17
Figure 7. Vacuum Control Valve and Steam Heat Exchanger .	19
Figure 8. Equipment Arrangement - Laboratory Area	20
Figure 9. Cross Section - Experimental Apparatus.	21
Figure 10. Experimental Apparatus.	23
Figure 11. Orifice, Needle and Stirring Motor	25
Figure 12. Remote Control Valving - Experimental Apparatus	26
Figure 13. Vent By-Pass Valve	27
Figure 14. Glass Dewar Assembly.	29
Figure 15. Control Panel	30
Figure 16. Large Spray	34
Figure 17. Fine Spray.	35
Figure 18. Solid Hydrogen Spray	37
Figure 19. Solid Spray Before Melt	38
Figure 20. Liquid-Solid After Melt.	39
Figure 21. Large Particles in Liquid	40
Figure 22. Freeze-Thaw Production Process	42
Figure 23. Fine Particles in Liquid.	43
Figure 24. Photographic Lighting Arrangement	51
Figure 25. Modifications of Experimental Space	54
Figure 26. Modifications of Experimental Space	56
Figure 27. Elevator and Grid Arrangement	58

List of Figures (Cont'd.)	<u>Page</u>
Figure 28. Experimental Dewar Assembly	59
Figure 29. Cross Section - Experimental Apparatus	61
Figure 30. Data Processing	64
Figure 31. Benson-Lehner Boscar Film Reader	65
Figure 32. Measurement of Particle Dimensions	67
Figure 33. IBM 7090 Digital Computer	68
Figure 34. Data Plotter	69
Figure 35. Liquid-Solid Hydrogen Mixtures - Age: 17 min. . .	72
Figure 36. Liquid-Solid Hydrogen Mixtures - Age: 5 hr., 15 min.	73
Figure 37. Liquid-Solid Hydrogen Mixtures - Age: 20 hr., 15 min.	74
Figure 38. Liquid-Solid Hydrogen Mixtures - Age: 40 hr., 15 min.	75
Figure 39. Terminal Velocity Determination	78
Figure 40. Solid Hydrogen Particle in Liquid at Triple Point. Magnification is 26 X, Age: 3 hr., 30 min.	81
Figure 41. Hydrogen Temperature - Entropy Diagram	83
Figure 42. Particle Size, Age: 27 min.	87
Figure 43. Particle Size, Age: 1 hr.	88
Figure 44. Particle Size, Age: 2 hrs.	89
Figure 45. Particle Size, Age: 3 1/4 hrs.	90
Figure 46. Particle Size, Age: 10 1/4 hrs.	91
Figure 47. Particle Size, Age: 15 1/4 hrs.	92
Figure 48. Particle Size, Age: 20 1/4 hrs.	93
Figure 49. Particle Size, Age: 30 1/4 hrs.	94
Figure 50. Particle Size, Age: 36 1/4 hrs.	95
Figure 51. Particle Length - 5, 25 and 41 hrs.	96
Figure 52. Particle Width - 5, 25 and 41 hrs.	97

List of Figures (Cont'd.)	<u>Page</u>
Figure 53. Percent of Particles Less Than 3 and 2 mm. Length	98
Figure 54. Typical Terminal Velocity Data	99
Figure 55. Terminal Velocity Measurement, Age: 68 min. . .	100
Figure 56. Terminal Velocity Measurement, Age: 3 1/2 hrs. .	101
Figure 57. Terminal Velocity Measurement, Age: 4 1/2 hrs. .	102
Figure 58. Terminal Velocity Measurement, Age: 68 min., 3 1/2 hrs. and 4 1/2 hrs.	103
Figure 59. Particle Size Data	108
Figure 60. Selected Distribution Functions	110
Figure 61. Data Comparison With Logarithmic Distribution .	112
Figure 62. Terminal Velocity Data	115
Figure 63. Terminal Velocity for Hydrogen Spheres and Experimental Data	116
Figure 64. Dewar Pressurization Apparatus	119
Figure 65. Preliminary Transfer Apparatus	123
Figure 66. Transfer Apparatus, Photo	125
Figure 67. Glass Transfer Line	126
Figure 68. Thick Liquid-Solid Hydrogen in Transfer Line . .	128
Figure 69. Thin Liquid-Solid Hydrogen in Transfer Line . . .	129
Figure 70. Freeze-Thaw Solid Formation, Time = 0	137
Figure 71. Freeze-Thaw Solid Formation, Time = 7 Milliseconds	138
Figure 72. T-S Diagram for Solid Production	140
Figure 73. Fraction of Triple-Point Liquid Vaporized vs. Quality	145
Figure 74. Quality Determination Apparatus	147

ABSTRACT

14628

Properties and characteristics of liquid-solid mixtures of hydrogen, including production methods, solid particle sizes, particle size distribution, aging effects, and terminal velocities of the solid particles in triple point liquid have been studied. Preliminary studies and dewar pressurization techniques for liquid-solid mixtures are discussed. Consideration has also been given to possible methods of obtaining homogeneous or colloidal mixtures. The equipment developed and the results described are part of an effort to determine techniques and parameters pertinent to the study of production, storage, and pipe line transport of this upgraded fuel.

Author

Key Words: Colloids, cryogenic, crystals, hydrogen liquid-solid phase, nucleation, particle size, production, rocket fuel, solid hydrogen, terminal velocity.

INTRODUCTION

The Cryogenics Division of the NBS-Institute for Materials Research is currently involved in an analytical and experimental study to characterize liquid-solid mixtures of hydrogen. The program entitled "Slush Hydrogen Production and Instrumentation Study" is sponsored by NASA-KSC under Purchase Request CC-14032. Work under this request number covers the period 1 March 1964 to 30 June 1965 and is described in the following sections of this summary report.

The major sections or parts of this report are chronological, giving details of experiments and analytical conclusions which in later sections may be modified or reversed. The format was adopted in the interest of completeness and reflects the fact that each of the parts A, B, and C were originally separate, informal reports to the sponsor. Parts A and B cover Phase I - Production and Solid Particle Size and Terminal Velocity Determination. Part C presents preliminary results in Phase II - Transport.

Liquid-Solid Technology

Space vehicles fueled with hydrogen in liquid form have required the development of new technology concerned with production, storage, and handling of the new fuel. Relatively high density at low pressure is realized by gas liquefaction but there are problems associated with handling and storing the low temperature fluid before, during, and after vehicle loading. Some of these problems are (a) short holding time caused by minimal insulation, (b) temperature stratification, resulting in pump cavitation problems, (c) sloshing of the liquid in such a manner as to affect flight stability, and (d) safety problems associated with the high vent rates before and after launch.

Further refrigeration of the liquid hydrogen to form a flowable slurry or mixture of solid and liquid should eliminate or reduce a number of the above problems. The use of slush hydrogen will increase holding time and reduce safety problems by providing a higher heat sink capacity before venting. Sloshing and temperature stratification problems may be reduced by the low fluidity or semi-solid nature of the slush mixture.

Previous to the present study, very little information was available on the subject of production, storage, and handling of mixtures of solid and liquid hydrogen. Instrumentation for the determination of slush quality and mass flow rate have not heretofore been explored in depth. Solid hydrogen, either in liquid hydrogen or in gaseous hydrogen, has been observed, but meaningful data have not been obtained. Most work involving hydrogen was carried out with other objectives in mind.

Objectives of Program

The present study is intended to be conducted on a laboratory scale. The objectives of the study pertaining to production and characterization are as follows:

1. Develop a knowledge and understanding of the various types (textures) of slush hydrogen that may exist for a series of given mixture ratios. These objectives will be accomplished by investigating the production parameters of slush hydrogen.
2. Through the application of analytical and experimental procedures, develop a method for analytically predicting pressure drop in slush hydrogen transfer lines.
3. Evaluate, correlate, and combine all known applicable physical properties of slush hydrogen.

4. Investigate the adaptability of the most promising production concepts to a large scale application for space vehicle slush hydrogen upgrading.

These objectives will be aimed at the establishment of standard specifications for instrumentation and production of flowable mixtures of solid and liquid hydrogen. The instrumentation section of the program will be covered in a separate NBS report, No. 8879, Slush Hydrogen Instrumentation Study.

SUMMARY

Two methods of producing liquid-solid mixtures of hydrogen were investigated. One method was to spray liquid through a small orifice into a chamber where the pressure was less than triple point pressure (52.9 torr). The particles produced were irregular in shape and of low density. The particle sizes and shapes were a function of orifice and pressure parameters. After production, the solid was converted to a liquid-solid mixture by increasing the pressure to slightly above 52.9 torr. This method of production proved to be a batch process and was not readily adaptable to large scale production. Little further work was done on the spray method.

A second method which generates reproducible particle sizes and is easily adaptable to large scale production was devised. This method of production was named the freeze-thaw process. In the process, solid is made by vacuum pumping on liquid; repeatedly cycling above and below the triple point pressure. When the pressure is reduced below 52.9 torr, a solid crust forms on top of the liquid. The solid drops into the liquid when the pressure is raised above 52.9 torr. By repeating the above pressure cycle, a dense, reproducible liquid-solid mixture may be easily generated. The freeze-thaw method of

production will produce particles of solid hydrogen in the liquid of a size ranging from 0.5 mm to 7 mm in size. The greatest number of particles are from 2.5 to 3.5 mm in size. A total of 17,000 particles was measured and the sizes recorded on data processing equipment.

The size distribution of the solid particles was also investigated. It was found that the particles do not have a normal distribution but rather a log-normal distribution.

The effect of aging on the slush mixture was determined. Slush made by the freeze-thaw process was aged for 43 hours. It was found that aging does have an effect on the particles. The freshly produced particles are friable and loosely connected. After approximately five hours, the particle voids start to fill in and the particle appears to be made up of small beads of solid which tend to grow in size and decrease in number. The particles lose protruding spikes and appear more rounded and much more dense. Most of the above change in configuration takes place within five hours after production. There was little change in the particles between five and forty-two hours. The particles do not increase in size but only change in appearance. There was no tendency for the particles to cohere during the aging experiment. It is believed the particle tends toward a minimum energy (spherical) configuration. The mechanics of the process is not completely understood.

Liquid-solid (slurry) flow expressions for flow through pipelines have been investigated for application to hydrogen slush flow. A treatment by Condolios [June, 1963] has been chosen. Work has progressed on using these flow expressions for predicting slush flow through insulated transfer lines.

Terminal velocity is one of the experimental parameters required to predict liquid-solid flow characteristics through pipelines. The terminal velocities of 182 particles were measured in triple-point liquid.

The terminal velocities lie in the range from 20 to 50 millimeters/second, the larger particles falling slightly faster.

Preliminary transfer techniques were investigated. A preliminary transfer apparatus was assembled and hydrogen slush was transferred at one atmosphere pressure from one glass dewar to another. High speed motion pictures were taken of slush flowing through a 3/4 inch, transparent, insulated transfer line. Helium and hydrogen pressurization was used to flow the slush.

A parahydrogen temperature-entropy diagram covering the solid, liquid, and vapor phases from 11° K to 23° K was prepared.

An analytical expression for the fraction of vapor removed from a triple-point mixture to produce a given liquid-solid quality was developed.

Solid hydrogen tubes were formed by bubbling gaseous helium through triple-point liquid. Very dense solid can be produced by this method.

High speed motion pictures were taken of the solid formation at the liquid-vapor interface during the freeze-thaw process. A better understanding of the production process was obtained by observing the solid form in slow motion.

The three progress reports for the overall program follow and constitute Parts A, B, and C of the summary report.

PART A. PRODUCTION

1. Introduction

The following is a portion of the first progress review for the project "Slush Hydrogen Production and Instrumentation." The work reported describes the progress made to September, 1964. Progress on the objectives of the instrumentation study are reported separately.

1.1 Activity Summary

A production apparatus was designed, fabricated, and tested. The apparatus allows production by two different methods. Two hydrogen experimental runs have been recorded on photographic film. A thermodynamic properties chart describing the liquid-solid-vapor region is being prepared. Properties of pressure, temperature, enthalpy, and entropy will be plotted on T-S coordinates.

Development of adequate photoinstrumentation techniques, including lighting, lens selection, film type, and exposure times were stressed during the reporting period. The solution of these problems is to a great degree trial and error, the objective being sharp, clearly defined, solid particle images in the vapor-solid and liquid-solid states. Data reduction methods will then allow accurate classification and particle size determination as a function of the controlling parameters.

The methods used to generate the liquid-solid mixtures were restricted to some form of vapor pressure reduction. That is, refrigeration is provided by the fluid itself through a mass-energy transfer at the phase interface. The resulting mixture varying in mass fraction from 0 to 50 percent will have characteristics dependent on the method of generation. Such variables as particle size, shape, dimensional stability, concentration, and terminal velocity all effect the transport

characteristics of the mixture.

The apparatus and photoinstrumentation techniques developed during the reporting period will allow determination of the most favorable method of forming a mixture with reproducible characteristics so that a transport system may be designed with confidence, based on existing slurry correlations.

The two methods used to generate the liquid-solid mixtures were the spray technique and the freeze-thaw technique. In the former, liquid hydrogen at a pressure and temperature between the normal boiling point and the triple point is expanded through a valve to a pressure well below the triple point pressure. The liquid cools and solidifies by evaporation and forms a quantity of polycrystalline solid particles. The pressure is then raised to the triple point and a liquid-solid mixture is formed by partial melting of the solid.

Freeze-thaw production involves a quantity of liquid hydrogen previously pumped to a pressure slightly above the triple point pressure. By further reducing the pressure to slightly below the triple point, solid forms at the liquid-vapor interface. If the pressure is then increased slightly above the triple point, the solid partially melts and sinks into the liquid since the solid is more dense than the liquid. By continuously repeating the pressure cycle, a dense, liquid-solid mixture is easily generated.

2. Equipment

The experimental studies were conducted in a laboratory located in the Liquefier Building at the National Bureau of Standards, Cryogenics Division. The building was originally designed as a liquid hydrogen production facility having the electrical and mechanical equipment within the building to meet the necessary safety requirements for handling hydrogen.

Hydrogen, helium, and nitrogen liquids and gases are readily available.

2.1 Description

Three vacuum pumps provide the necessary pumping capacity to produce a liquid-solid mixture of hydrogen at its triple point. The piping and valving arrangements allow use of one, two, or three pumps. Specifications for these pumps are given in figure 1. Figure 2 shows a curve of the pumping capacity versus pressure for a single pump. A photograph of the three vacuum pumps is shown in figure 3.

Two higher vacuum pumps are also available for use in the system. The specifications for these pumps are also given in figure 1. Figure 4 is a photograph of one of these pumps.

All vacuum pumps are connected to a common piping header. A six-inch diameter copper pipe extends from the header through a vacuum control valve and a heat exchanger to the test apparatus. A flow schematic of the system showing all valving and piping involved is shown in figure 5.

The vacuum control valve, designated as S-510 on the schematic, is pneumatically operated by a diaphragm motor. The valve is of the butterfly type with a soft rubber seat for a vacuum tight seal. A precisor incorporated with the pneumatic motor maintains the valve position relative to the input signal independent of the flow forces on the butterfly. The vacuum valve and the precisor are shown in figure 6.

The vacuum valve input signal is provided by a pneumatic controller which may be operated in a manual or automatic mode. The controller receives a pressure signal from a differential converter. The differential converter proportions an input air supply to the controller based on the pressure in the test chamber. A reference pressure of 5 microns absolute is supplied to the differential converter by a

WORTHINGTON VACUUM PUMP SPECIFICATIONS

Type : Horizontal Reciprocating , 2 Stage

Bore and Stroke : 31 x 13 inches

Positive Displacement : 1425 CFM

Horsepower : 75

Capacity : 1150 CFM at 50 Torr

0 CFM at 2 Torr

KINNEY VACUUM PUMP SPECIFICATIONS

Type : Rotary High Vacuum

Horsepower : 10

Ultimate Pressure : 10 microns with closed intake

Figure 1. Pump Specifications

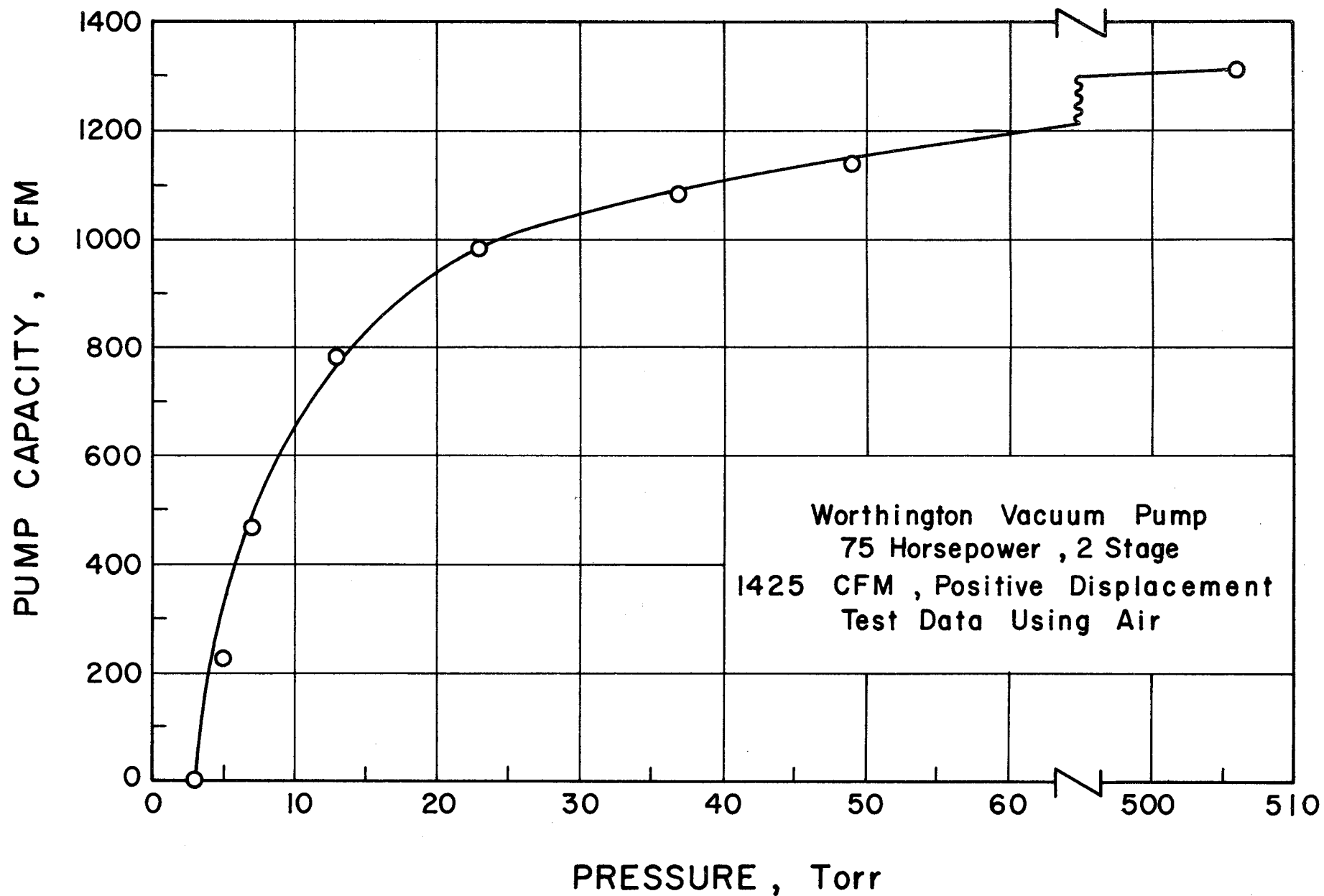


Figure 2. Pumping Capacity - Worthington Pumps

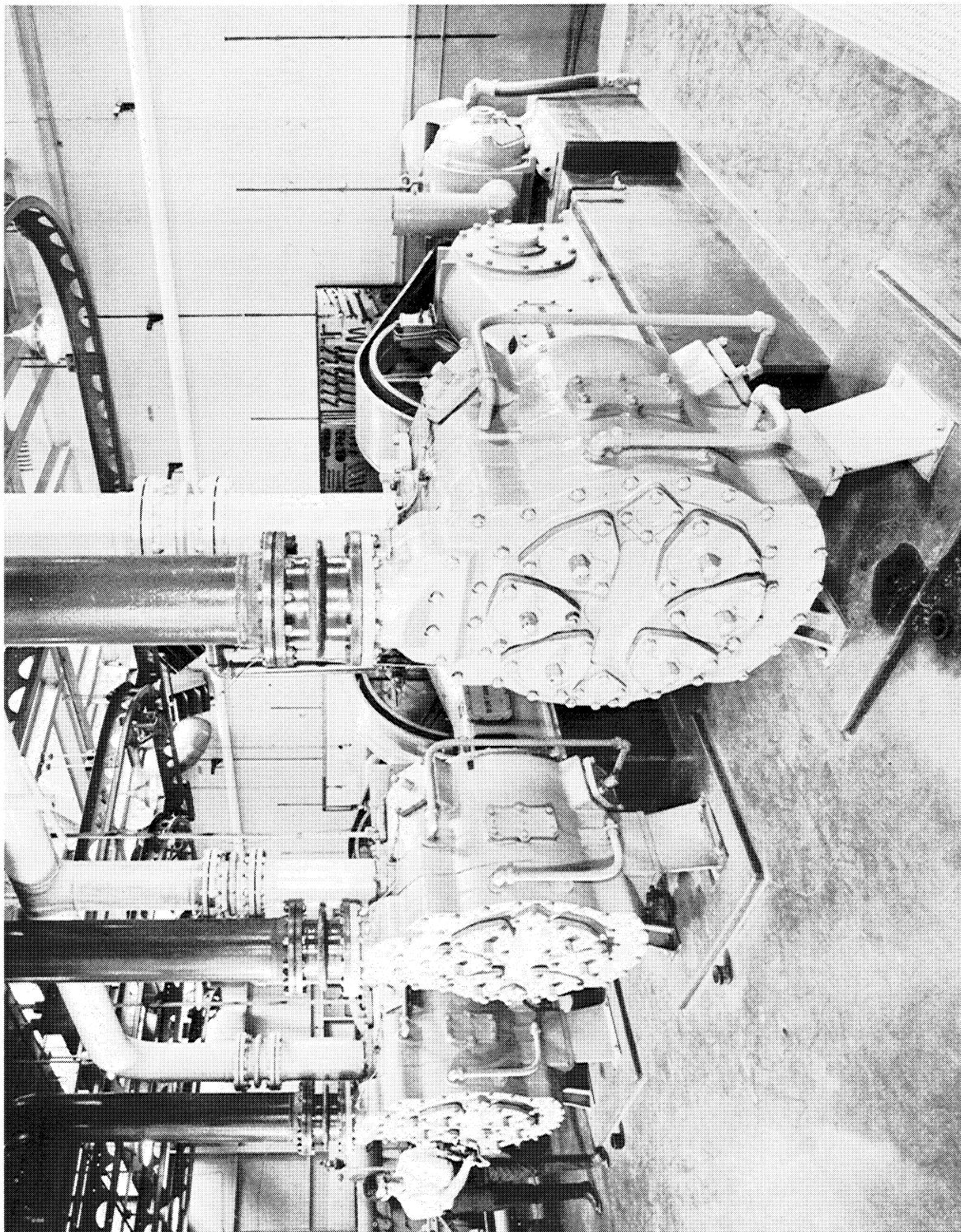


Figure 3. Three Rough Vacuum Pumps - Liquefier Building

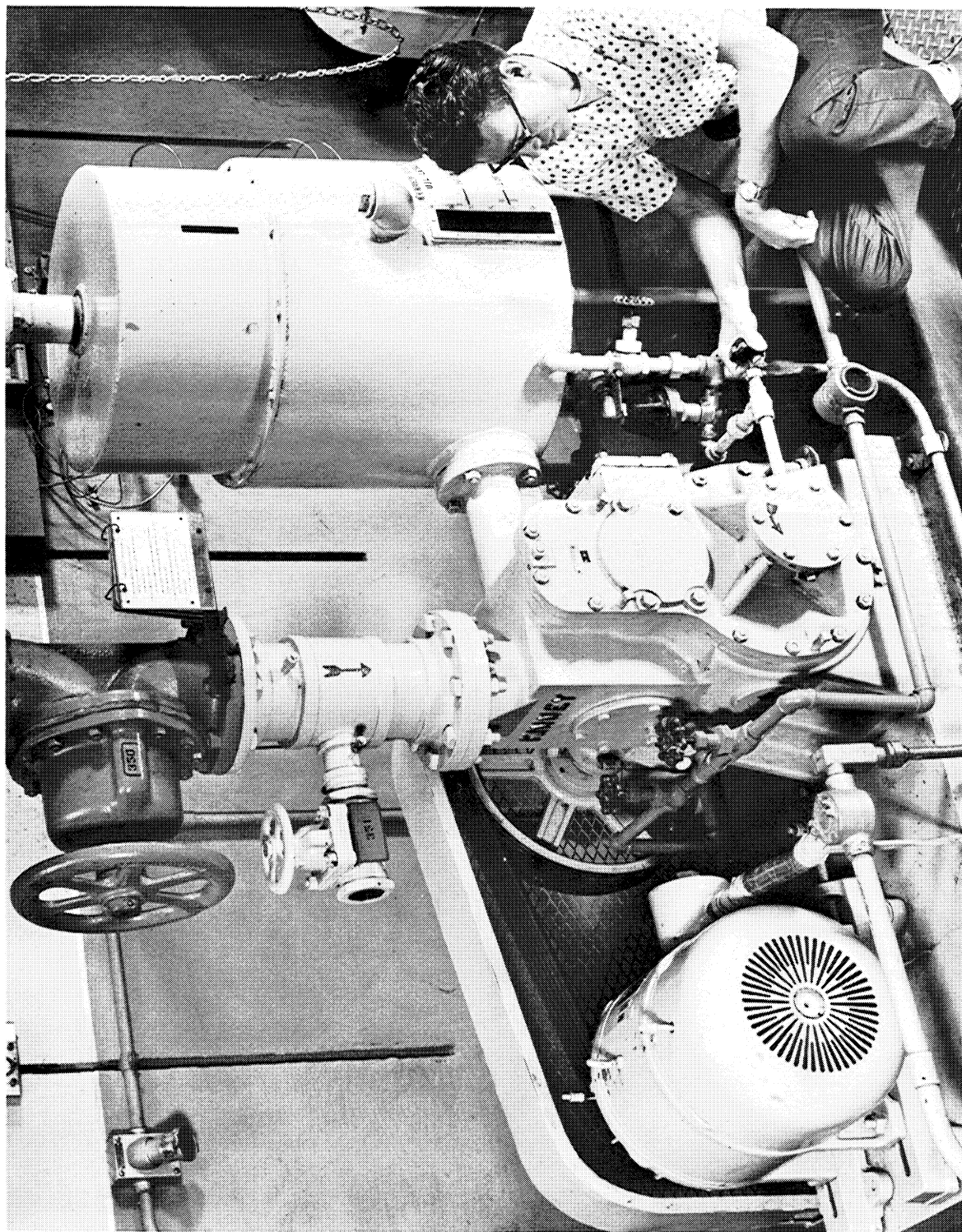
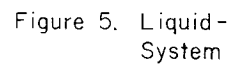
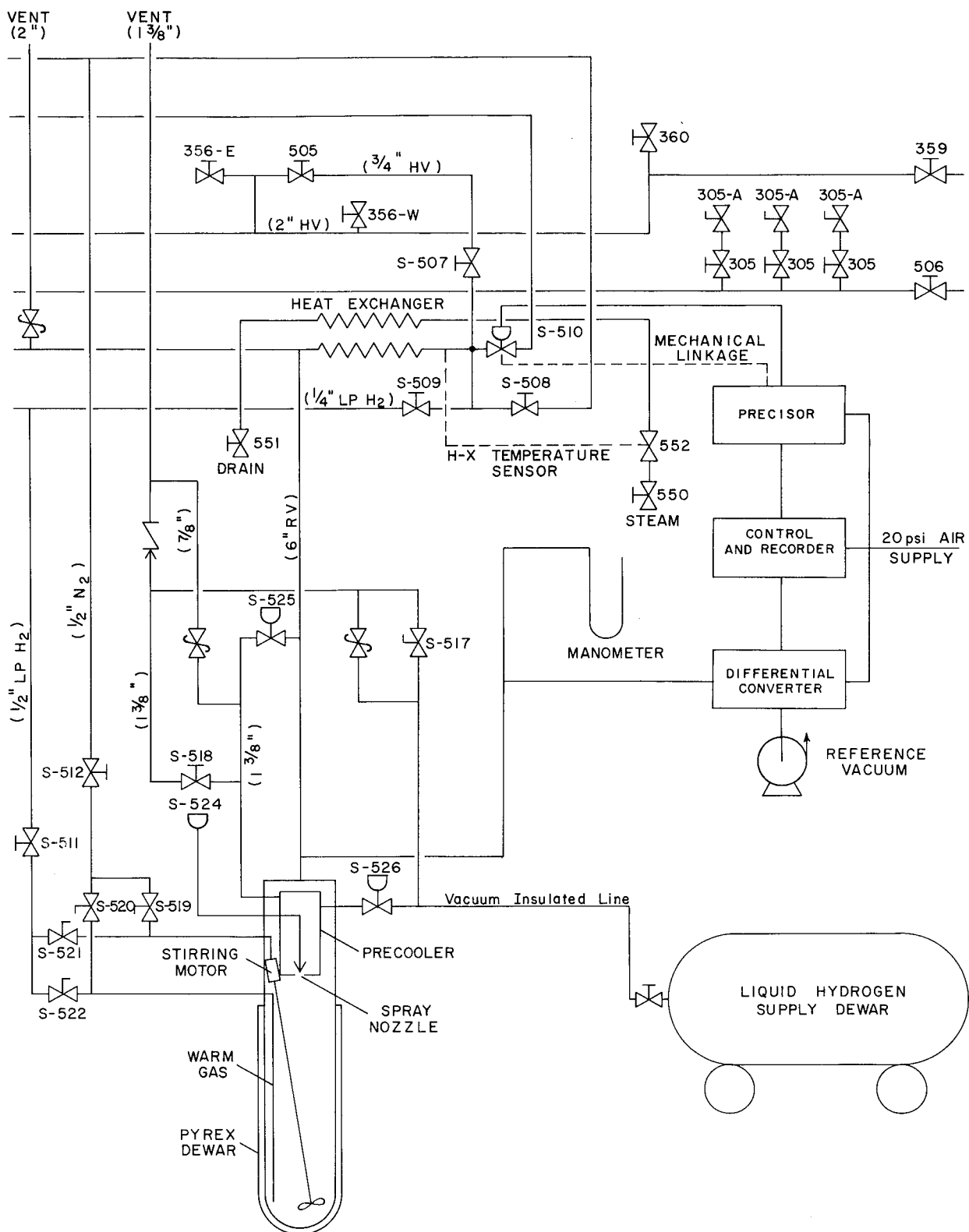


Figure 4. 10 HP High Vacuum Pump - Liquefier Building





Solid Hydrogen
Flow Schematic

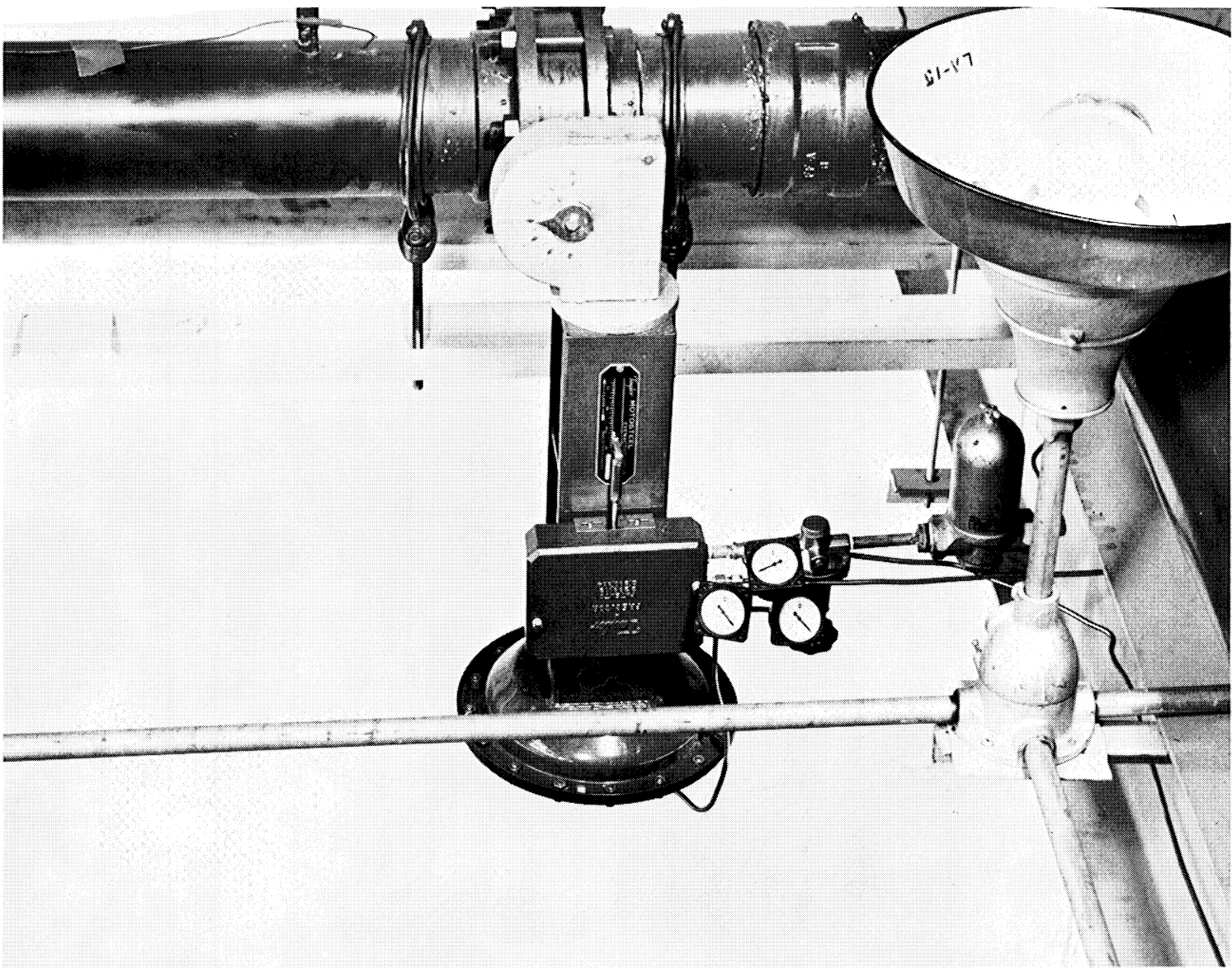


Figure 6. Vacuum Control Valve and Precursor

rotary vane pump.

In the manual mode, the controller provides direct control of the butterfly opening in the vacuum valve. In the automatic mode, the controller maintains a selected test chamber pressure by modulating the vacuum valve. The test chamber pressure is controlled to plus or minus one torr over the range of 0 to 374 torr. A continuous recording of the test chamber pressure is made on a strip chart recorder provided with the controller.

A steam heat exchanger precedes the vacuum valve in the system. The heat exchanger warms the pumped gas to near ambient temperature to assure a warm environment for the soft rubber seat of the vacuum control valve and for the vacuum pumps. The heat exchanger is of the single pass reverse flow type, consisting of a 12-inch diameter pipe surrounding the 6-inch diameter vacuum pipe and a 3-inch diameter pipe running through the center of the vacuum pipe. The temperature of the pumped gas is sensed between the vacuum valve and the heat exchanger. The steam flow is automatically controlled from the temperature sensor. Figure 7 shows the vacuum valve, the steam supply line, and the exit end of the heat exchanger.

From the heat exchanger, the vacuum pipe extends to the test apparatus and to a second presently unused stack. A view of the heat exchanger and both stacks is shown in figure 8.

The test apparatus consists of a glass dewar, a pretreatment chamber, a spray nozzle and controls, a vacuum insulated liquid transfer line, a stirring motor, and the necessary vent and control valves. A cross section of the apparatus is shown in figure 9 and a photo of the apparatus is shown in figure 10.

Liquid hydrogen is supplied from a remote dewar through the vacuum insulated line and fill valve to the pretreatment chamber. The

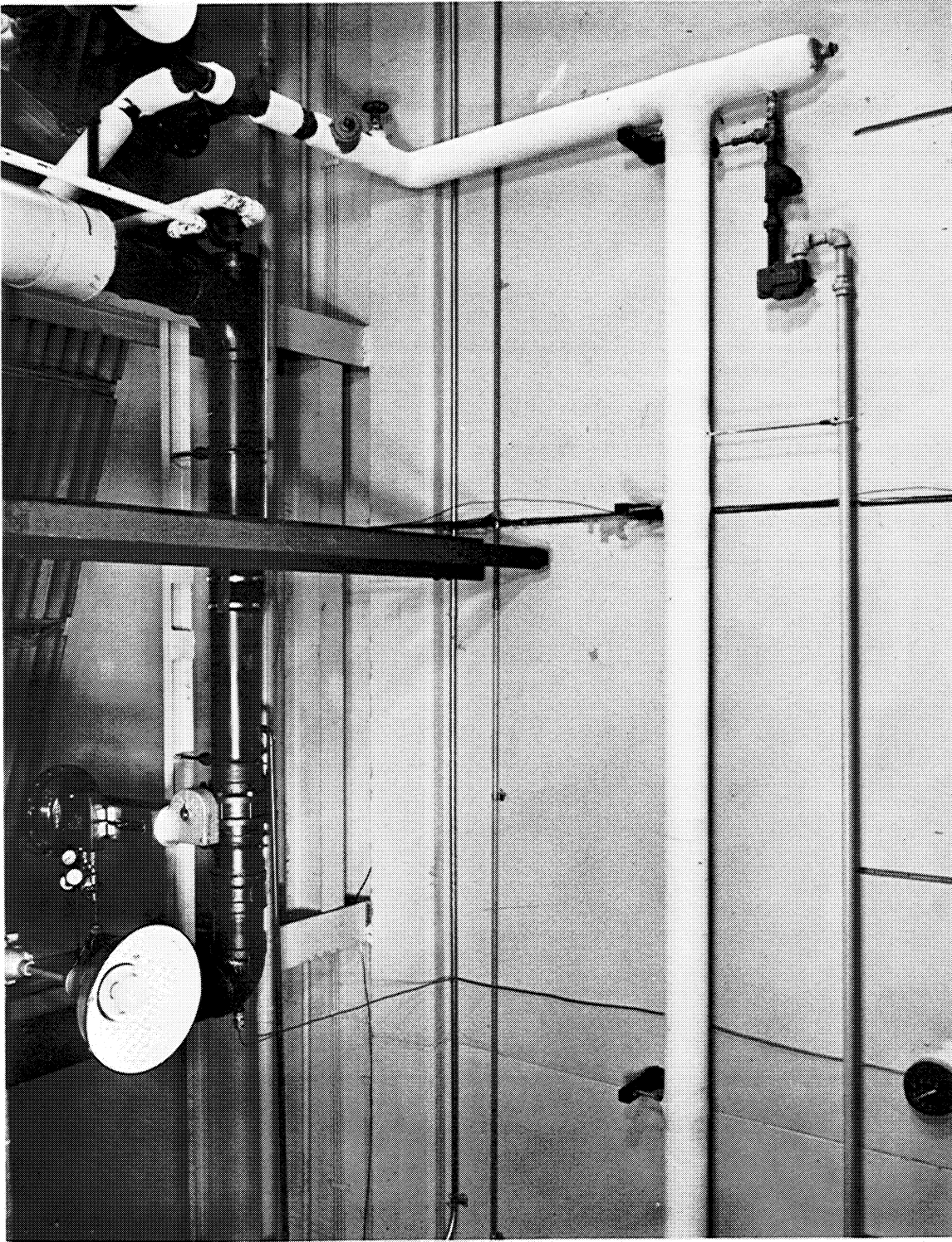
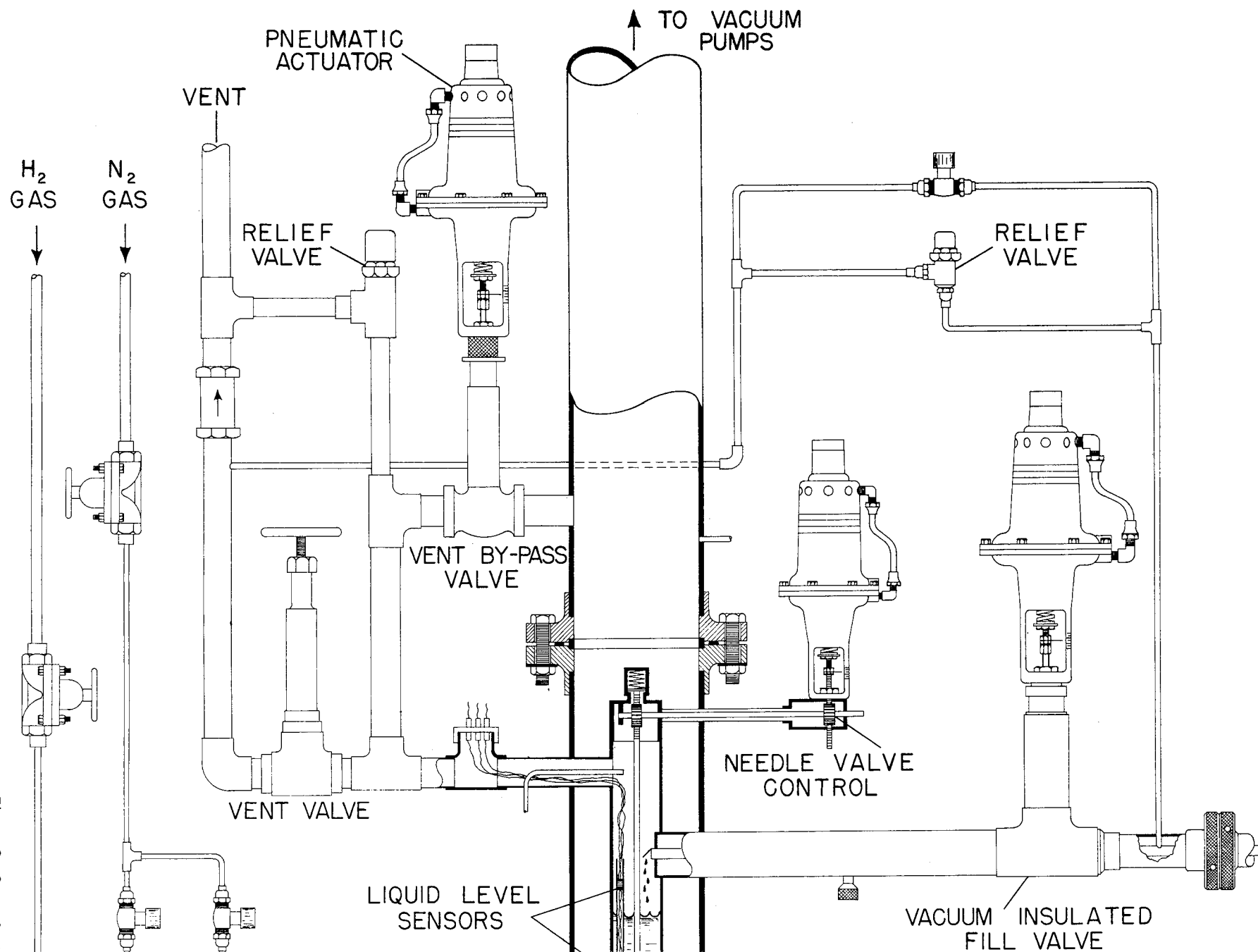


Figure 7. Vacuum Control Valve and Steam Heat Exchanger



Figure 8. Equipment Arrangement - Laboratory Area



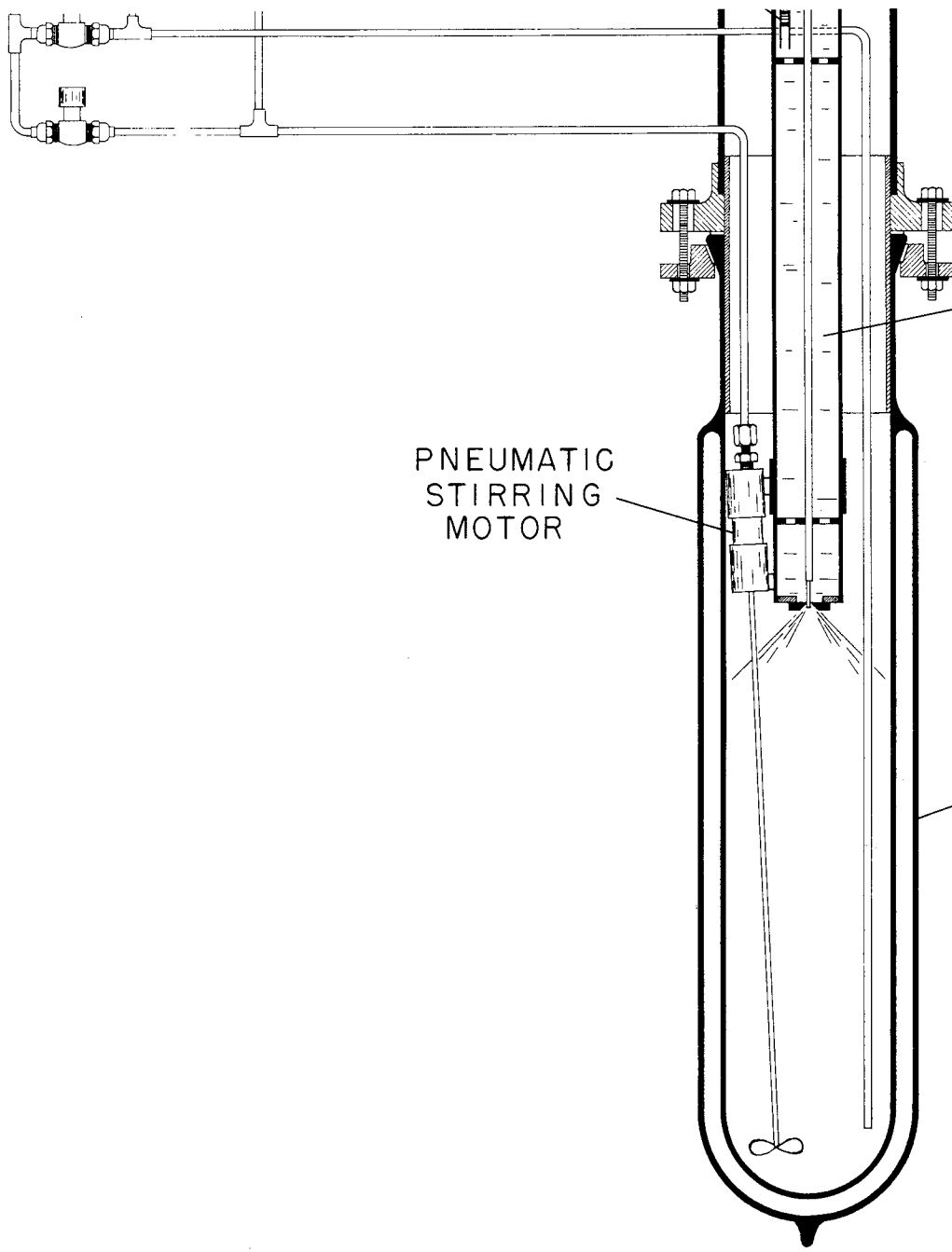
2

- Experimental

PNEUMATIC
STIRRING
MOTOR

PRETREATMENT
CHAMBER

NON-SILVERED
GLASS DEWAR



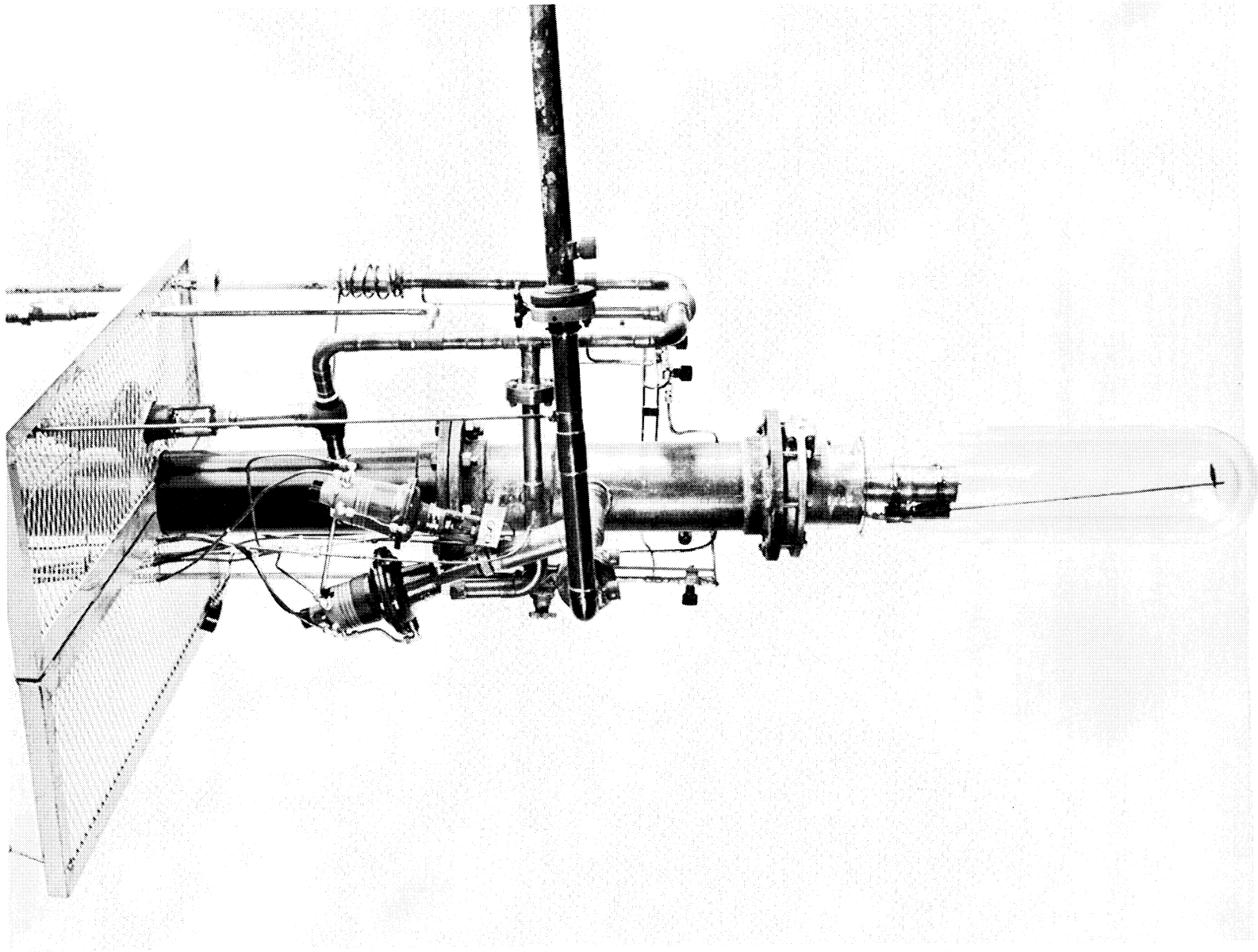


Figure 10. Experimental Apparatus

fill valve is a modulating remote controlled valve, shown in the foreground of figure 10. A by-pass valve and pressure relief valve vent the fill line during initial flow and provide for relief of trapped gases after the fill valve is closed.

The fill line empties into the pretreatment chamber, which is a 2-5/8 inch diameter by 30 inches long copper pipe. Within the pretreatment chamber are two carbon resistor liquid level sensors. An orifice is located at the bottom of the chamber and a tapered needle is centered in the orifice. The orifice and needle make up the spray nozzle. Both the orifice plate and the needle are replaceable. Figure 11 shows the needle extended through the orifice. The needle is fixed to a control rod extending up through the pretreatment chamber and through a double rack and pinion arrangement to an external pneumatic motor. The pneumatic motor and outer rack and pinion box are shown in figure 12 to the right of the fill valve. The rotating shaft is sealed with an "O" ring, and both the gear box and the "O" ring are purged with helium gas during operation.

The upper end of the pretreatment chamber is vented with a 1-3/8 inch diameter line. The vent line contains a manual, extended stem valve and a check valve. Both of these valves are by-passed by a pressure relief valve. The vent line also contains a 1-1/4 inch vent by-pass valve which opens into the six inch vacuum pipe. The vent by-pass valve is pneumatically operated by remote control. Figure 13 shows the vent by-pass valve. The valving arrangement allows the absolute pressure of the pretreatment chamber to be controlled between the glass experimental dewar pressure and the supply dewar pressure.

The glass dewar is attached to the pumping line with bolted flanges and a teflon gasket. The glass dewar is 6 inches I. D. x 8 1/4

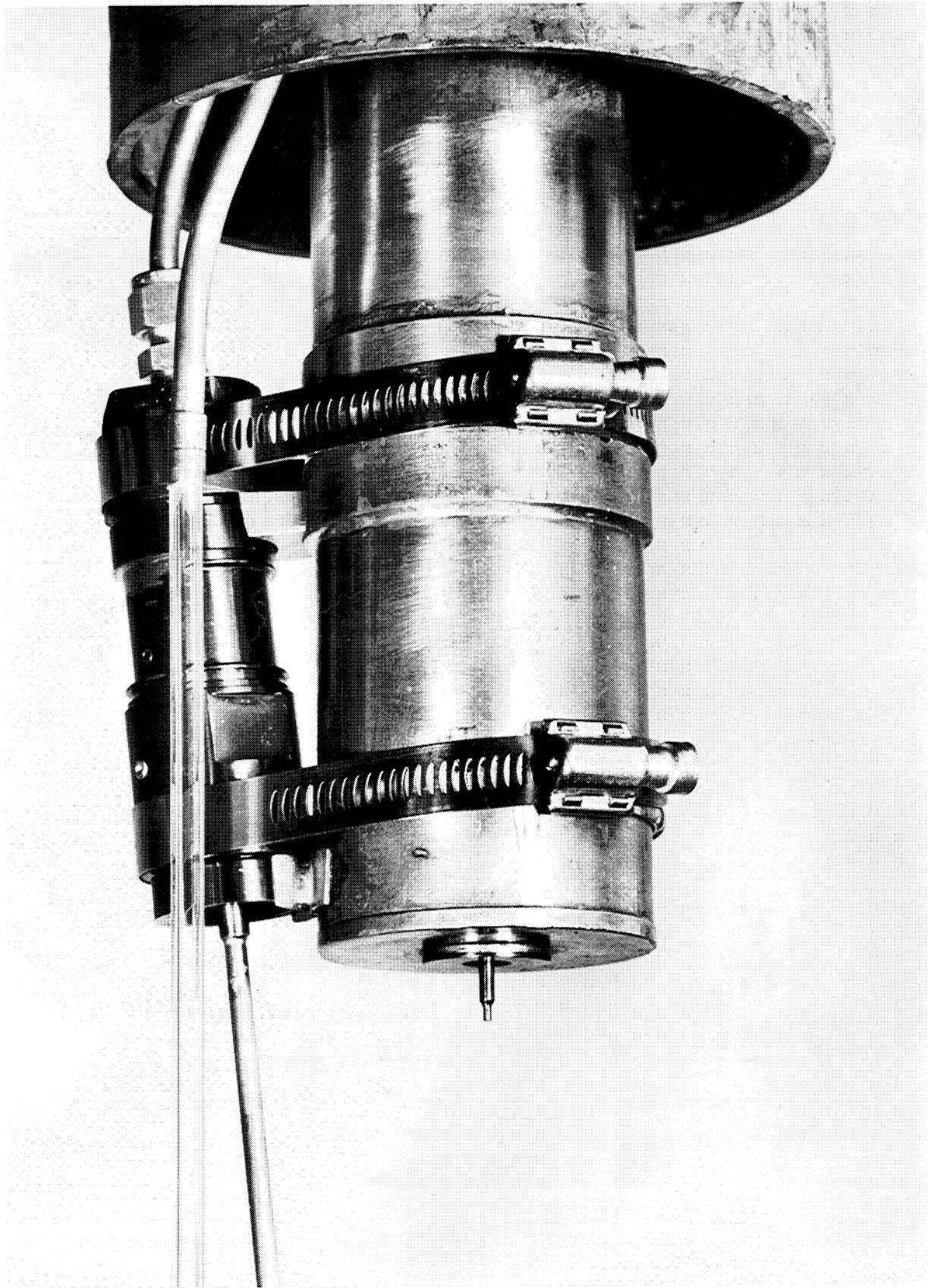


Figure 11. Orifice, Needle and Stirring Motor

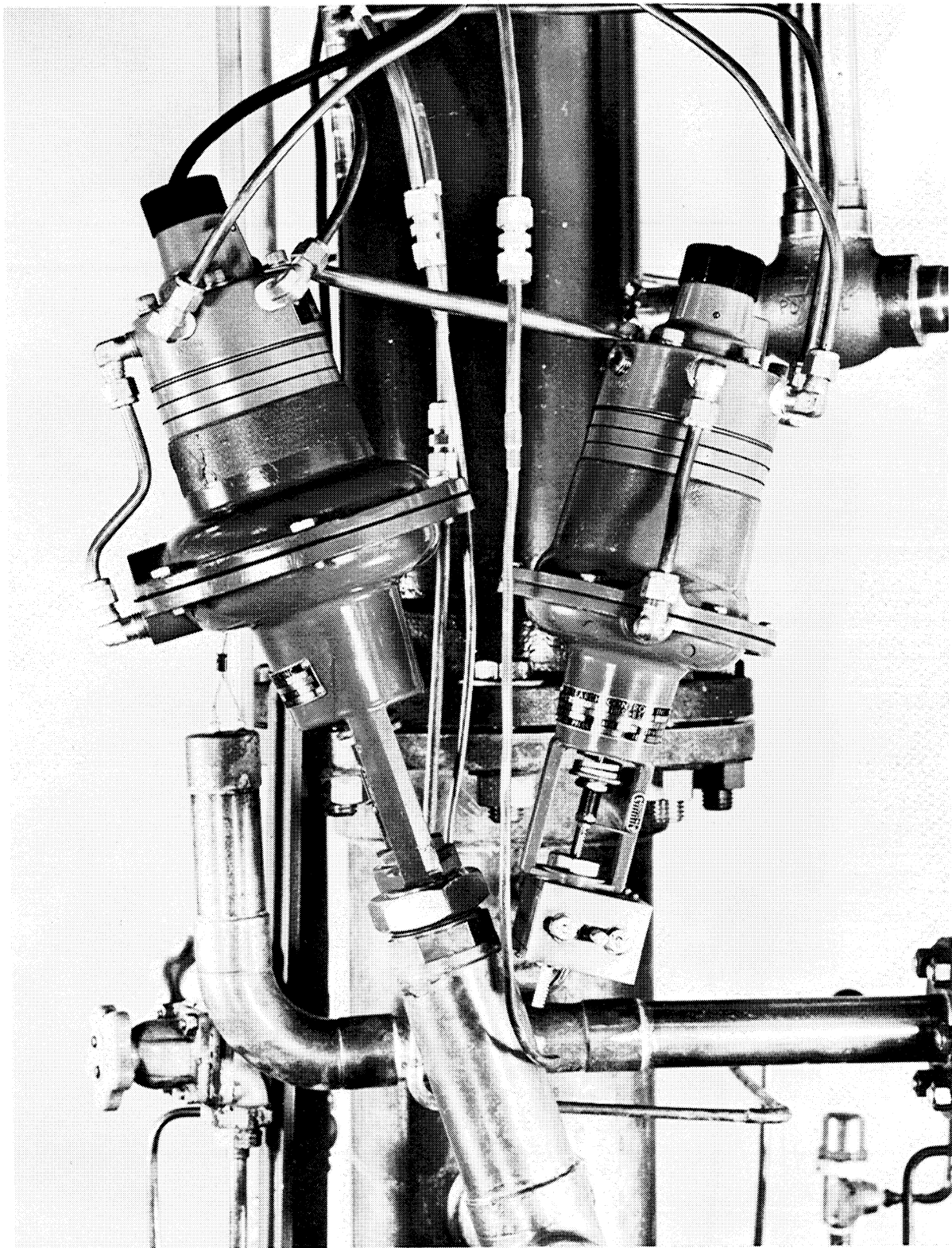


Figure 12. Remote Control Valving - Experimental Apparatus

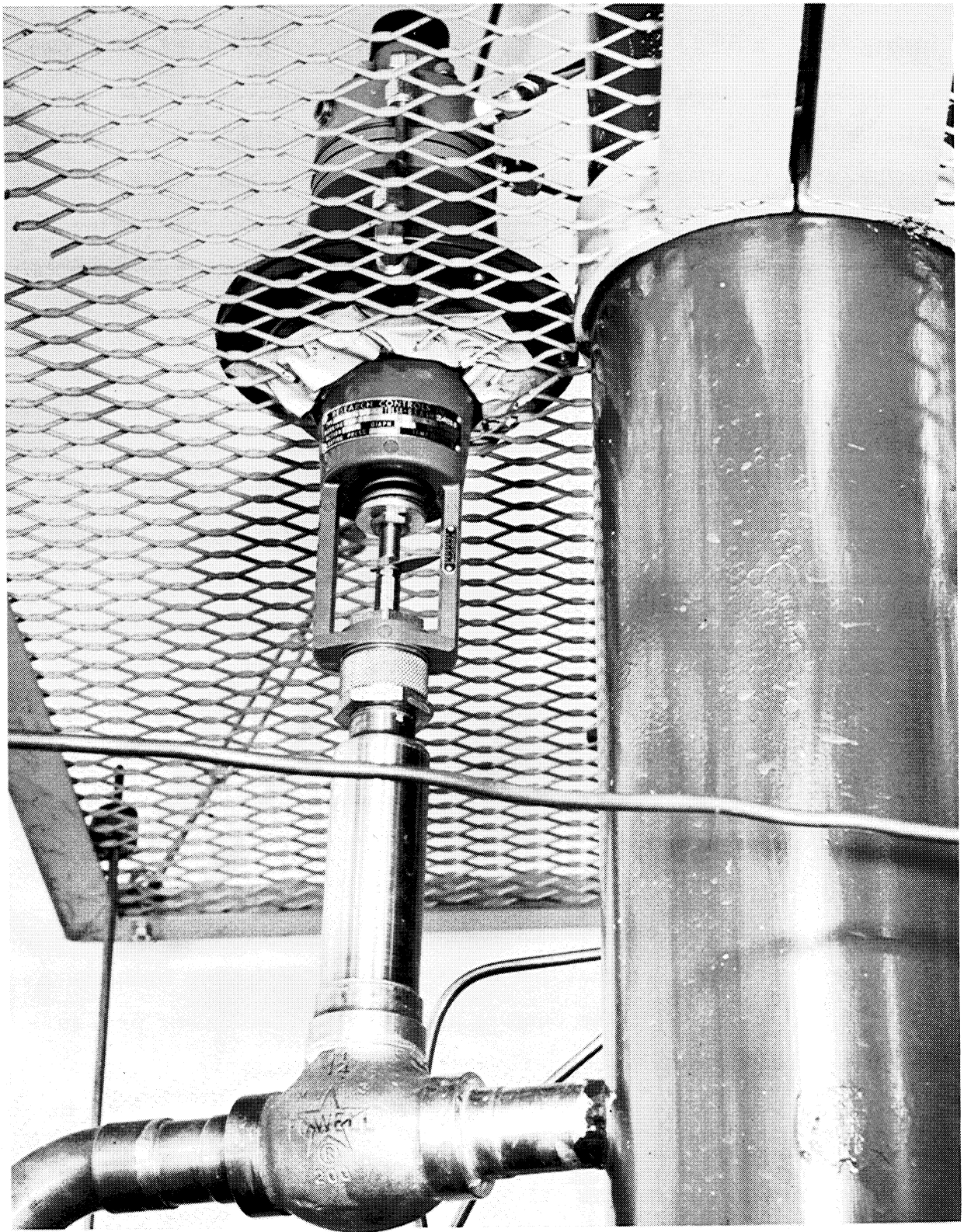


Figure 13. Vent By-Pass Valve

inches O. D. x 35 1/2 inches long. A stirring device which consists of a pneumatic motor and extended shaft with propeller stirrer is attached to the lower end of the pretreatment chamber. The extended shaft places the propeller near the bottom of the dewar. The entire assembly can be seen in figure 14. A close-up photograph of the motor and mountings is shown in figure 11. The stirring motor may be driven by hydrogen gas and the exhaust is discharged directly into the main pumping line.

A 1/4-inch tube enters above the glass dewar flange and continues to the bottom of the glass dewar. This tube provides hydrogen gas for warming the dewar contents or to assist in stirring. A second glass dewar filled with liquid nitrogen is used as an additional heat shield for the apparatus dewar when required.

The control panel for operation of the vacuum control valve, the needle valve, the vent by-pass valve, and the fill valve is shown in figure 15. At the top of the panel are three compound gauges. The upper left gauge indicates the pretreatment chamber pressure. The upper right gauge gives an approximate value for dewar pressure. The lower left gauge indicates the transfer line pressure. The absolute mercury manometer is a precise indication of the dewar pressure.

To the left of the manometer is the vacuum valve controller and attached recorder. The dial and three pointers at the top indicate the butterfly valve position, the control pressure, and the dewar pressure. The strip chart continuously records the dewar pressure.

Below and to the left of the manometer are the controls for the hydrogen fill valve, the vent by-pass valve and the needle control valve. The small knobs control the valve positions by modulating the air signal to the valve motors. The panel below contains the power supply and control for the 16 mm motion picture camera. The extreme lower

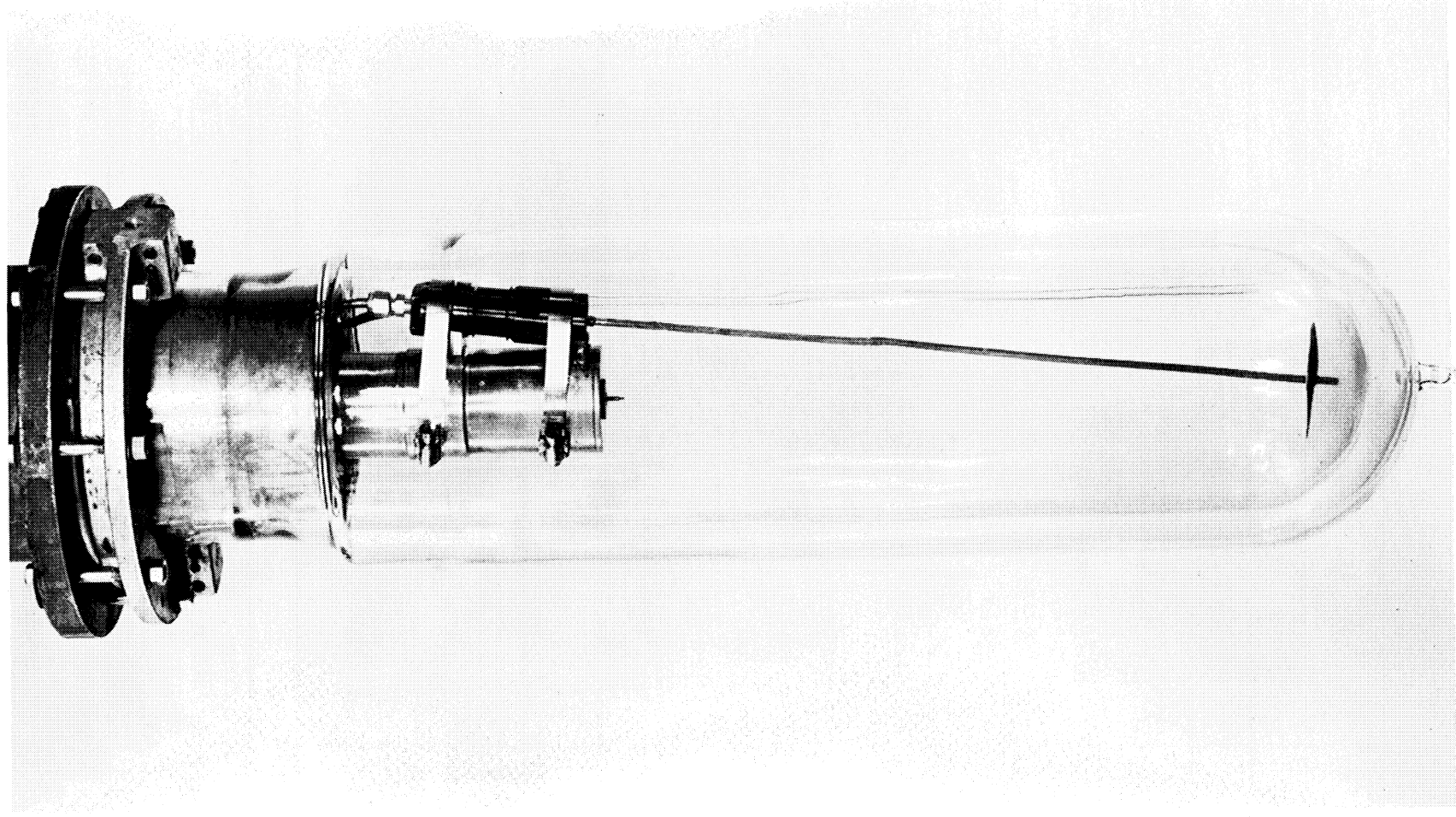


Figure 14. Glass Dewar Assembly

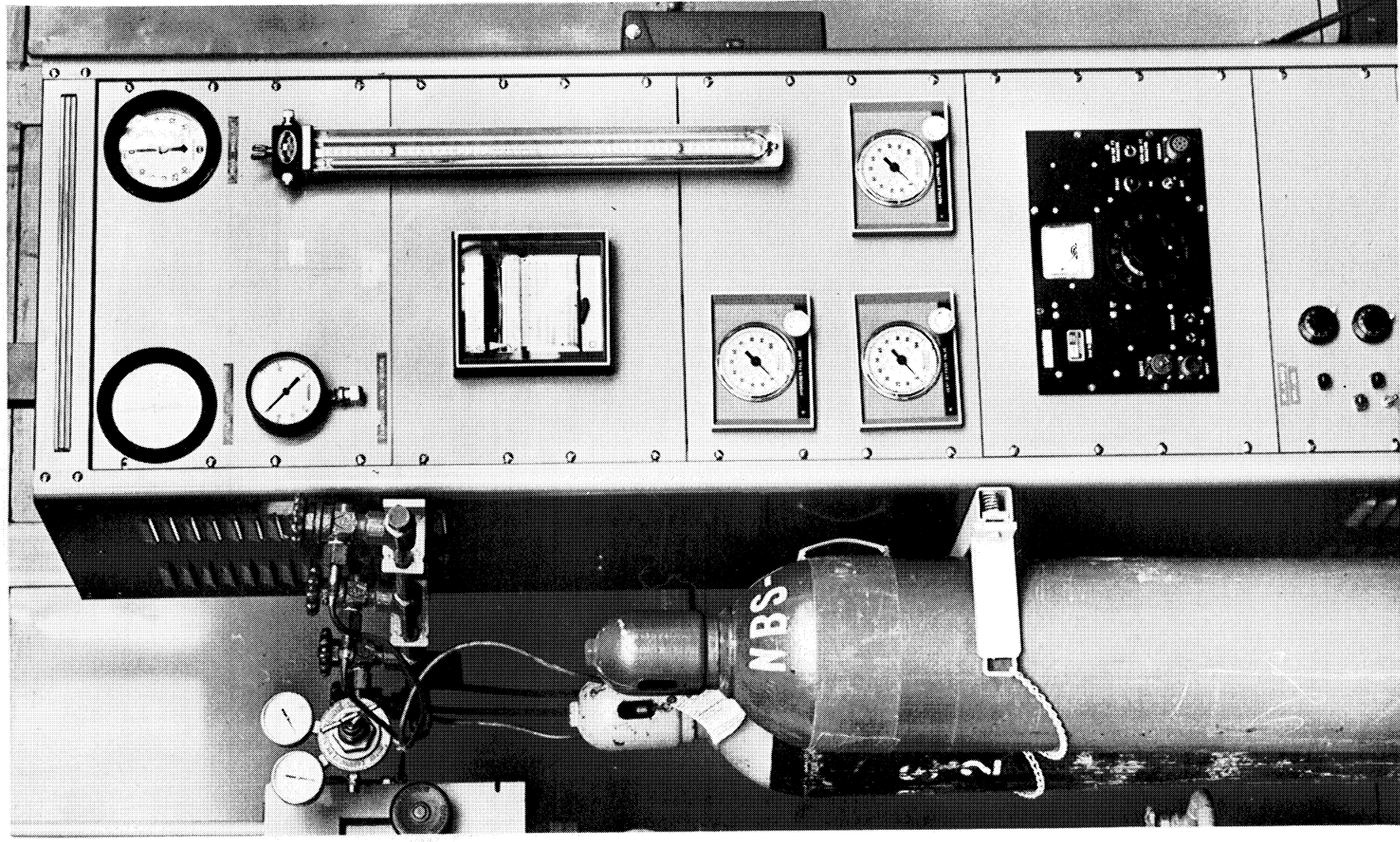


Figure 15. Control Panel

panel contains the controls and indicator lights for the pretreatment chamber liquid level sensors.

2.2 Operation

To form a liquid-solid mixture by the spray method, liquid hydrogen is passed into the pretreatment chamber through the liquid transfer line and the fill valve. The dewar pressure is reduced below the triple point by setting the required pressure on the vacuum valve control. The pretreatment chamber pressure can be maintained at the desired level through operation of the vent by-pass valve. When the lower liquid level sensor is covered, indicating an adequate supply of the liquid, the needle valve is opened to the desired position and the spray enters the dewar. At dewar pressures below the triple point, the liquid turns to solid, the heat of fusion being removed by evaporation. When the dewar is filled with solid particles, the pressure is raised above the triple point by introducing hydrogen gas. This warmer gas, combined with the heat leak of the apparatus, melts some of the solid particles and a liquid-solid mixture remains in the dewar.

To produce a liquid-solid mixture by the freeze-thaw method, the needle valve is opened during filling, permitting the liquid to spray into the dewar. The glass dewar pressure is maintained above the triple point. When sufficient liquid has accumulated in the glass dewar, the pressure is cycled above and below the triple point. When the dewar pressure is reduced below the triple point, some of the liquid vaporizes carrying off the heat of fusion and a layer of solid forms. Raising the pressure slightly above the triple point melts some of the solid and the remaining solid layer settles to the bottom of the dewar. The liquid-solid mixture can be upgraded by repeating the cycle as many times as desired.

3. Results

Results to date cover development and refinements of photo-instrumentation techniques and preliminary observations of liquid-solid mixtures produced by two different methods.

3.1 Photoinstrumentation

Considerable emphasis has been placed on photography during the present reporting period. High-speed photography will be used to investigate the effects of orifice and needle parameters on spray particle variables and liquid-solid parameters such as size, shape, and ratio of length to diameter. Other parameters necessary for transport study such as terminal velocity, particle size distribution, tendency to agglomerate, and the effect of aging the solid particles will also be determined with the aid of high-speed photography. Consequently, much of the effort to date has been toward determining optimum photographic techniques.

Photographic equipment, supplies, and personnel of the photographic laboratory of the National Bureau of Standards were used in the development of the photoinstrumentation. Two still cameras and three 16 mm motion picture cameras were available for use. Two of the motion picture cameras were evaluated for high-speed documentation, a Wollensak Fastex WF 1 and a Photo-Sonics, model 1B. Various types of light sources, screens, baffles, reflectors, and film were also evaluated.

The high speed Photo-Sonics camera, model 1B, with a rotating prism and variable shutter opening proved to be the best camera for particle studies. The Photo-Sonics camera has a frame rate of 12 to 1000 frames per second with respective exposure times of 1/60 second to

25 microseconds. The lens is a f-2 Navitar with a 50 mm focal length. The resolution of the present lens is adequate, but the magnification of 0.08X does not allow analysis of particles less than about 10 μ m. A lens modification will be required to increase the magnification to about 0.5X, a value necessary for adequate analysis.

The best lighting for taking pictures of particle spray was found to be a 1000 watt, quartz-iodide light source at right angles to the camera and at the same level as the camera. The best lighting for photographing the liquid-solid mixture was found to be a 1000 watt, quartz-iodide light source 180 degrees from the camera and about 12 inches above the lens.

The photographs in figures 16 through 21 were reproduced from 16 mm motion picture film taken with the above lighting conditions and the Photo-Sonics camera.

3.2 Production by Spray Method

Solid hydrogen particles can be easily produced by spraying liquid hydrogen through an orifice into a chamber whose pressure is below the triple point (52.9 torr). It was found that the particles would vary in size and texture, primarily dependent upon the orifice and needle configuration. The needle was 0.125 inches diameter and tapers to 0.120 inches near the tip. The original orifice plate had a 30 degree taper on the bottom, extending outward from the hole as shown in figure 11. With the taper on the bottom, the orifice produced large particles. Agglomerates would accumulate on the bottom of the orifice and break off in particle sizes to two centimeters long with various shapes. One of these large particles is shown in figure 16.

To reduce the agglomerate accumulation on the bottom, the orifice plate was reversed. This placed the taper on the inside and the sharp edge hole on the bottom. With the orifice in the reverse position,



Figure 16. Large Spray

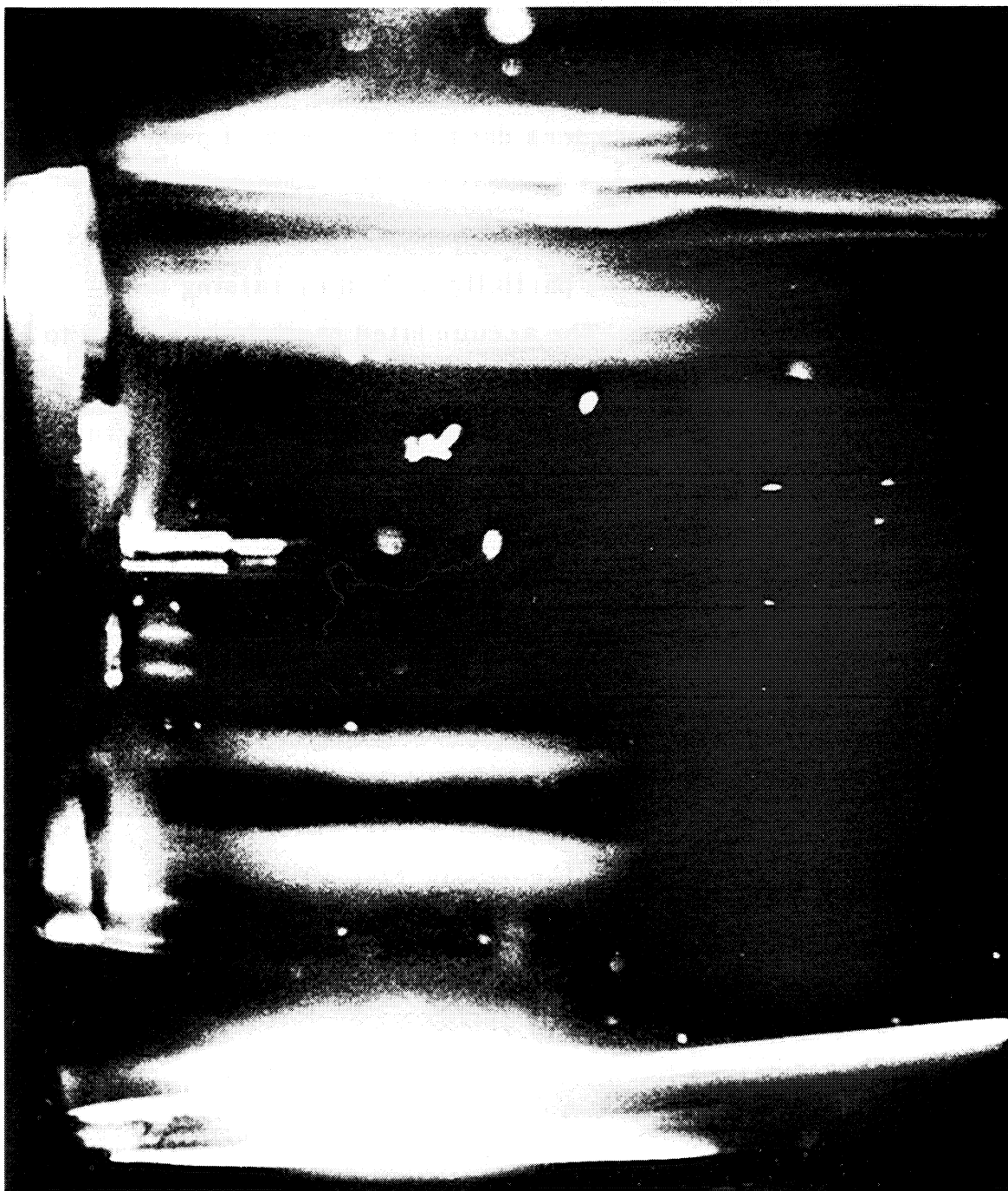


Figure 17. Fine Spray

fine spray particles were produced as shown in figure 17. Varying the needle position in the orifice had a slight effect on particle size, but not as pronounced as changing the orifice configuration.

Hydrogen particles, as shown in figure 18, are produced rapidly with the spray method. The particles appear to be very light and fluffy in texture and are much less dense than the solid produced by the freeze-thaw method.

The glass dewar is usually filled with spray particles, as shown in figure 19. These particles are partially melted by raising the pressure above the triple point. The accumulated particles collapse to a much smaller volume of liquid-solid mixture in the bottom of the dewar. A photograph of the solid immediately after a melt is shown in figure 20. If the liquid-solid mixture is stirred after the melt, the solid breaks up into irregular particles as shown in figure 21. No microscopic study of the spray particles has been made to date. Pre-treatment chamber pressure, dewar pressure, heat leak, and orifice and needle configurations are all parameters that appear to affect spray particles. The effect of these parameters will have to be investigated so that reproducible particles may be generated.

3.3 Production by Freeze-Thaw Method

Solid hydrogen can also be produced by vacuum pumping on the surface of the liquid. Pumping on the surface provides refrigeration by evaporation. After the liquid comes to triple point temperature (13.8°K), additional pumping removes the heat of fusion and a crust of solid forms at the surface. The solid crust continues to grow thicker as long as the pressure is kept below the triple point. When the pressure is allowed to go above the triple point, the solid begins to melt and the crust slowly falls to the bottom of the liquid. By alternately pressure cycling



Figure 18. Solid Hydrogen Spray.

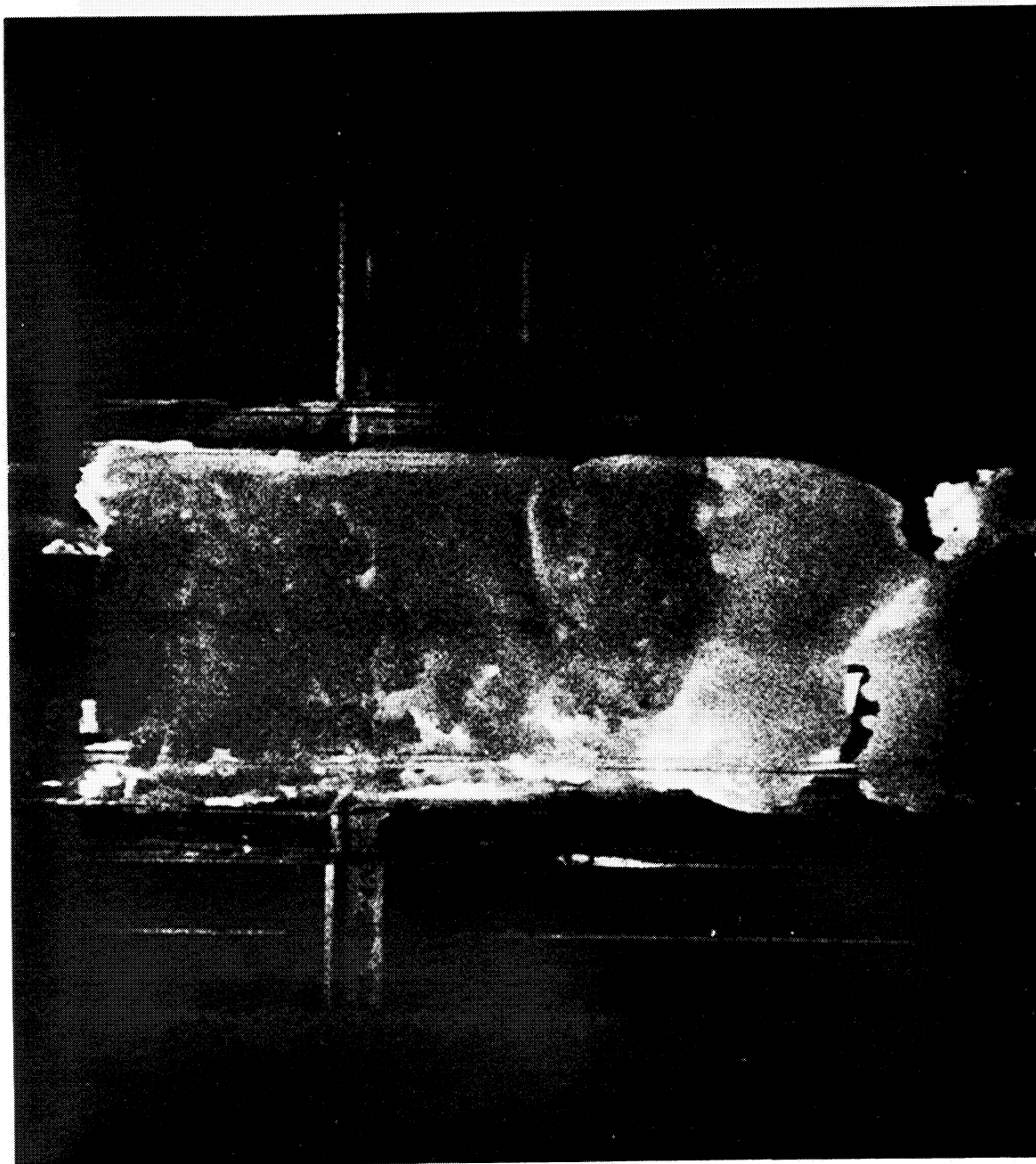


Figure 19. Solid Spray Before Melt.

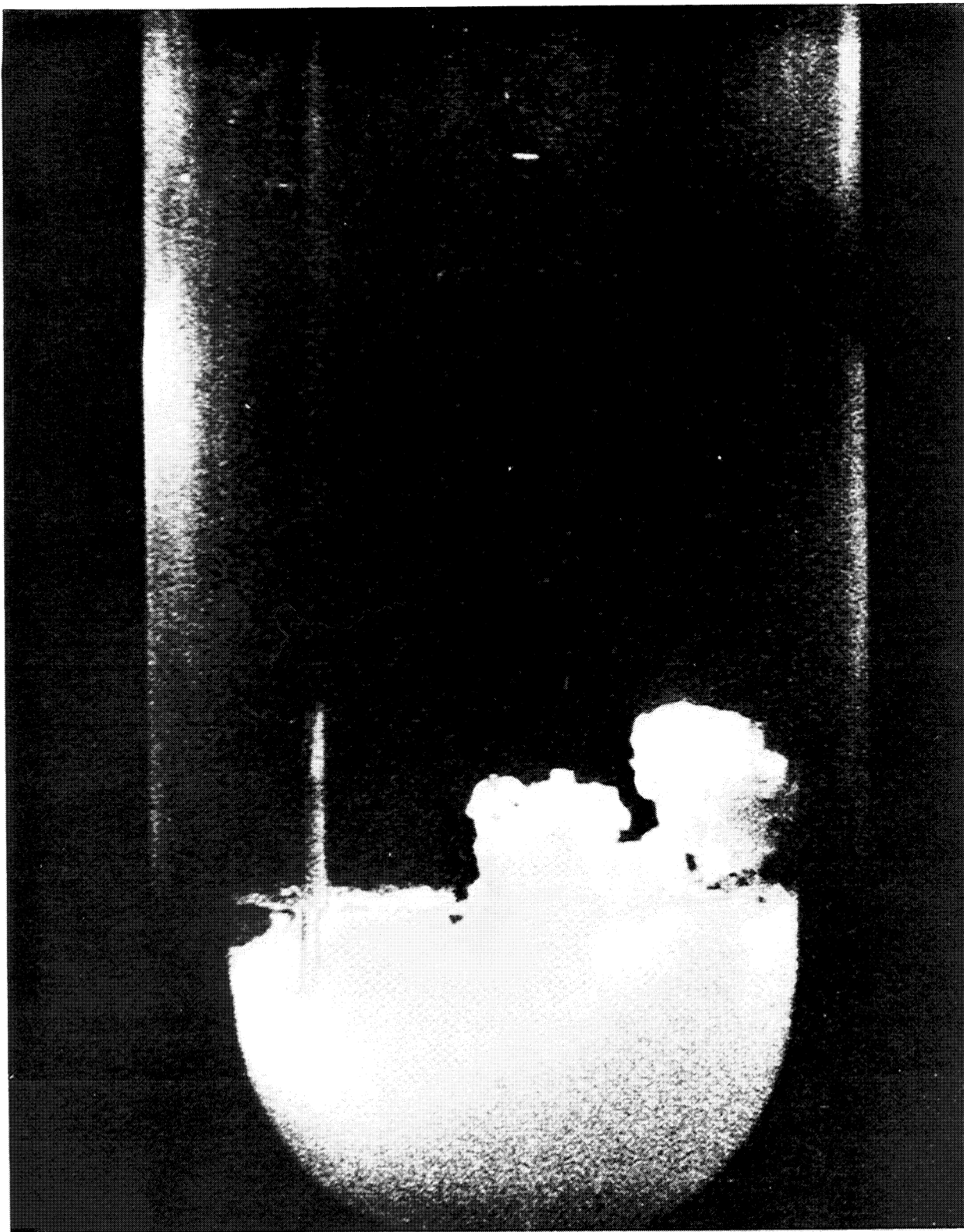


Figure 20. Liquid-Solid After Melt

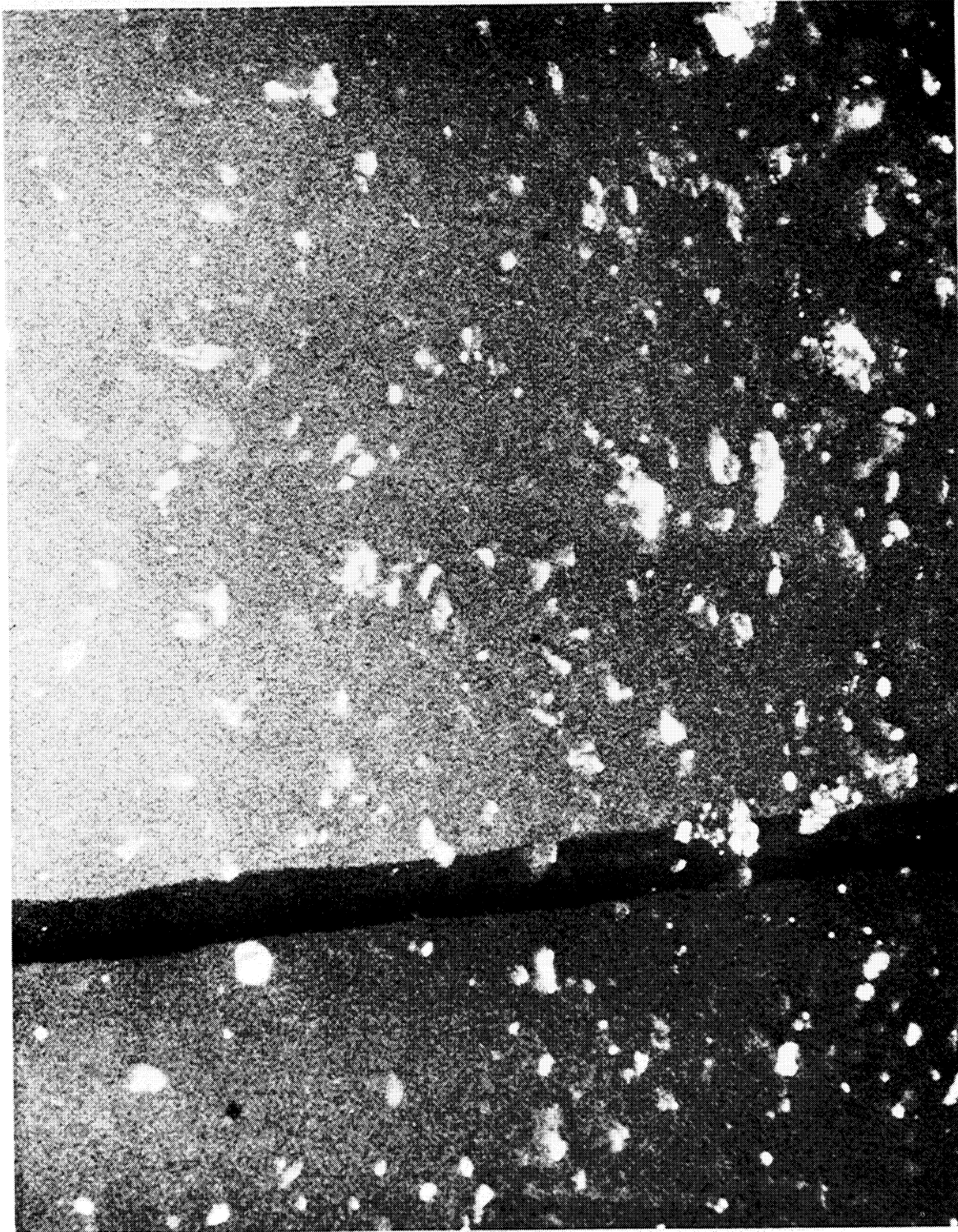


Figure 21. Large Particles in Liquid

above and below the triple point, mixtures of liquid-solid hydrogen can be quickly produced as shown in figure 22.

By use of mechanical agitation for breaking the crust and stirring, a homogeneous mixture of liquid-solid can be produced. After a short period of time, the solid particles settle to the bottom and appear to be of relatively uniform size as shown in figure 23. There appears to be no tendency for the particles to agglomerate while in this state.

3.4 Liquid Nitrogen Shielding

Liquid nitrogen shielding is not necessary for making hydrogen solid by either of the two methods, but it is necessary to reduce the heat leak for long term measurements of particle characteristics and behavior. The optical distortion produced by four layers of glass and a layer of boiling nitrogen was not as great as expected. Nitrogen bubbles tending to hinder photography can be momentarily eliminated by pressurizing with nitrogen gas. Figures 21 and 23 are photographs made through nitrogen shielding.

4. Future Work

Results of the program to date are preliminary. Production apparatus, photoinstrumentation and mixture handling have been determined and tested in a general sense. The incorporation of a quality meter into the apparatus and the general subject of data analysis have not been considered extensively. Anticipated activity in these areas are considered in the following sections.

4.1 Production Apparatus

No modifications are anticipated. The expansion valve orifice and needle may be modified slightly to give optimum particle size in the spray method of mixture generation. A scoop or lift to raise the

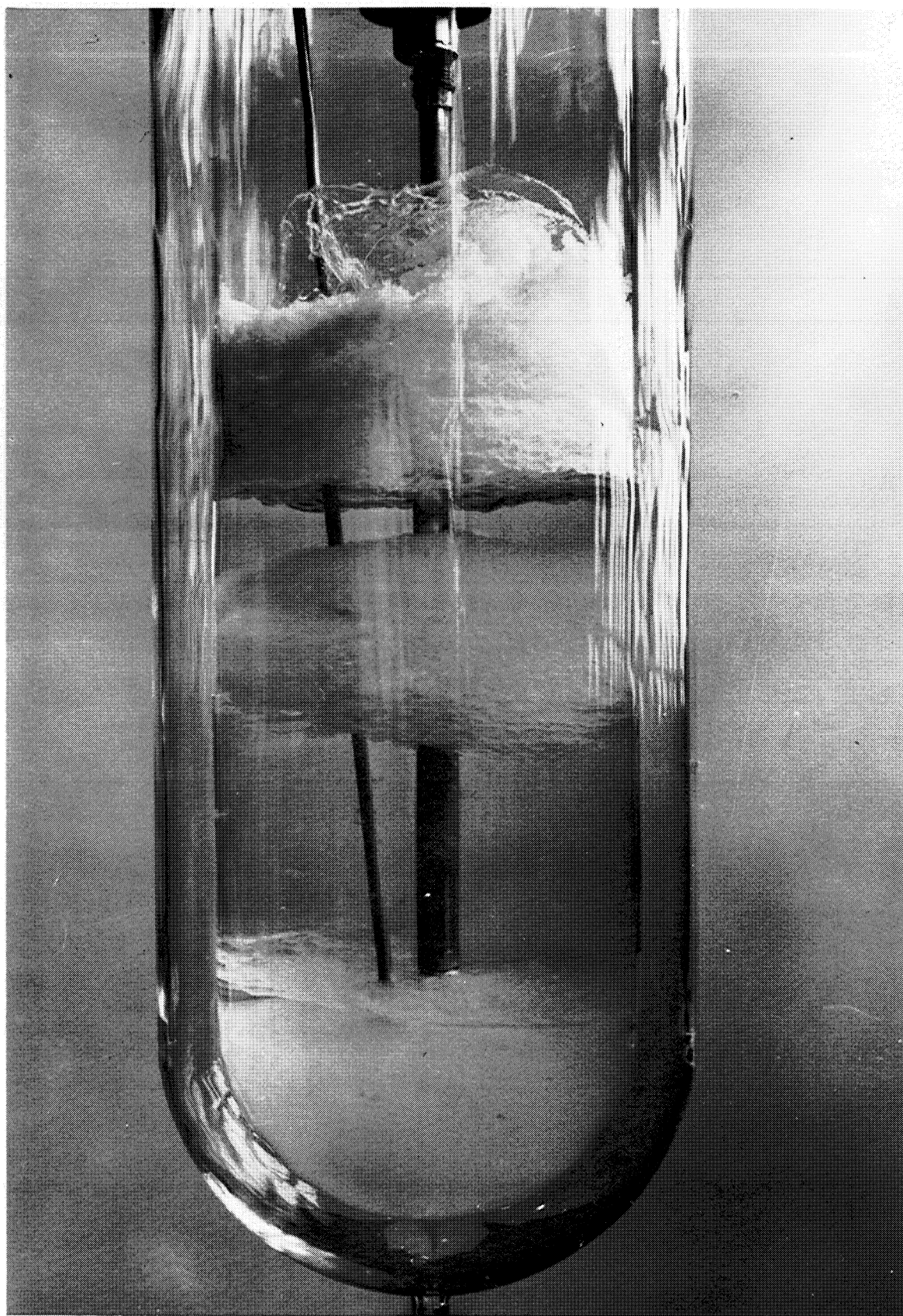


Figure 22. Freeze-Thaw Production Process



Figure 23. Fine Particles in Liquid

solid particles into the liquid region for particle size and terminal velocity measurement will be devised. Minor modifications of the venting system will be made to assure safe operation. With these minor changes, the apparatus is believed adequate to complete Phase I of the study.

4.2 Photoinstrumentation

The present film image size of particles is not adequate for detailed analysis. In addition, no fixed size reference is available on the present film. Particle sizes may be calculated from lens and object-image distance data, but a more accurate method would be to photograph a true linear scale simultaneous with the particle.

The particle film image will be increased by increasing the lens to image distance or using a lens of longer focal length. Both of the above modifications would reduce the depth of field and therefore the number of particles visible per frame.

Three methods of obtaining a size reference on the 16 mm film will be considered. The first method would use a beam splitter or a partially reflecting piece of glass set at 45° to the camera-particle axis. The beam-splitter, located outside the glass dewar and in the camera line-of-sight, would reflect into the lens an image of a reference grid set at 90° to the camera-particle axis and at the same focal distance as the particle. Since the beam-splitter is only partially reflecting, the image of the particle would also be recorded on the film.

The second method of recording a reference grid would employ the use of a photo-relay lens which incorporates a lens system and grid reticle in such a way that the grid is placed at a known focal distance from the particle. Since the relay system is mounted with the existing lens, a particle image and the reference grid are superimposed.

The third method would be to place a transparent reference grid within the liquid hydrogen above the slush level. The solid particles and reference grid would both be within the depth of field of the camera and would be photographed simultaneously.

Lighting for particle size determination in the liquid-solid mixture is presently adequate. These are continuous quartz-iodide lamps of 1000 watt rating. Additional lighting, if required, can be achieved by adding a condensing lens system to the existing lights. The determination of the particle size of the spray is not adequate. The continuous light source and the 25 microsecond exposure time are not sufficiently fast to stop the particles spraying from the orifice. A high speed strobe light will be used to decrease exposure time to 1 microsecond in an attempt to analyze these particles.

4.3 Liquid-Solid Mixture Study

The determination of particle size as a function of production method will be conducted by varying the controlling parameters and observing the effects. Since, in all the observed cases so far, the particles vary in size within a particular set of production parameters, a statistical treatment of the experimental data seems indicated.

Once reproducible particle sizes have been determined, as a function of the production method, the particle sizes and terminal velocity of the particles in the liquid can be measured. This will be done photographically with a few modifications to the existing apparatus. The needle valve and orifice plate will be removed and an extension to the control rod added. The control rod will terminate near the bottom of the glass dewar and will be fitted with a scoop. A mixture of liquid and solid will be generated in the glass dewar so that the settled solids will occupy about half the total volume, with the remainder being liquid. The scoop at the bottom of the control rod will then be lowered into the solids.

A portion of the solids will flow onto the top of the scoop and remain there while it is raised into the liquid region. After the mixture has settled, the control rod may be moved slightly, causing some of the particles to fall from the scoop and settle through the liquid. Motion pictures will be taken of the settling particles. Particle sizes and terminal velocities will be determined from a grid and from accurate timing marks on the film.

Particle growth and agglomeration will be studied using lapse-time photography over a period of several days. A mixture of liquid and solid will be produced and thermally shielded to limit heat leak effects. Several feet of motion picture film will be taken periodically to secure a compressed time sequence of aging effects.

A quality meter developed under the instrumentation program will be incorporated into the above described tests as soon as it is available. The effect of the instrument will then be added to the already defined experiments.

4.4 Data Analysis

Once the solid particle is recorded on photographic film, its accurate size and shape may be studied. In order to analyze and correlate these data, a Benson-Lehner Boscar film reader will be used. This is an existing system available at the laboratory.

The Boscar film reader projects the 16 mm frame image on a accurately positioned ground glass screen with a magnification of about 8X. Cross hairs are then positioned on film reference marks and the x-y axis normalized and calibrated to fix the exact magnification. Two x-y points on the particle will allow length/diameter ratios to be determined with good accuracy since the film may be rotated and the particles are random oriented. As each x-y point is defined by the cross hairs,

the point is punched on an IBM card through an 026 card punch attached to the Boscar.

These data cards are then used as input to an analysis program to be run on the IBM 7090 digital computer. Different computer programs will be used depending on the nature of the analysis. In addition to a statistical treatment of particle size and shape, the analysis technique will be used to determine terminal velocities and aging effects. The results of the data analysis will be used to predict transport characteristics and design the transport experimental apparatus of Phase II.

PART B. SOLID PARTICLE SIZE AND TERMINAL VELOCITY DETERMINATION

1. Introduction

The following is a portion of the second progress review for the project "Slush Hydrogen Production and Instrumentation." The instrumentation portion of the program is reported separately. The work reported describes progress made from September 1964 to February 1965.

1.1 Activity Summary

Progress during the present reporting period has resulted in a further refinement of equipment and techniques and the measurement of certain critical liquid-solid mixture characteristics.

A number of significant decisions were made. The study of the spray production method was set aside in favor of the more promising freeze-thaw production technique. It was found that using the present experimental apparatus, the spray production method, in addition to being a batch process, resulted in mixtures of a non-reproducible nature. Large solid agglomerates, in excess of 5 cm in size, were produced indicating that further crushing may be necessary to establish good transport characteristics.

Production of liquid-solid mixtures by the freeze-thaw method resulted in particles less than 10 mm in size and on a reproducible basis. The freeze-thaw method is potentially very efficient, as the refrigeration process is nearly isothermal. Large scale production should be relatively inexpensive and may be accomplished either at the liquefaction site or at "on-site" storage. Also, the method is more conducive to schemes for production on a continuous basis. Therefore, no further work was done on the spray method. The following sections are concerned with mixtures produced only by the freeze-thaw method.

The experimental effort has been concentrated in three general areas:

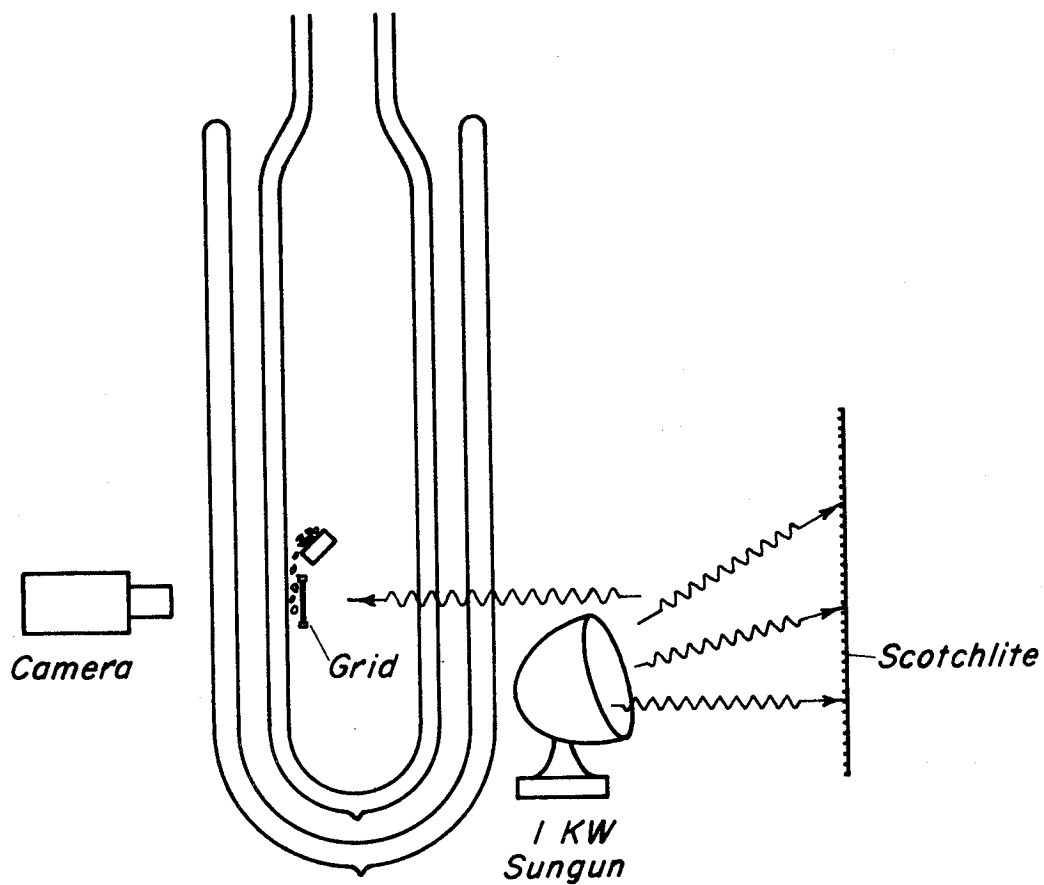
- 1) particle size determination - the actual measurement of the particle size and statistical correlation of data,
- 2) aging effects - the observation and statistical correlation of any changes in the particle size, shape or configuration as a function of storage time, and
- 3) terminal velocity - the measurement of the maximum velocity attained by a particle as it falls through undisturbed liquid.

Data in the above areas have been recorded on approximately 3000 feet of 16 mm film. A large portion of the film has been processed through a data reduction system and the provisional data for all three areas are presented.

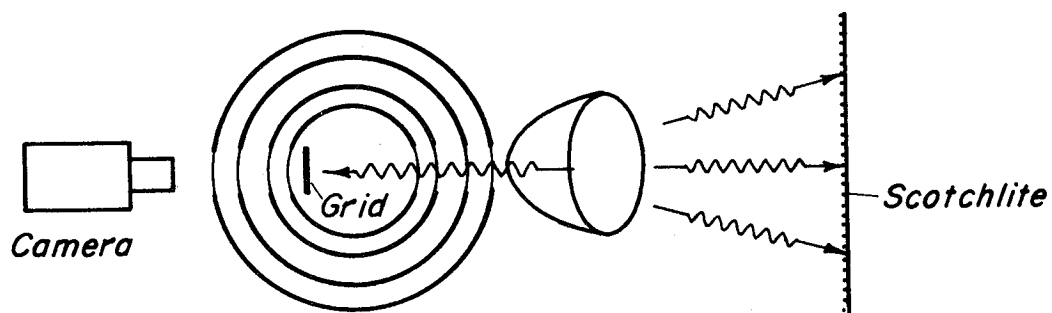
2. Photoinstrumentation

Considerable effort was devoted to photoinstrumentation and lighting in the present reporting period. Any form of direct lighting with the 1 KW quartz-iodide lamp was found to introduce excessive heat and would start melting the solid particles to be photographed. Smaller, less powerful lights would not give the required light for film exposure. After trying several schemes, it was decided that reflected light from Scotchlite (#244-Signal Silver) gave the best lighting and particle contrast.

A sketch of the lighting arrangement used for the particle size and terminal velocity tests is shown in figure 24. A 1 KW quartz-iodide element was mounted inside an explosion proof fixture and positioned near the outer dewar immediately below the elevation of the grid. The light was positioned just under the camera-particle axis and aimed slightly upward at the Scotchlite where it was reflected back through the non-silvered strips of the two dewars and grid to the camera lens. The



SIDE VIEW



TOP VIEW

Figure 24. Photographic Lighting Arrangement.

Scotchlite was positioned about 40 inches from the center of the dewars. As the clear solid particles pass in front of the grid, the irregular shaped crystals scatter the reflected light. The scattering makes the edges of the particles appear black against the white Scotchlite background and provides excellent particle definition as shown in the particle photos of figures 35 through 38.

The camera was positioned to take photographs, through the non-silvered strips of the dewars, of particles falling in front of the grid against the white Scotchlite background. The motion picture camera is a 16 mm Photo-Sonics, model 1B. It has a rotating prism and variable shutter opening which gives a high speed capability of 1000 frames/second and a minimum exposure time of 25 microseconds. The lens is a 50 mm., f-2.0 Navitar with a standard magnification of 0.08X. Accessories include a boresight for focusing and aiming the camera, and a timing light for accurately recording the true speed of the film.

The magnification of 0.08X is not adequate for detailed analysis of particles. The particle film image was increased by increasing the lens to image distance. This was accomplished by placing a lens spacer between the lens system and the camera. A lens spacer of 2.15 cm was inserted for all the particle size and aging studies. The modification increased the magnification to 0.05X but decreased the depth of field from 7.4 cm to 3.3 mm for a lens opening of f-11. The increased magnification was greatly needed and the limited depth of field proved to be no problem.

For the terminal velocity studies, it was necessary to increase the object distance in order to focus near the center of the inner dewar. This was accomplished with a lens spacer of 1.1 cm, giving a magnification of 0.3X and a depth of field of 10 mm at f-11.

Several pictures were taken of solid agglomerates resting on a lucite pillar using a variable 7-30X Bausch and Lomb microscope and a 35 mm stereo camera designed to take photographs through a microscope. The lighting arrangement was the same as shown in figure 24.

3. Heat Leak

In order to age or store solid hydrogen at the triple point without upgrading, a container of very low heat leak is necessary. Since the heat leak to the existing nitrogen shielded apparatus was excessive, additional measures were required. Strip silvered dewars were purchased to replace the non-silvered dewars used in preliminary experiments. Additional tests indicated that excessive radiation was being emitted by the copper apparatus and pretreatment chamber just above the dewars. These radiation sources were minimized by installing two radiation shields of low emissivity at the bottom of the pretreatment chamber. Two thin copper discs were nickel plated and thermally connected to the bottom of the pretreatment chamber as shown in figure 25. A standpipe was installed inside the pretreatment chamber as shown in figure 29. The arrangement made it possible to flow liquid hydrogen into the pretreatment chamber and maintain the level of the liquid at any point below the holes in the top of the standpipe, without allowing flow of liquid hydrogen into the liquid-solid mixture in the glass dewar. By periodically transferring hydrogen into the bottom of the pretreatment chamber, it was possible to maintain the temperature of the shields near 14°K . The use of the shields, and the strip silvered dewars, decreased the heat leak to a value of about 0.05 watts. With the heat leak minimized, and the continued refrigeration being supplied by liquid hydrogen evaporating at the surface, it became feasible to conduct a solid hydrogen aging run which could last 40 to 100 hours.

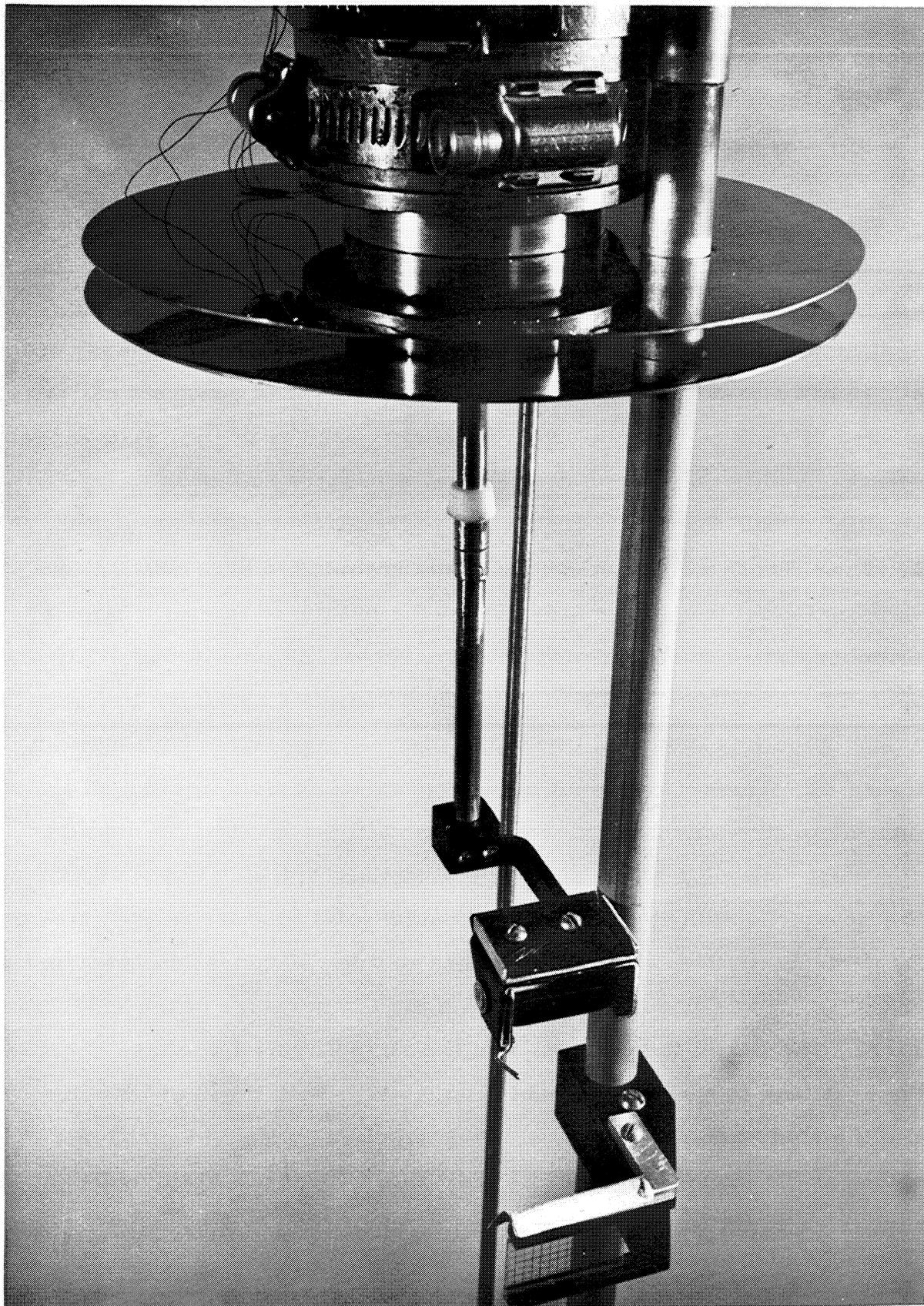


Figure 25. Modifications of Experimental Space

4. Particle Size and Aging Study

The particle size distribution of the liquid-solid mixture is required to determine transfer characteristics. Classical methods of predicting transfer characteristics in liquid-solid mixtures require particle size and distribution as a known variable. To correlate particle size data with particles of classical liquid-solid mixtures, a particle was considered to be any formation of attached crystals that may be distinguished from any other such formations. In some instances a particle was made up of one crystal, in others a group of attached crystals.

Aging studies were made to determine the effect of time and storage on the solid particles. Parameters such as shape, size, structure and density of the individual particles were investigated. Any tendency toward an interaction among the individual particles, such as melting or freezing together to form large agglomerates or one large solid mass, was also considered.

4.1 Experimental Apparatus and Modifications

To observe individual particles, they must be separated from the mass of settled solid. The apparatus was modified to provide an elevator to lift solid particles from the settled solid into the clear liquid. The elevator tilted automatically, allowing the particles to fall immediately in front of a transport grid. Figure 26 shows the elevator and the grid. The elevator is supported by a rod with an 18 inch rack soldered to the upper end. The rod and rack extend through the pretreatment chamber where the rack engages a pinion gear. The pinion gear shaft extends outside the test apparatus. The shaft is manually operated to give 18 inches of elevator capability. The rod used to support the elevator replaced the rod previously used for the needle in the spray nozzle. A teflon stopper was secured to the rod in a position so that it can be drawn against the hole in the bottom of the pretreatment chamber to contain the liquid.

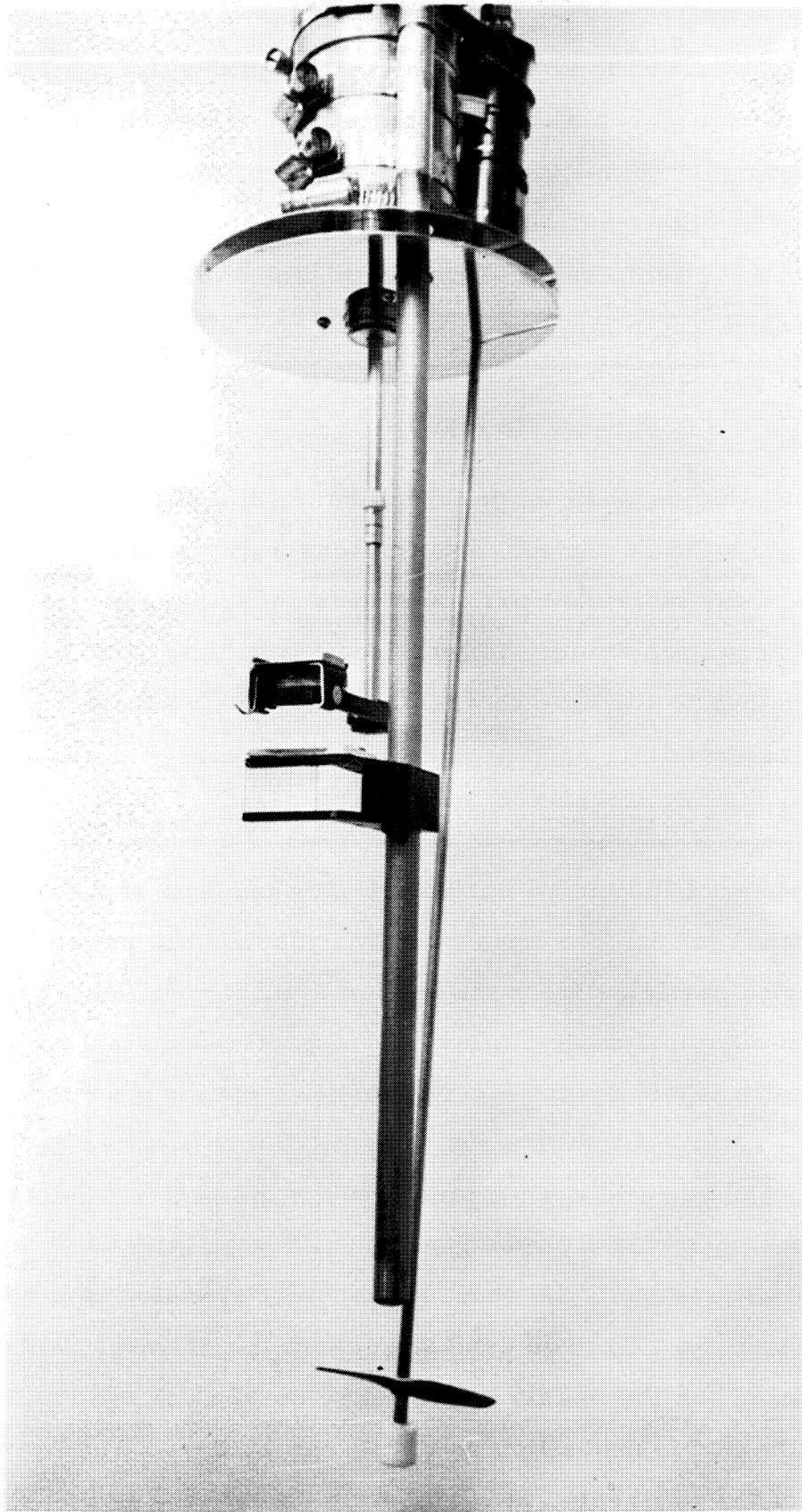


Figure 26. Modifications of Experimental Space

The grid is made by the standard glass lantern slide photographic technique. The spacing is 2 millimeters. The glass is mounted in an aluminum support using teflon tape edging. A thin walled stainless steel tube mounted to the lower end of the pretreatment chamber supports the grid mount and also serves as a warm-up gas tube. Figure 27 is a close up of the grid and mount. The entire assembly inside the silvered dewar is shown in figure 28.

4.2 Experimental Procedure

The tests were started by filling the glass dewar with liquid hydrogen and reducing the pressure to the triple point. Solid was then formed at the liquid surface in cycles by raising and lowering the pressure across the triple point. During the formation of the solid, the stirring motor operated continuously. The stirring broke up the layers of solid as they settled into the liquid. The process was continued until the dewar was filled with the liquid-solid mixture. After a period of time, the level of the solid settled below the grid. At this time, the elevator was used to lift solid above the grid and release it across the grid face. A 16 mm motion picture camera (Photo-Sonics model 1B) was used to photograph particles crossing between the grid and dewar wall. An exposure time of 1/800 second was required to assure photographs of well defined particle boundaries. The lighting and photographic arrangements were discussed in section 2. Scenes of 15 to 20 seconds were photographed at frequent intervals. Each scene taken during the test was identified by an initial shot of a sequence number. All data pertinent to the scene were recorded and referenced to the sequence number.

During the aging runs, the pretreatment chamber was kept partially filled with liquid hydrogen to keep the heat shield described in section 3. as near the triple point temperature as possible. The pressure on the

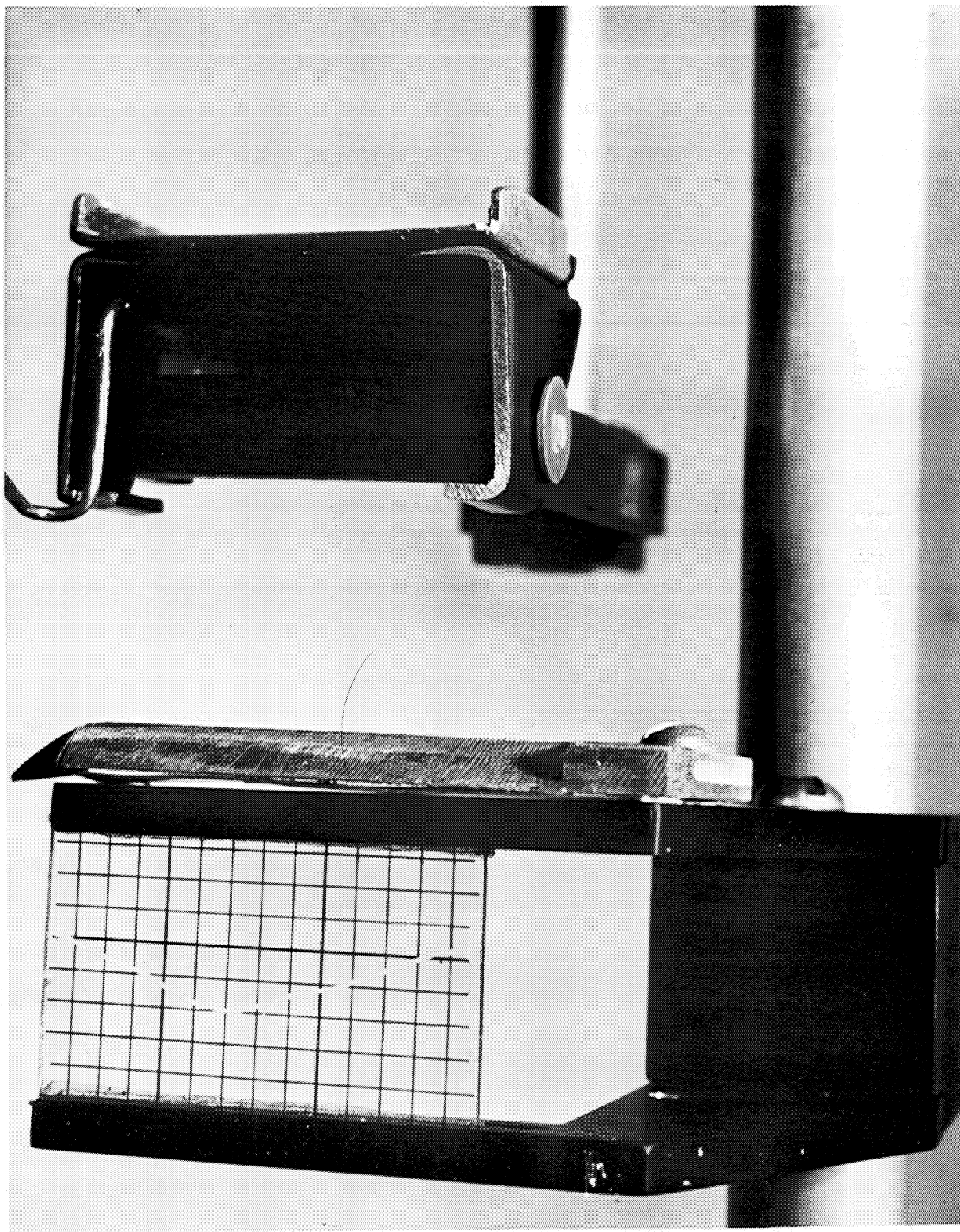


Figure 27. Elevator and Grid Arrangement

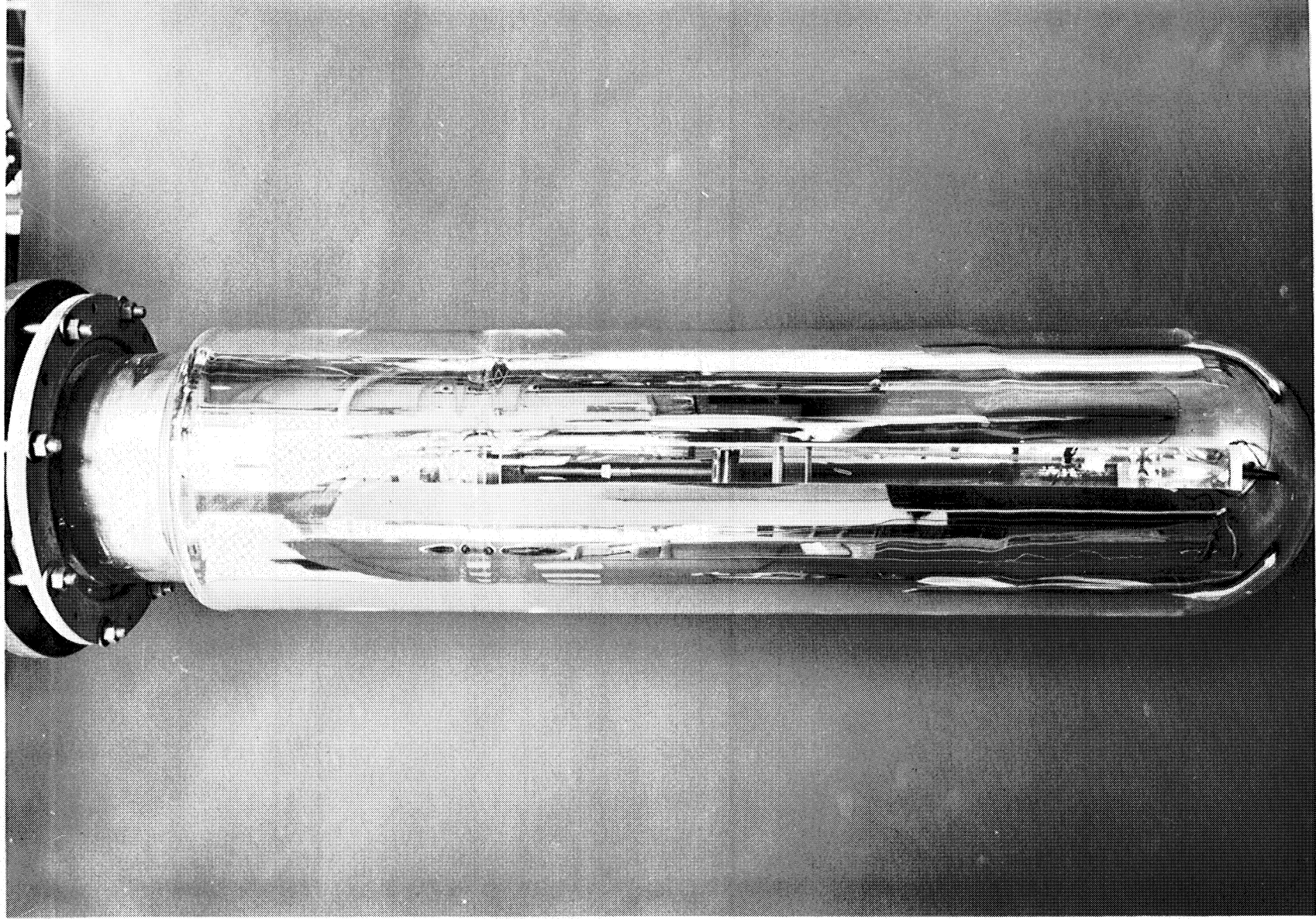


Figure 28. Experimental Dewar Assembly

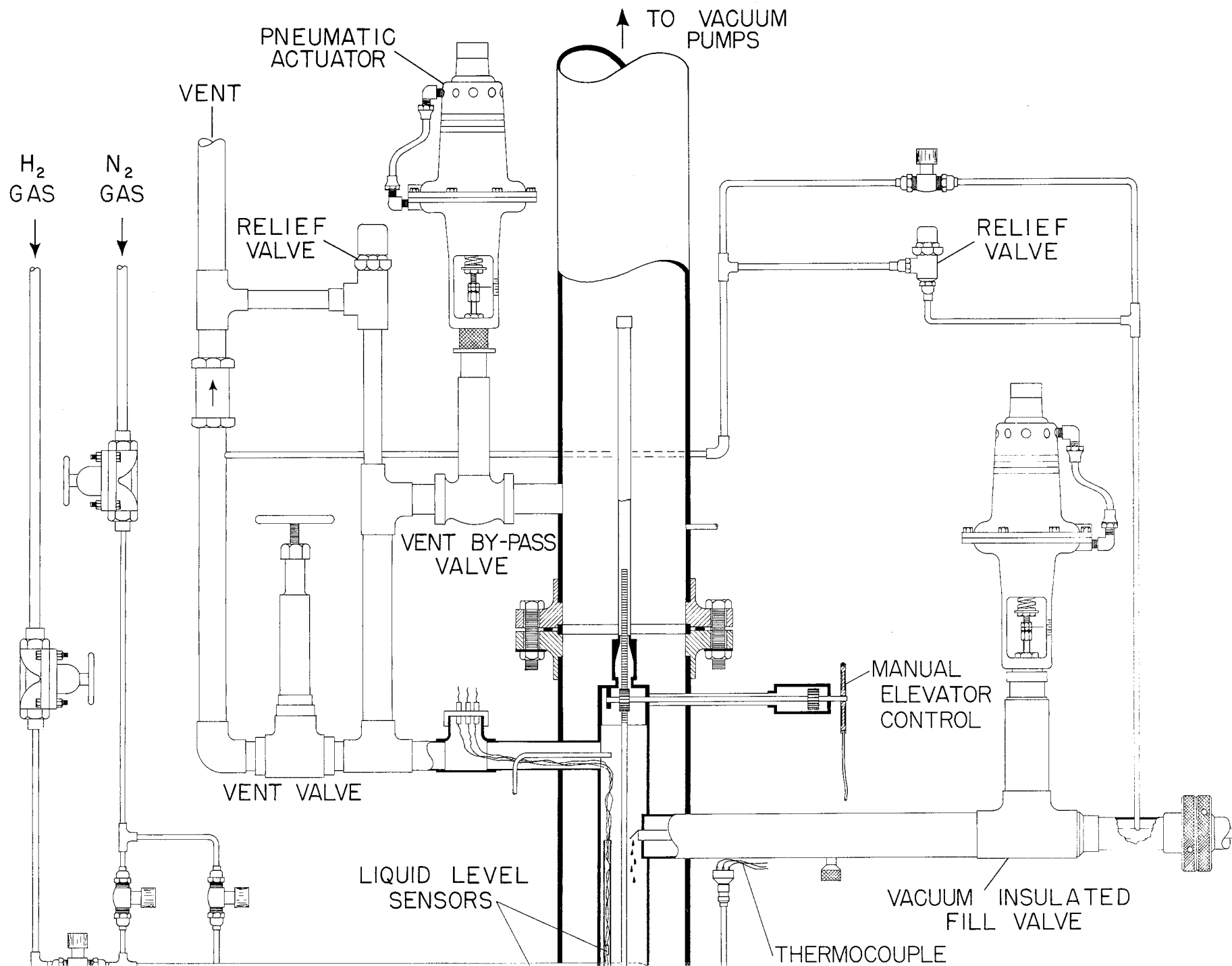
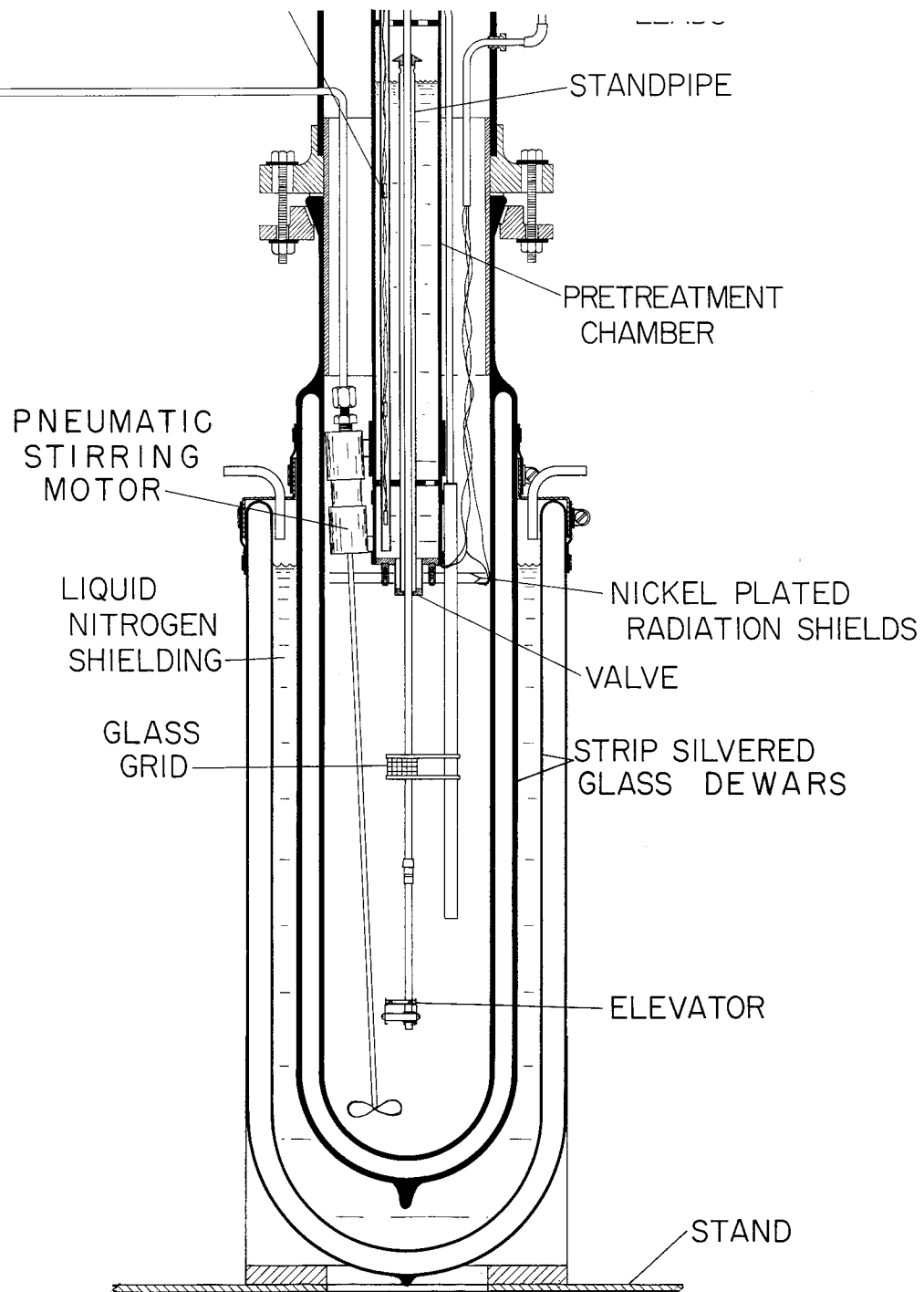


Figure 29. Cross Section - E
Apparatus

rimenta



liquid in the pretreatment chamber was maintained slightly above triple point pressure. Liquid in the pretreatment chamber was replenished at 15 minutes intervals.

The liquid nitrogen shielding dewar was kept full; a seal between the shielding dewar and the test dewar, shown in figure 29, allows slight pressurization of the liquid nitrogen while photographing the particles. Pressurization momentarily suppressed boiling and eliminated bubbles.

The pressure in the hydrogen dewar was maintained at approximately 60 torr. Heat leak down the dewar wall was absorbed by the liquid near the surface. This was replaced periodically to maintain the liquid level well above the grid to assure liquid temperatures at the grid level to be near the triple point.

Four aging tests were conducted during the present reporting period. The test durations were 2.5, 4, 10.5, and 42 hours. During these tests, 2200 ft. of 16 mm motion picture film were taken and 4565 liters of liquid hydrogen and 9330 liters of liquid nitrogen were used.

4.3 Data Processing

Figure 30 is a flow diagram for the processing of data. Reduction of the data on the 16 mm film was accomplished in three separate systems.

4.3.1 Benson-Lehner Film Reader

The film was read on the Benson-Lehner film reader (Boscar). The system is made up of a film viewer which magnifies the film approximately eight times, an IBM card punch, and a typewriter. Figure 31 shows the viewer in operation. The viewer contains a moveable X, Y cross hair and a system for recording the position of the cross hair in arbitrary units on the card punch and typewriter. The viewer head is also moveable allowing any orientation of the film frame relative to the X, Y cross hair. The particles were measured by positioning the

DATA PROCESSING

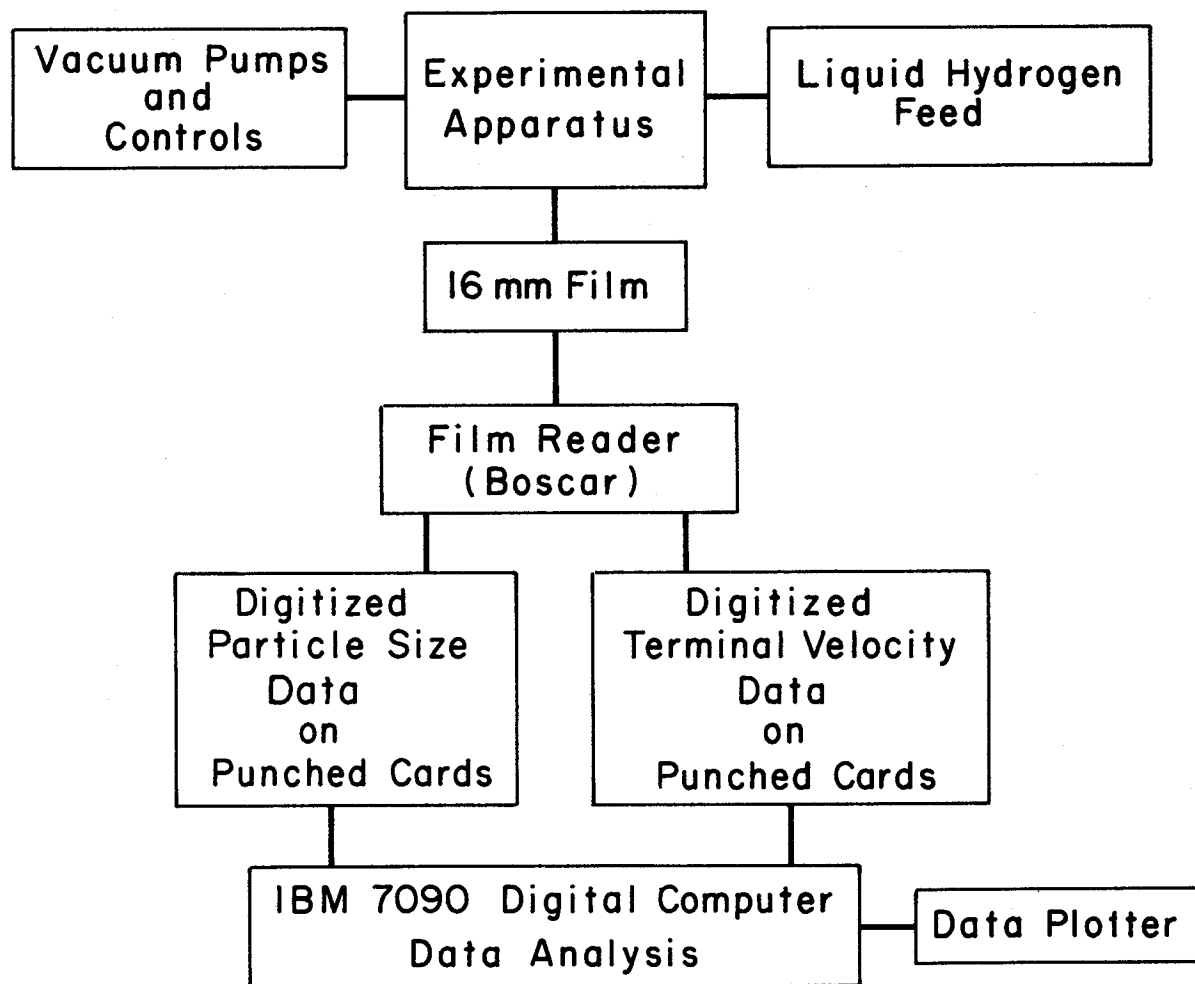


Figure 30. Data Processing

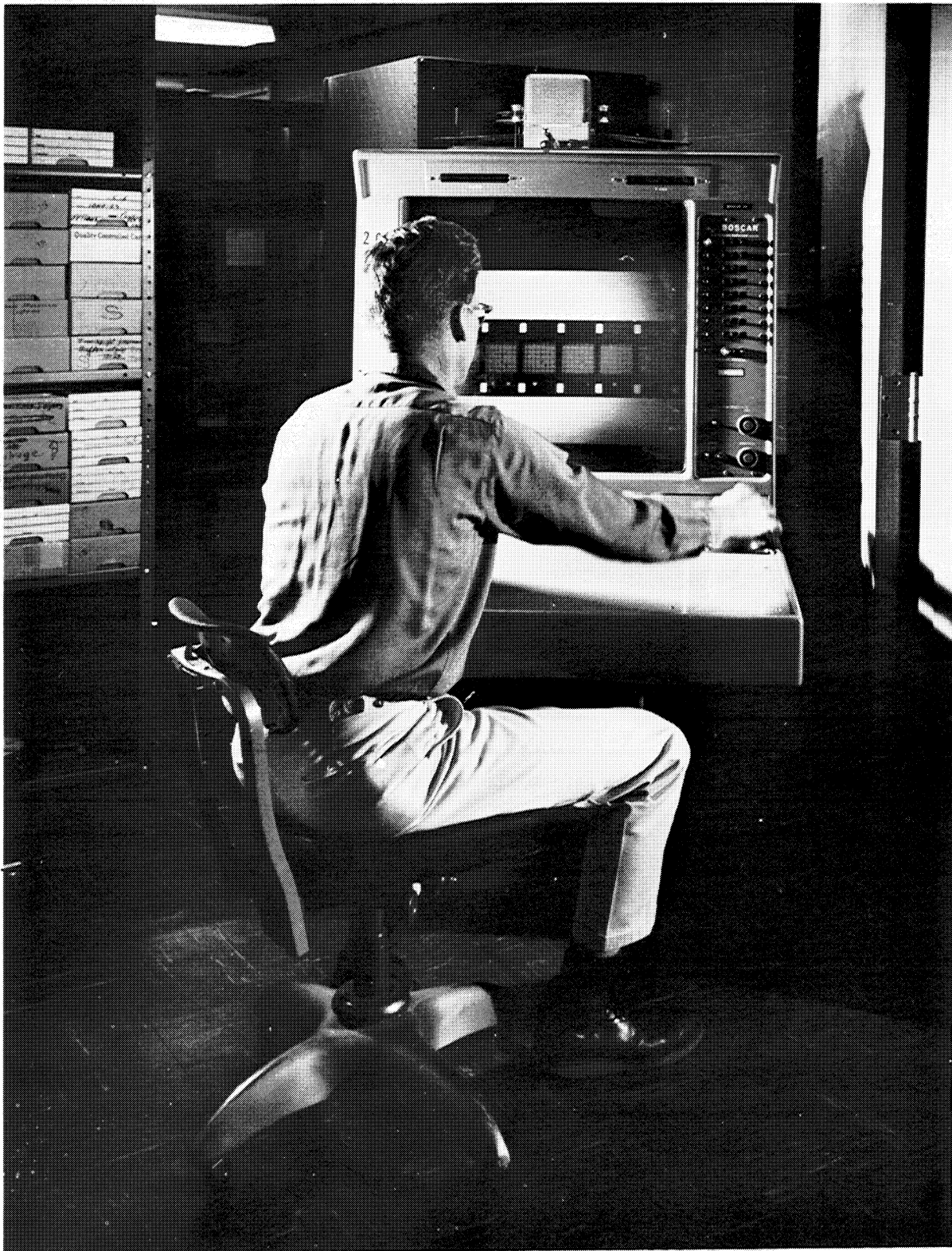


Figure 31. Benson-Lehner Boscar Film Reader

apparent length of the particle parallel to either cross hair. The X, Y cross hairs were then placed on the far left and upper most boundary of the particle. These X, Y values were recorded as X_1 Y_1 . The cross hairs were then moved to the far right and lower boundary of the particle. These were recorded as X_2 Y_2 . Figure 32 illustrates the measurement of a particle. Each IBM card contained both X, Y values for four particles. Each frame was considered to be a new event and all particles in focus were measured. Particles were measured in 22 separate film sequences. The 22 sequences cover solid aged from 17 minutes to 41.25 hours. A total of 13,400 particles were measured. The grid which appears in each frame was measured to obtain a scale factor from Boscar units to millimeters.

4.3.2 IBM 7090 Computer

The cards punched by the Boscar were used as input data for a program on the IBM 7090 data processing computer shown in figure 33. The program determines the particle length and width from the X, Y values and the scale factor. The difference between X_1 and X_2 , and Y_1 and Y_2 are found. The largest is designated as the length and the smallest the width. All particles measured in one film sequence are scanned for the largest and smallest particle. This span is divided into forty equal increments. The percent of particles in each of these increments is determined and the accumulative percent versus particle size from smallest to largest particle is printed out. The program also makes a tape of the output.

4.3.3 Plotter

The tape produced by the IBM 7090 program is used on the plotter which is programmed to plot final curves of percent of particles versus particle size. The plotter is shown in figure 34.

MEASUREMENT of PARTICLE DIMENSIONS

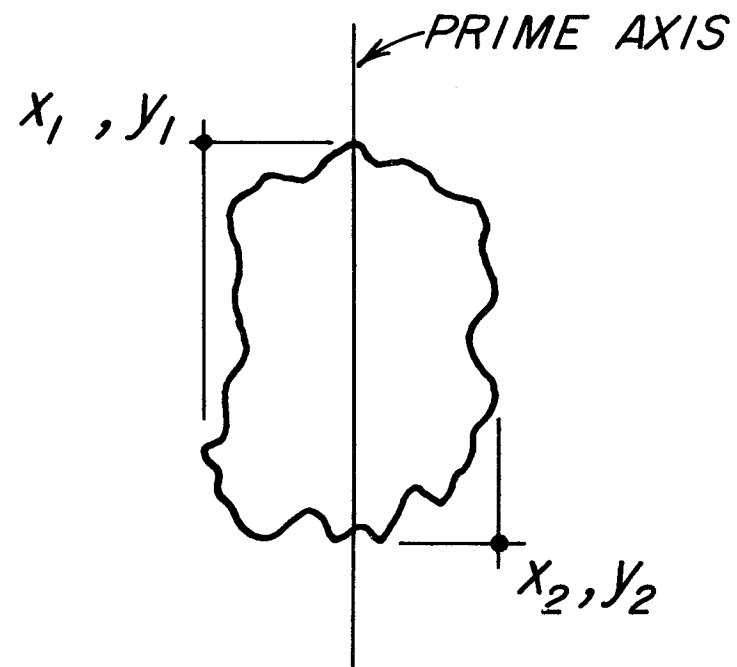


Figure 32. Measurement of Particle Dimensions



Figure 33. IBM 7090 Digital Computer

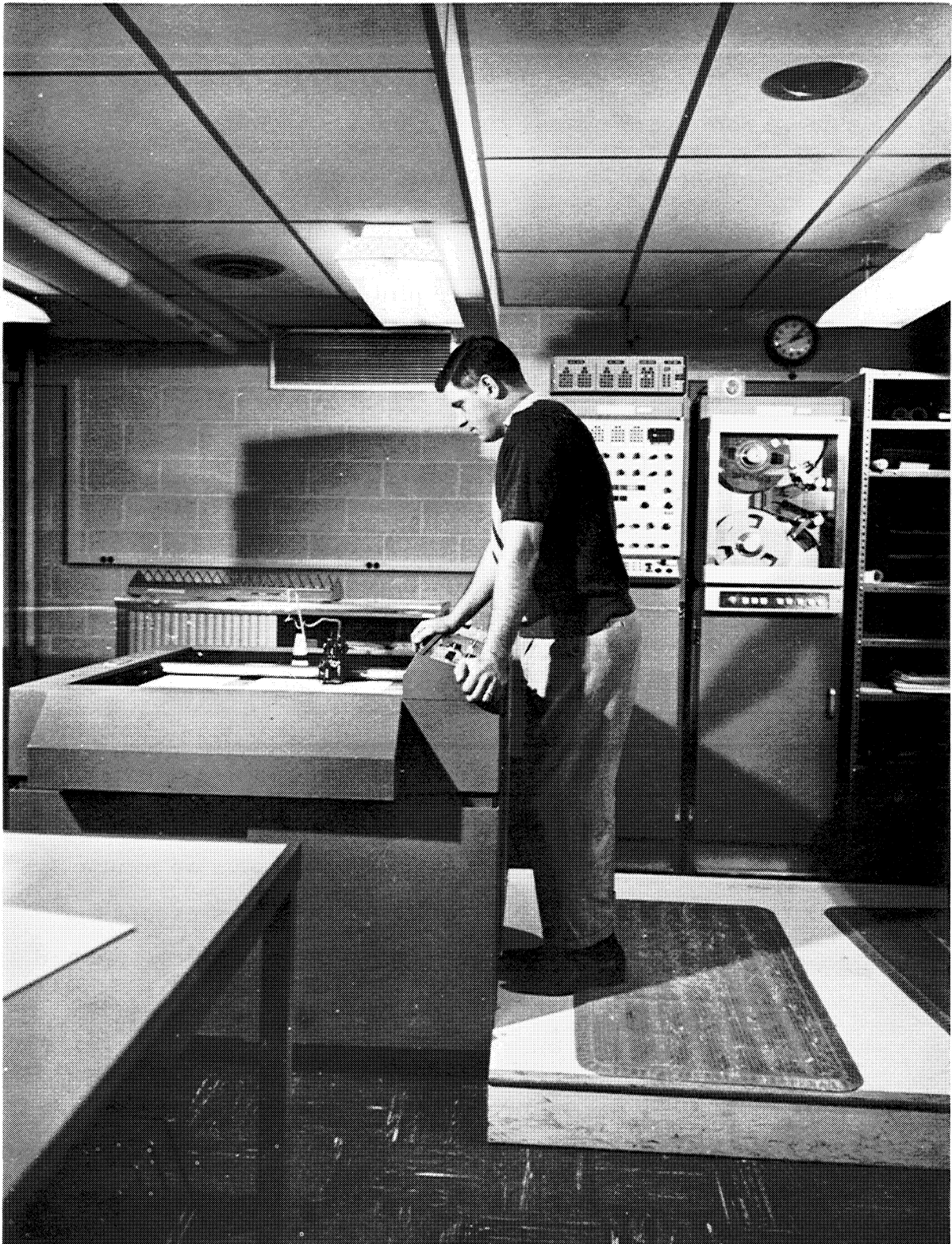


Figure 34. Data Plotter

4.4 Accuracy

Accuracy of measurement of particle sizes was influenced by many variables. Some of the most significant are as follows:

1. distortion of the grid and particle through the four dewar walls, the liquid nitrogen shield, and the liquid hydrogen,
2. the contraction of the grid at liquid hydrogen temperature,
3. the effect of the depth of field of the camera lens system,
4. the distortion of the projected picture by optics in the Boscar,
5. the accuracy of positioning of the cross hairs of the Boscar, and
6. the repeatability of the Boscar recording system.

Determination of individual effects of each of these variables on the accuracy was not feasible. To obtain a realistic figure for the accumulated error, the following procedure was used. The grid was measured at the normal boiling point of liquid nitrogen, thus eliminating most of the thermal effects. The apparent grid size was then determined at test conditions using the same procedure as that used to measure particles. The two were compared and agreed within plus or minus five percent. This procedure includes all mentioned variables except the effect of the depth of field of the camera lens. This was calculated and it was determined that the effect was less than one half percent when particles in focus were the only ones measured.

Other factors involving accuracy, not previously mentioned, are the ability to position the particle in the Boscar to obtain the maximum dimension for length and the inability to measure the third dimension of the particle. Because these factors could not be evaluated, a large number of particles were measured (an average of 600 per sequence) to provide a statistical profile of particle size.

4.5 Experimental Results

The character of the solid changes considerably with age. Solid hydrogen less than one half hour old has the appearance of an intricate network of very small crystals loosely attached. Figure 35, which is enlarged 12.5 times, illustrates the texture. The grid spacing on the figure is 2 millimeters. As the particle ages, some of the small crystals apparently grow at the expense of others and the particle becomes an agglomerate of spherical shaped crystals. Figure 36 shows solid particles of 5.25 hours old. At approximately five hours, the particles are made up of still larger crystals with some particles being a single crystal. They still have the tendency to be spherical in shape, with 90 percent of the particles having lengths less than three times their width. Figures 37 and 38 are particles 20.25 and 40.25 hours old. The appearance of the particles has not changed noticeably from those five hours old.

5. Terminal Velocity Measurements

Considerable work has been done on the transportation of solids through pipelines and various analytical expressions are available for slurry flow. Solids such as coal, sand, ore, pulpwood, and sewage using water as the liquid medium have been studied. With this existing knowledge of slurry flow, plus the flow parameters and characteristics obtained from the present work on liquid-solid hydrogen, it is hoped that a meaningful analytical expression can be resolved for the flow of the mixture through insulated transfer lines. There are many flow parameters to be considered in such an expression. Particle size, shape, equivalent diameter, density, and terminal velocity are the main particle variables.

The terminal velocity, or the drag coefficient calculated from terminal velocity, is a parameter always present in slurry flow expressions. For irregular particle shapes, this is best obtained by experimental

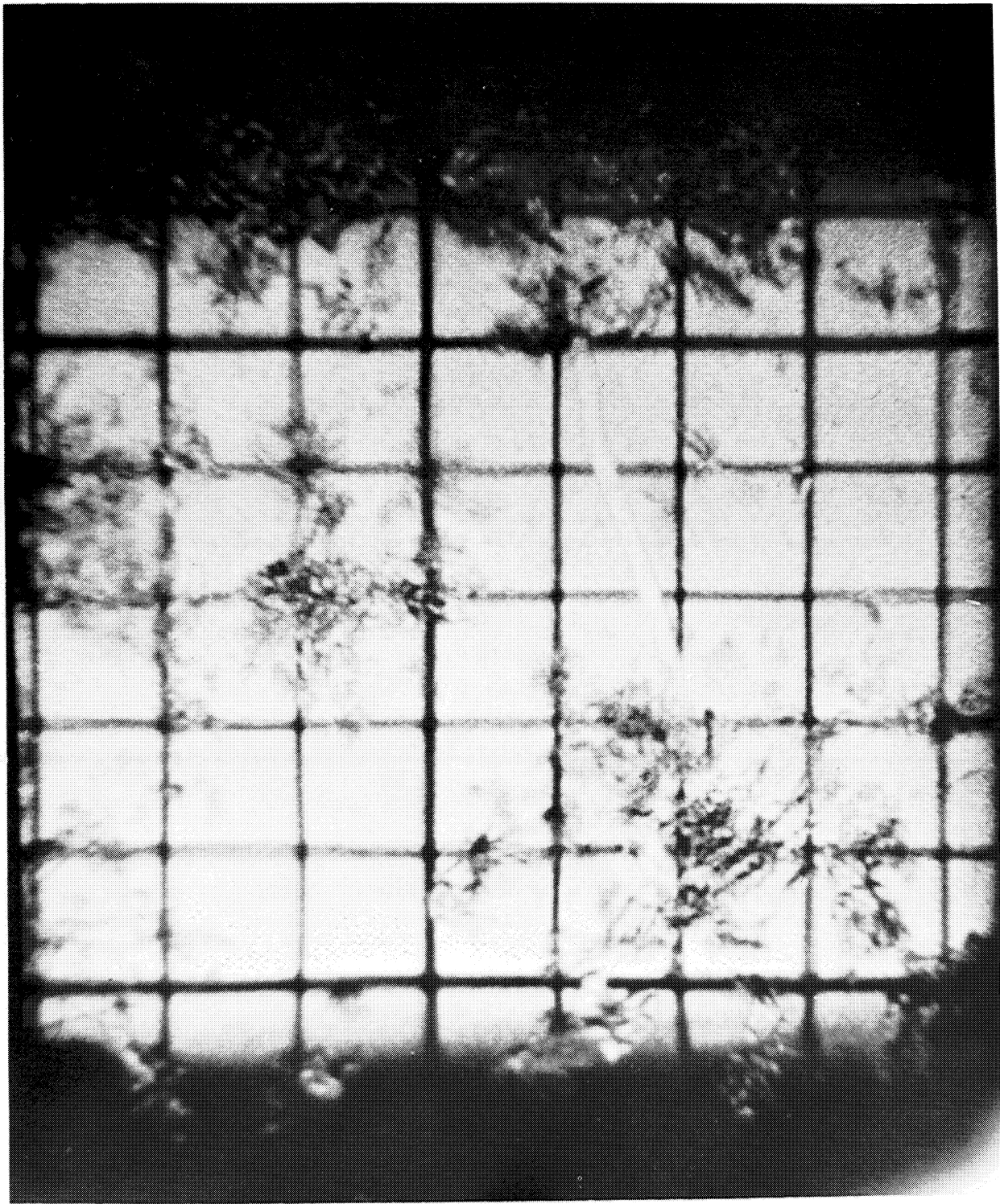


Figure 35. Liquid-Solid Hydrogen Mixtures - Age: 17 min.

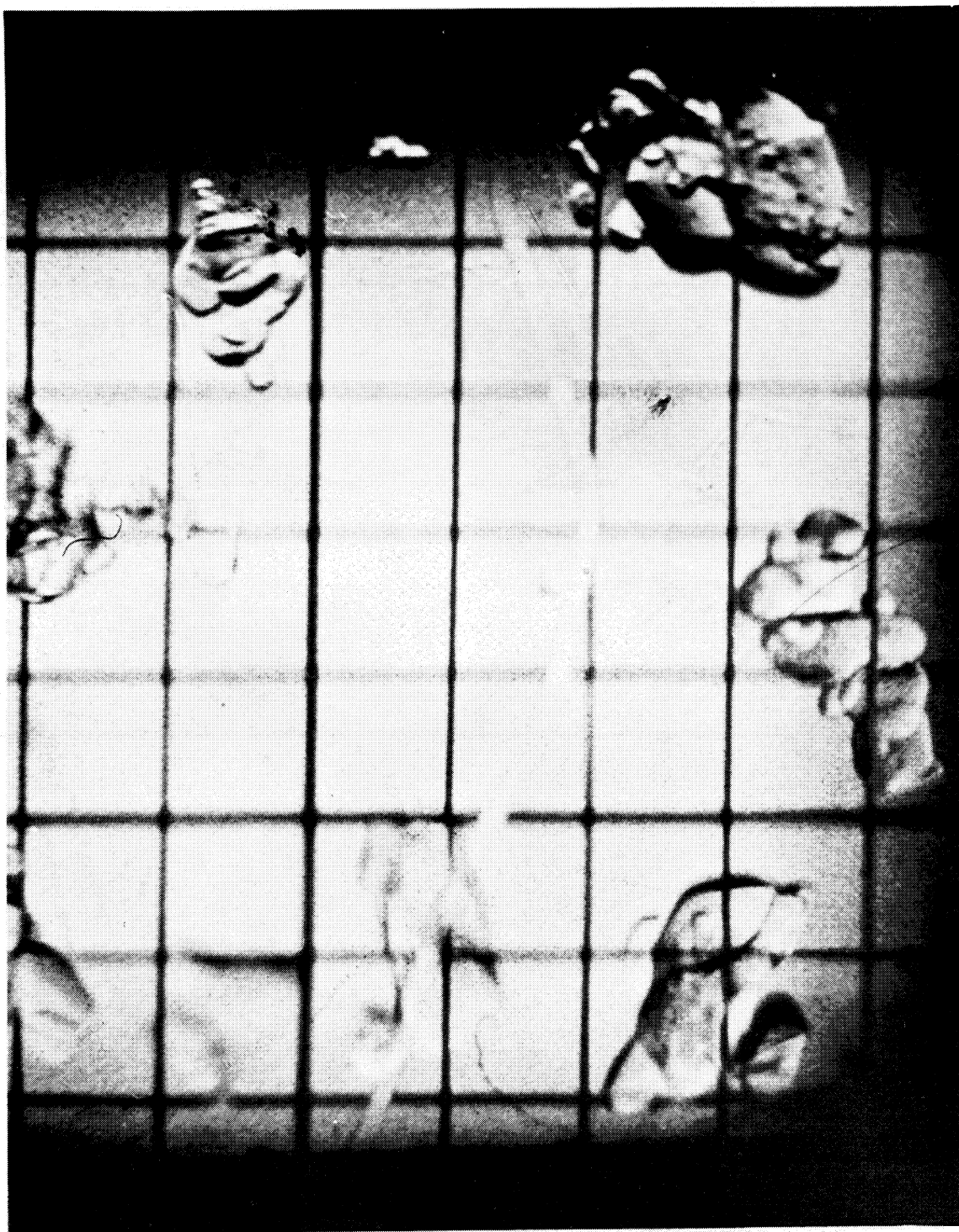


Figure 36. Liquid-Solid Hydrogen Mixtures - Age: 5 hr., 15 min.

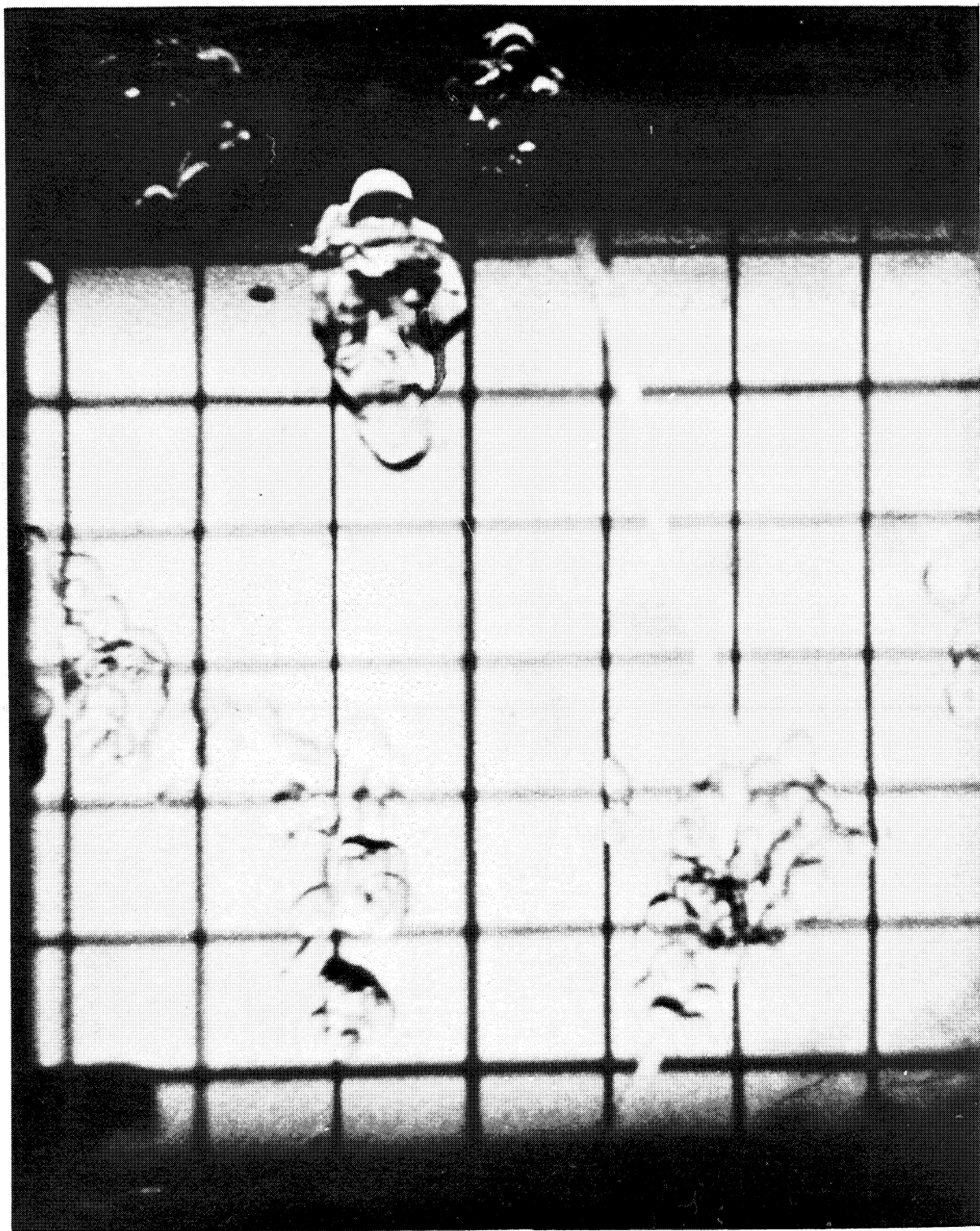


Figure 37. Liquid-Solid Hydrogen Mixtures - Age: 20 hr. , 15 min.



Figure 38. Liquid-Solid Hydrogen Mixtures - Age: 40 hr., 15 min.

methods. Therefore, the terminal velocity of the irregular solid hydrogen particles was measured. Two terminal velocity runs of 1.5 and 4.5 hours duration were made.

5.1 Experimental Apparatus

The apparatus used for measuring terminal velocity was the same as that previously explained for the particle size and aging studies except for one modification. The glass grid and elevator were moved away from the dewar wall almost to the center of the dewar to assure no interference to the free fall of the particles.

5.2 Experimental Procedure

The experimental procedure for the terminal velocity studies was the same as previously explained for particle size and aging studies, except for photographing the particle. The grid was photographed first for a scale reference measurement and then the camera was repositioned below the grid. The solid particles were released just above the grid as before, but in order to eliminate the turbulence caused by dumping and to be certain that the particles had reached terminal velocity, they were allowed to fall approximately four inches before they were photographed.

The camera was modified for the terminal velocity work. It was necessary to focus near the center of the dewar which required a longer object distance. A thinner lens spacer was used to accomplish this. An explanation of the spacer and its effects are given in the photoinstrumentation section.

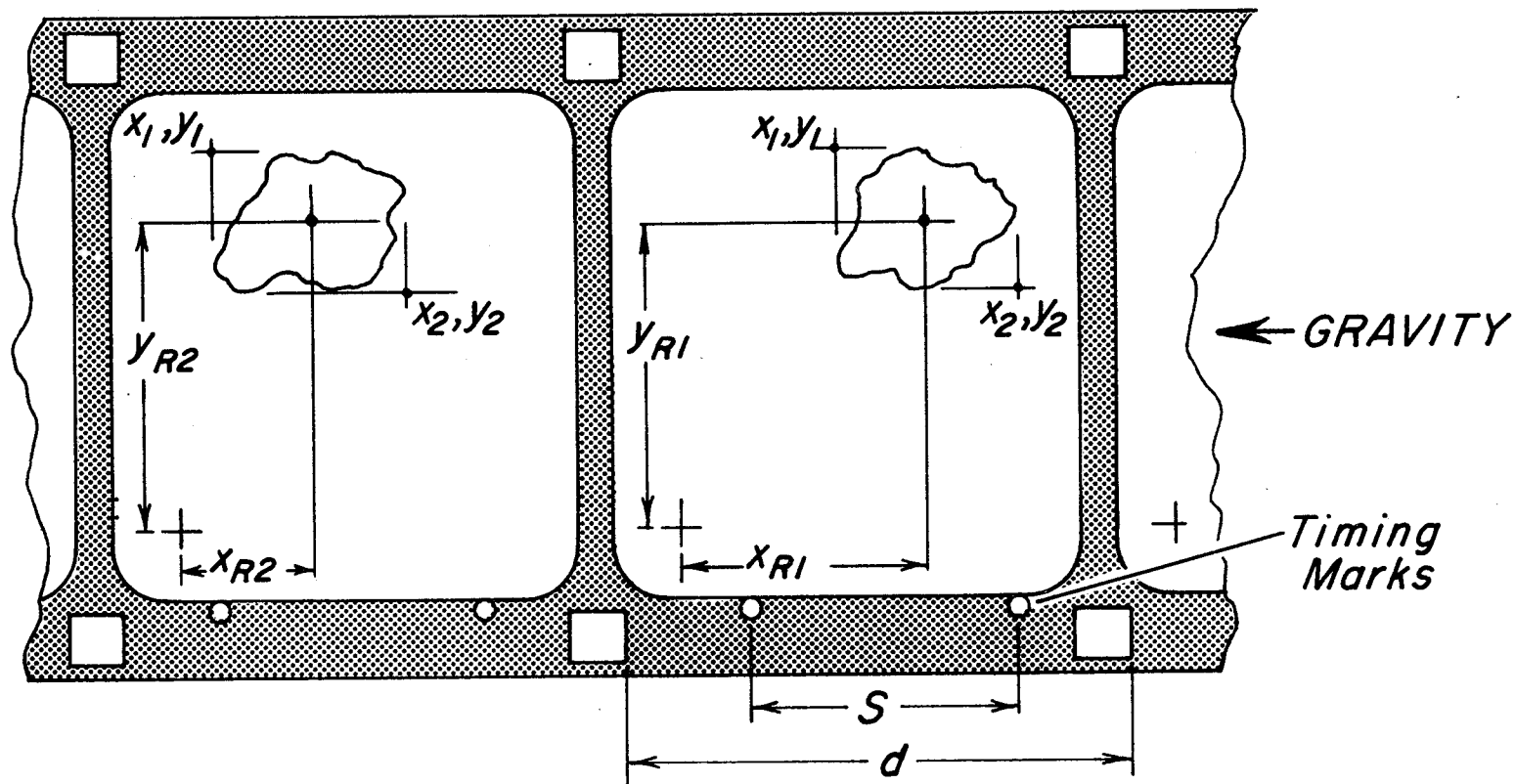
Eight hundred feet of 16 mm film was exposed during the two terminal velocity tests. Data film was taken at periodic intervals covering solids of age ten minutes to 4.5 hours.

5.3 Data Processing

The 16 mm data film was analyzed on a Benson-Lehner (Boscar) film reader, previously described. The particle terminal velocity was measured as shown in figure 39. A scale factor to determine actual particle size and distance is calculated from an initial view of a grid of known size as before. The edge of the 16 mm film is maintained parallel to the X axis of the film reader during the entire measurement sequence. The measurement sequence is as follows. A reference point to determine particle movement is taken on each frame. The corner of the sprocket hole was used for a reference point. The particle size is measured by taking two X-Y points as described previously. The film speed is determined by measuring the distance (s) between two precision timing light exposures made on the film while photographing the particle and the known distance (d) between the sprocket holes. The above sequence is repeated for a given number of frames or until the particle passes the field of view or goes out of focus. Certain discretion must be exercised in selecting a particle to be measured. The measured particle should fall straight downward, not be too close to another particle, and be in focus for at least 10-15 frames. Each particle measured in the above manner was given a number.

IBM data cards with the above information were next programmed into the IBM 7090 computer. The program calculates the center of the rectangle enclosing the particle as shown in figure 39 and also calculates the distance from the particle center to the reference point. The velocity of the particle is calculated from the known time interval and the known distance (d) between the sprocket holes. The quantity V_T must equal V_X , the velocity in the X direction, to indicate the true terminal velocity. The computer then calculates and prints out the average particle size, the average particle velocity and the average frame rate.

TERMINAL VELOCITY DETERMINATION



$$V_t = \sqrt{(x_{R2} - x_{R1})^2 + (y_{R2} - y_{R1})^2} \left(\frac{S}{d} \right)$$

V_t must be equal to V_x to indicate True Terminal Velocity.

Figure 39. Terminal Velocity Determination

5.4 Accuracy

In order to determine the error involved in measuring particle velocity by the above method, a simple test was performed on the film reader. A fixed point on the grid was measured, instead of the usual particle, for a series of 12 frames. The measured distance should have been constant indicating a zero velocity. The average X measurement from the reference point was 10.2 mm. The smallest measurement was 9.87 mm and the largest was 10.45 mm. The deviation from the average of 10.2 mm was $\pm 3\%$. This simple test gives a reasonable indication of the total accumulated errors involved in measuring the terminal velocity of a particle by the above method. It is felt that the average particle velocity calculated with the average frame rate should lie within $\pm 5\%$ of true value.

5.5 Experimental Results

Data on 77 particles were processed and evaluated at the end of the present reporting period. Particle sizes ranged from 0.7 to 7.6 mm. The individual particles were followed through an average of 15 frames on 16 mm film. The film sequences covered liquid-solid mixtures of ages 50 minutes, 68 minutes, 3.5 hours, and 4.5 hours.

The terminal velocities of the first 32 particles of age 50 minutes varied considerably. The velocity of each particle was consistent but there was considerable scatter in comparing the velocities of all 32 particles. The terminal velocity data on the older particles of age 68 minutes through 4.5 hours were much more consistent. This is understandable when comparing the fresh particles to the older particles as shown in figures 35 and 38. The fresh particles have a different texture and the shapes are more irregular, while the older particles have a more consistent texture, less irregular shape, and appear to be more dense.

A typical data plot is shown in the Appendix. The straight line indicates that the particle has indeed reached terminal velocity and the deviations from a straight line are negligible. Other plots of terminal velocity versus the dimension of the particle normal to the velocity are shown. There are four plots; one each for particles of ages 68 minutes, 3.5 hours, 4.5 hours, and one composite graph containing all these points on one plot. From these plots, several preliminary observations can be made. There is a trend toward increasing velocity for the larger particles. The terminal velocity for most of the particles lies within the range of 20-50 mm/sec. This is reasonable agreement considering the irregular shape of the particles. It is hoped that additional consistent terminal velocity data can be obtained for particles older than five hours.

6. Solid Particle Microphotography

The solid hydrogen particle shown in figure 40 was photographed using a Bausch and Lomb Stereo-Zoom microscope with a GraFlex Stereo 35 mm camera. The particle magnification is 26X. The small crystals that make up the particle agglomerate can be clearly seen. The particle has been aged about 3.5 hours and the growth of the crystal-like centers is believed to be of interest in the general problems of production, storage, and transport of liquid-solid mixtures. For example, as the sub-particles grow, the number of individual crystals apparently decreases, with the final result that the agglomerate increases only slightly, if at all, in size. The density of the agglomerate is increased and the effect of the heavier smoother particle can be found in the higher terminal velocities.

The present restriction to the continuation of this study is the degree of illumination of the particle. Present lighting is a 3200° F source reflected from Scotchlite. The lighting arrangement is required to reduce high heat input to the particle which would cause rapid melting. Proper selection of film and possible use of a strobed light source should allow an

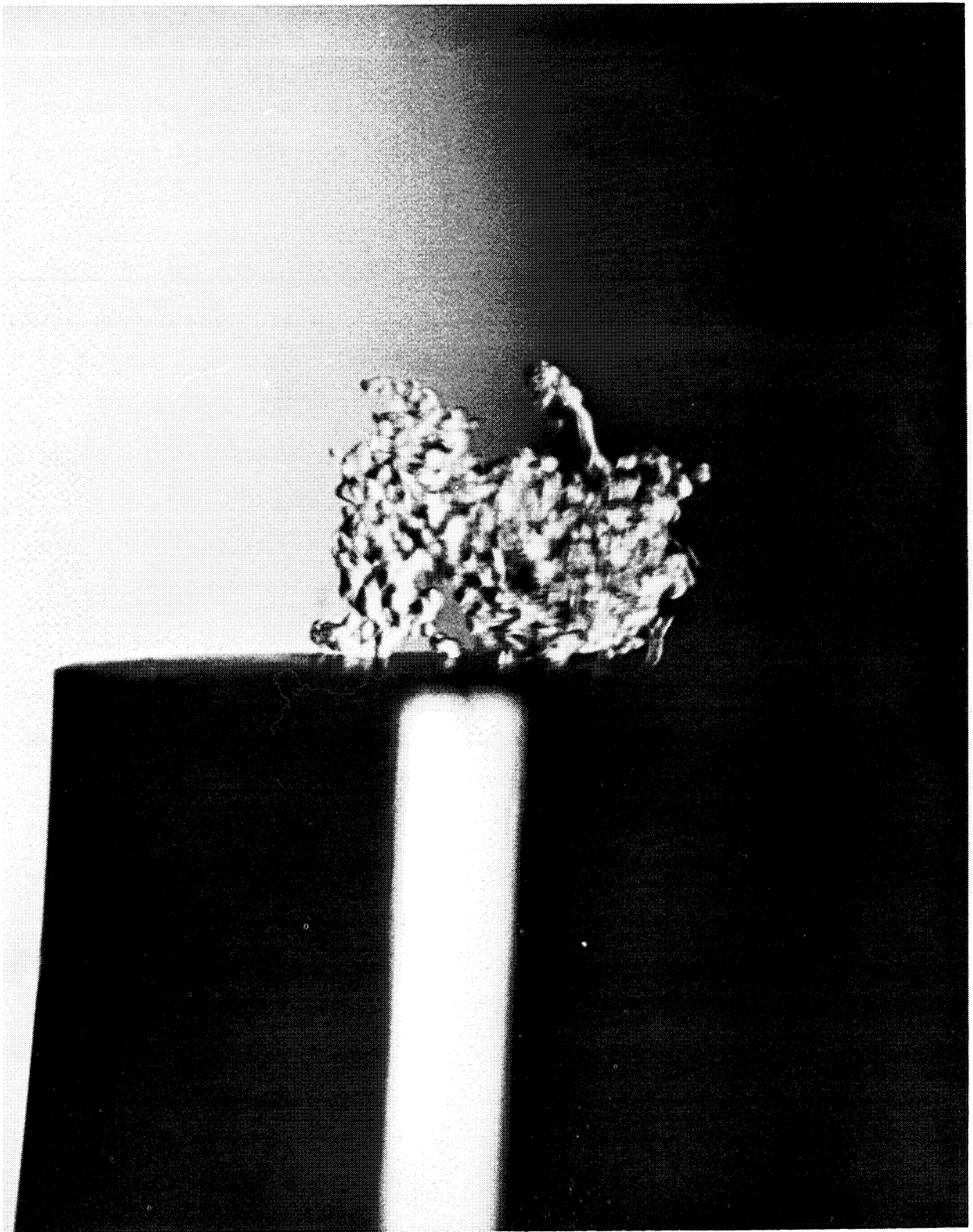


Figure 40. Solid Hydrogen Particle in Liquid at Triple Point
Magnification is 26 X, Age: 3 hr., 30 min.

increase in magnification of about five times using presently available equipment. These small crystal-like centers could then be studied to determine their effect on existing mixtures and the possible production of mixtures where the solid particles are of micron size.

7. The T-S Diagram

A temperature-entropy diagram covering the solid, liquid, and vapor phases from 11°K to 23°K was completed and is presented in figure 41. Information for constructing the diagram was taken from work by Cook et. al. (1964), Mullins et. al. (1961), Roder et. al. (1963) and Woolley et. al. (1932). The enthalpy and entropy base used is the same as that used by Roder. The temperature data used by Mullins were adjusted to the scale. The entropy of the normal boiling point from the Mullins data was 0.33 joules/gm°K higher than the entropy from the Roder data.

The liquid and liquid-vapor region was taken from Roder, the only changes being units conversion. The solid-vapor region was taken from Mullins, with changes in entropy and temperature noted above. The saturated solid line from the triple point to 18.5°K was constructed with data from Cook and Woolley. The dashed portion of the line was extrapolated. Data from Dwyer et. al. (1964) became available after completion of the diagram. These data would shift the saturated solid line 0.25 joules/gm°K lower at 300 atmospheres pressure and 0.05 joules/gm°K higher at 100 atmospheres pressure. The lines of constant specific volume in the liquid region were constructed from cross plots of entropy versus specific volume with lines of constant pressure and temperature. The specific volume along the saturated solid line was calculated using the Clapyron equation, the equation for specific volume of saturated liquid for solidification from Roder, and the heats of fusion. All other parameters were calculated directly from the data given by Mullins and Roder.

8. Conclusions

It is possible, based on the existing provisional correlation of data and other experimental observations, to draw a number of conclusions about liquid-solid mixtures of hydrogen made by the freeze-thaw process.

- 1) The freeze-thaw production method will produce fine particles of solid hydrogen in the liquid of a size ranging from 0.1 mm to 10 mm in size. The greatest number of particles are from 1 to 3 mm in size.
- 2) Large agglomerates (to 8 cm in size) formed during the production process are easily broken up by stirring or agitating the mixture.
- 3) The apparent density of the mass of undisturbed solid particles increases markedly because of progressive settling.
- 4) After 43 hours of relatively undisturbed aging, the mixture could be stirred easily, appearing very fluid. The particles do not tend to cohere to form large masses.
- 5) An observed particle of freshly produced solid is apparently made up of a large number of small nucleation centers. The individual sub-particles increase in size and decrease in number as the liquid-solid mixture ages. The particles do not appear to increase greatly in size but only change in appearance.
- 6) As the particles age, the rough outer surfaces are smoothed and internal voids are filled in to form a solid that is clear and rounded in appearance. The aging process is essentially complete within 4-6 hours after production.

7) The measured terminal velocities of the particles seem to follow the classical pattern of laminar and turbulent settling. The small particles passing slowly through the liquid in the typical laminar mode and the larger heavier particles falling at a faster rate as suggested by turbulent settling.

8) Aging of the particle increases its terminal velocity. The smoothing of the outer surface and the increase in density result in a heavier particle offering less resistance to flow through the fluid.

9) Values of terminal velocities vary from 20 to 40 mm/sec for particles of about 1 mm in size, to 35 to 45 mm/sec for particles of 4 - 5 mm in size.

These statements can be supported by photographic record and data plots included in the appendix.

9. Future Work

The program will proceed, as planned, to predict transport properties of liquid-solid mixtures based on the accumulated data of particle size and terminal velocity. The model to be used is that previously developed for non-cryogenic slurry flow. Experimental verification and possible modification of the model will be accomplished by the construction of a flow apparatus. This equipment will allow visual and photographic observations of steady state pipe flow, entrance and exit phenomena, and transport characteristics which may appear at elbows, valves, or other flow restrictions. In addition, instrumentation will be used to determine pressure drops and other pertinent flow parameters.

Further study of the individual particles may be made using the techniques of microphotography. This may lead to methods of production

giving much smaller particles with better flow characteristics and higher storage densities.

10. Appendix - Provisional Data

Provisional data from the particle size and aging study are presented in figures 42 through 53. The data in figures 42 through 50 show the percent of particles versus the length and width of the particle in millimeters. The data in figures 51 and 52 show length and width respectively of three ages of solid. From these two graphs it can be seen that, in general, the particle size and distribution changes very little after five hours aging. Figure 53 indicates the percent of particles smaller than 2 and 3 millimeters length. It can be seen that solid less than five hours old has a higher percentage of small particles. After five hours, 60 to 70 percent of the particles are 0.2 to 3 millimeters in length.

Following the data from the particle size and aging study are five figures of preliminary data from the terminal velocity investigation. Figure 54 is a typical data plot of particle movements. The relative movement of the particle in the X direction with respect to a known reference point of each frame can be seen. The line is nearly straight indicating the particle has reached a constant terminal velocity. Figures 55, 56 and 57 indicate the terminal velocities of solid particles of ages 68 minutes, 3.5 hours, and 4.5 hours, respectively, as a function of the dimension of the particle perpendicular to movement (Y_d). Figure 58 is a composite of the previous three graphs.

These preliminary data indicate that the terminal velocities of most of the particles lie in the range from 20 to 50 mm/sec. There also appears to be a slight trend toward higher velocity for the larger particles. Similar data for solid older than 4.5 hours have not been taken.

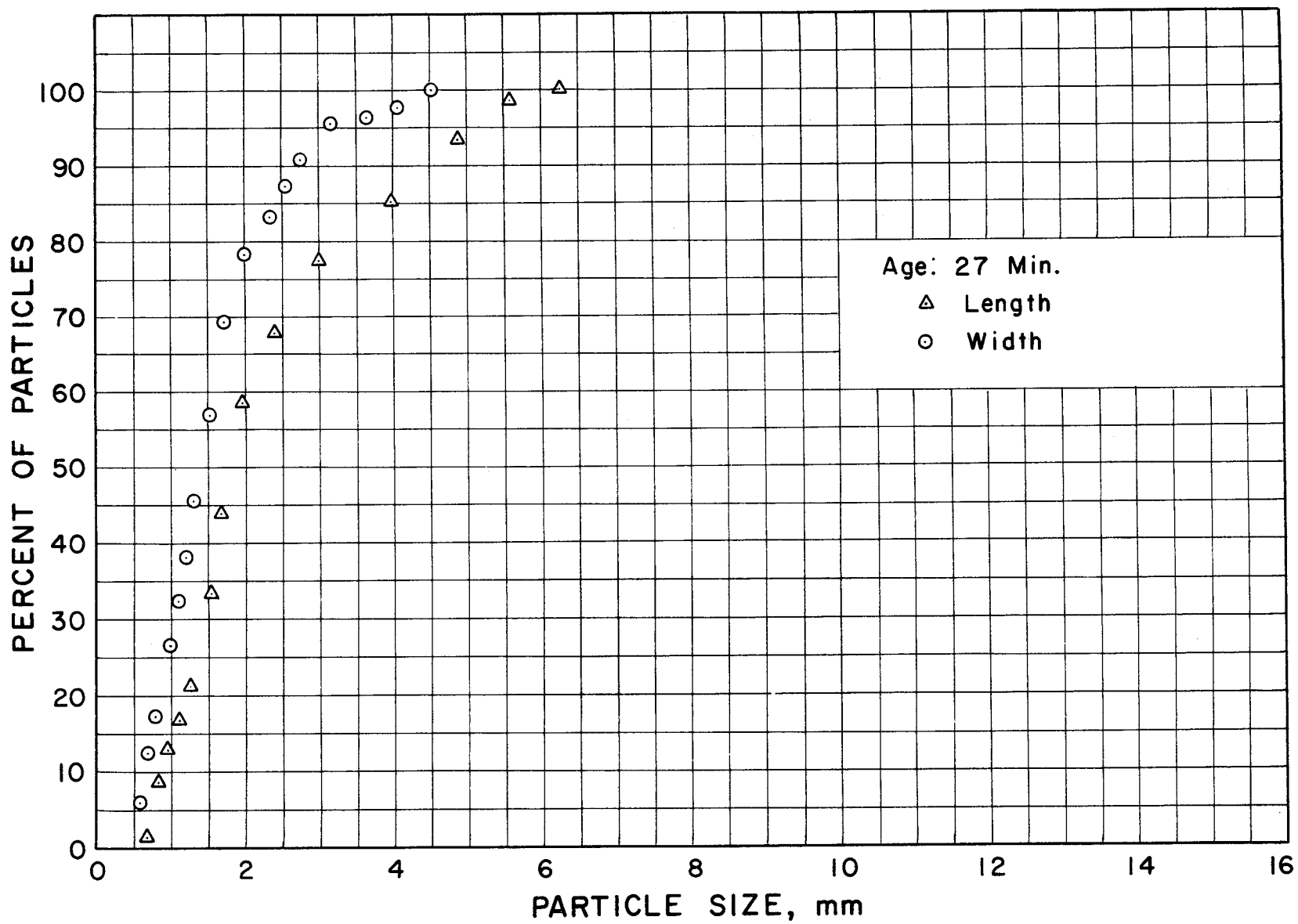


Figure 42. Particle Size, Age 27 Minutes.

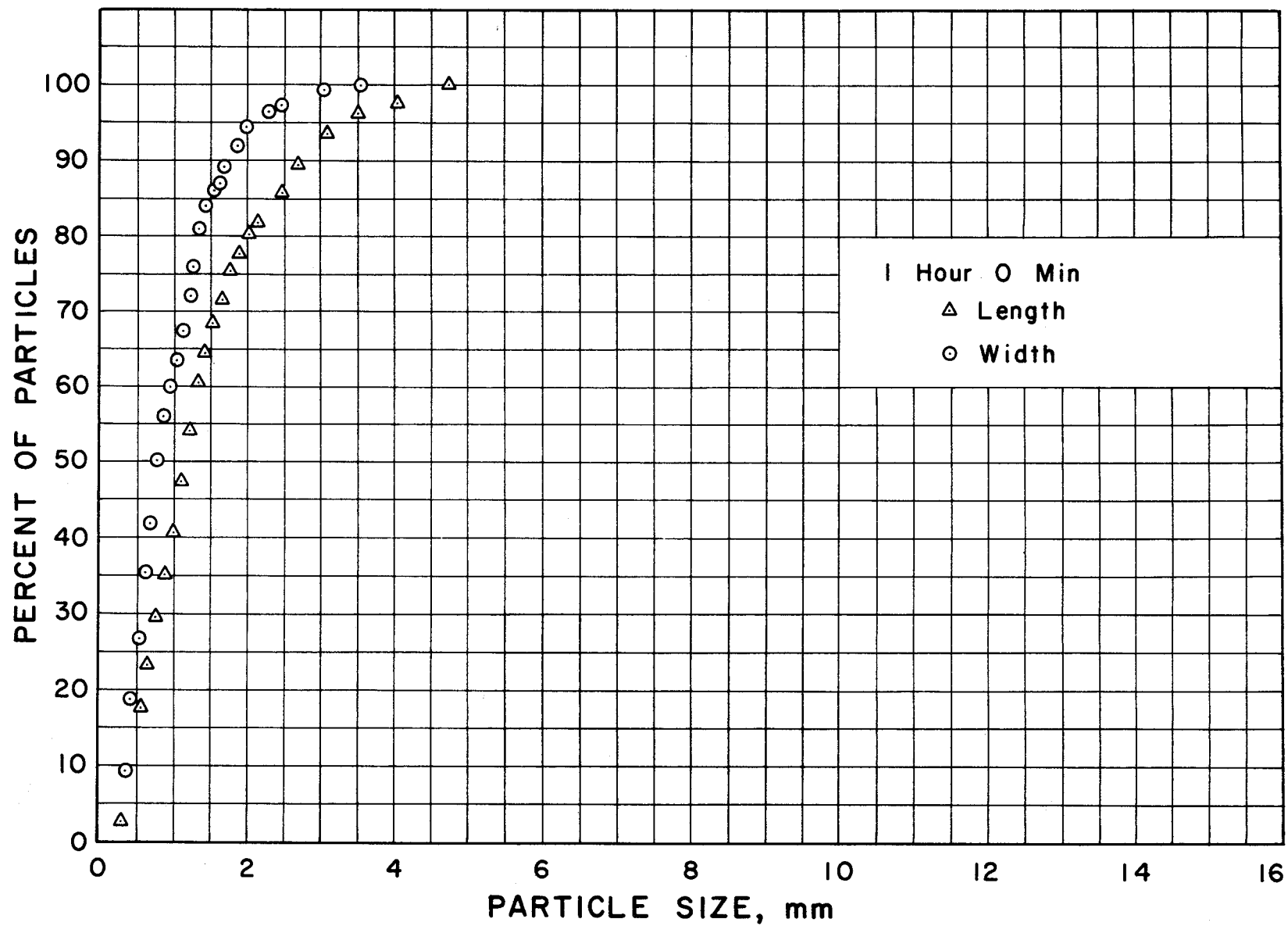


Figure 43. Particle Size, Age 1 Hour.

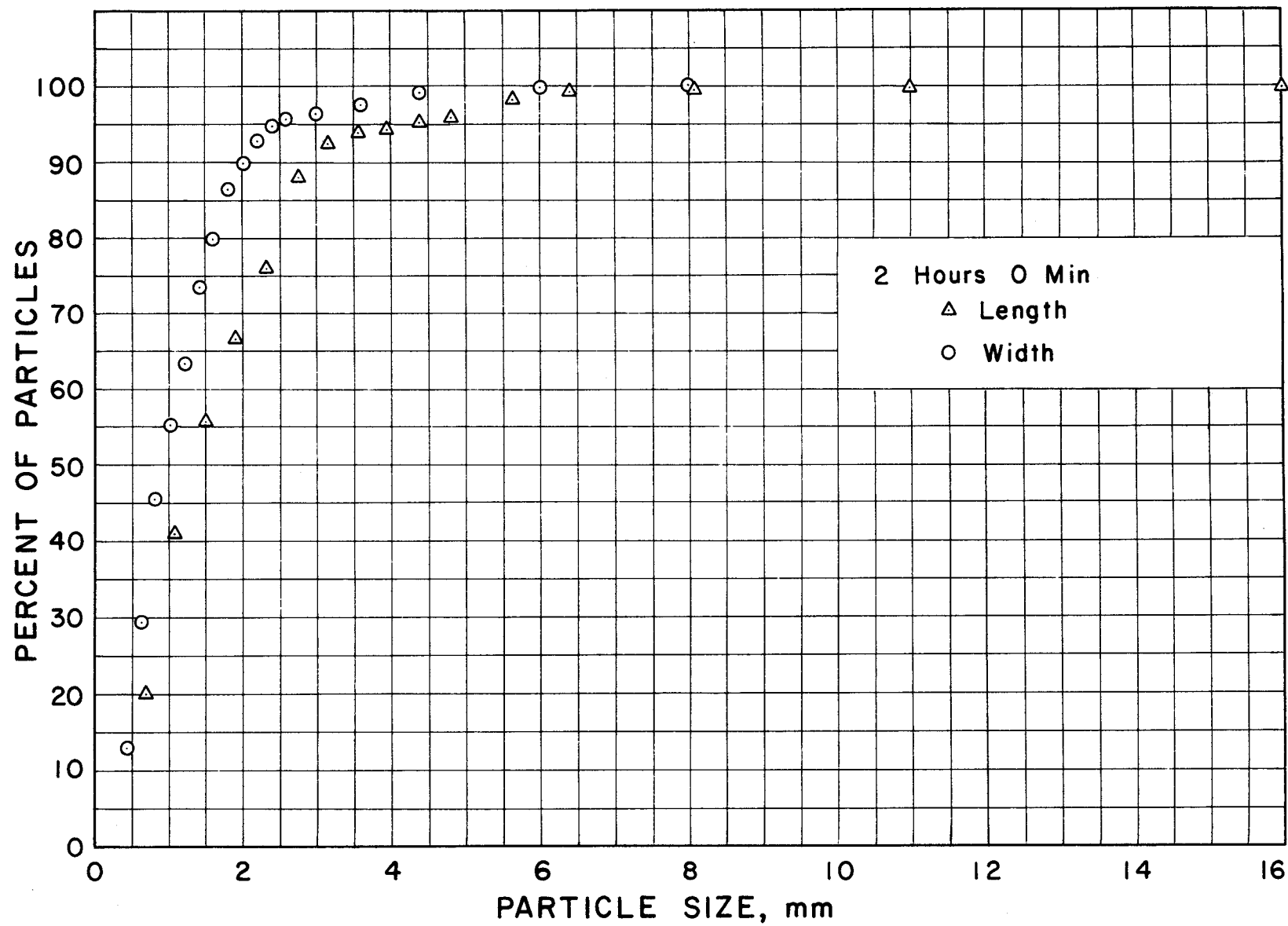


Figure 44. Particle Size, Age 2 Hours.

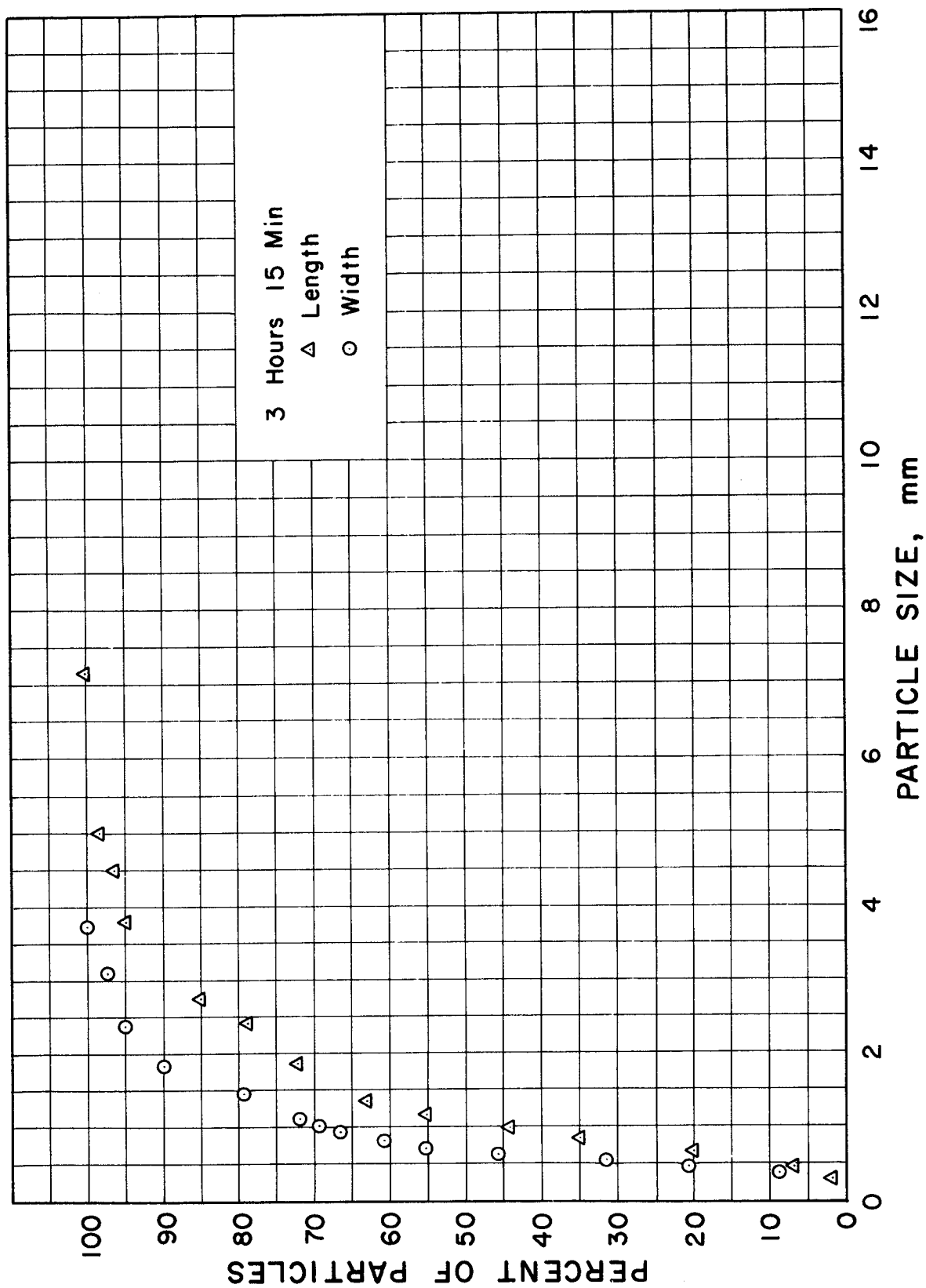


Figure 45. Particle Size, Age 3 1/4 Hours.

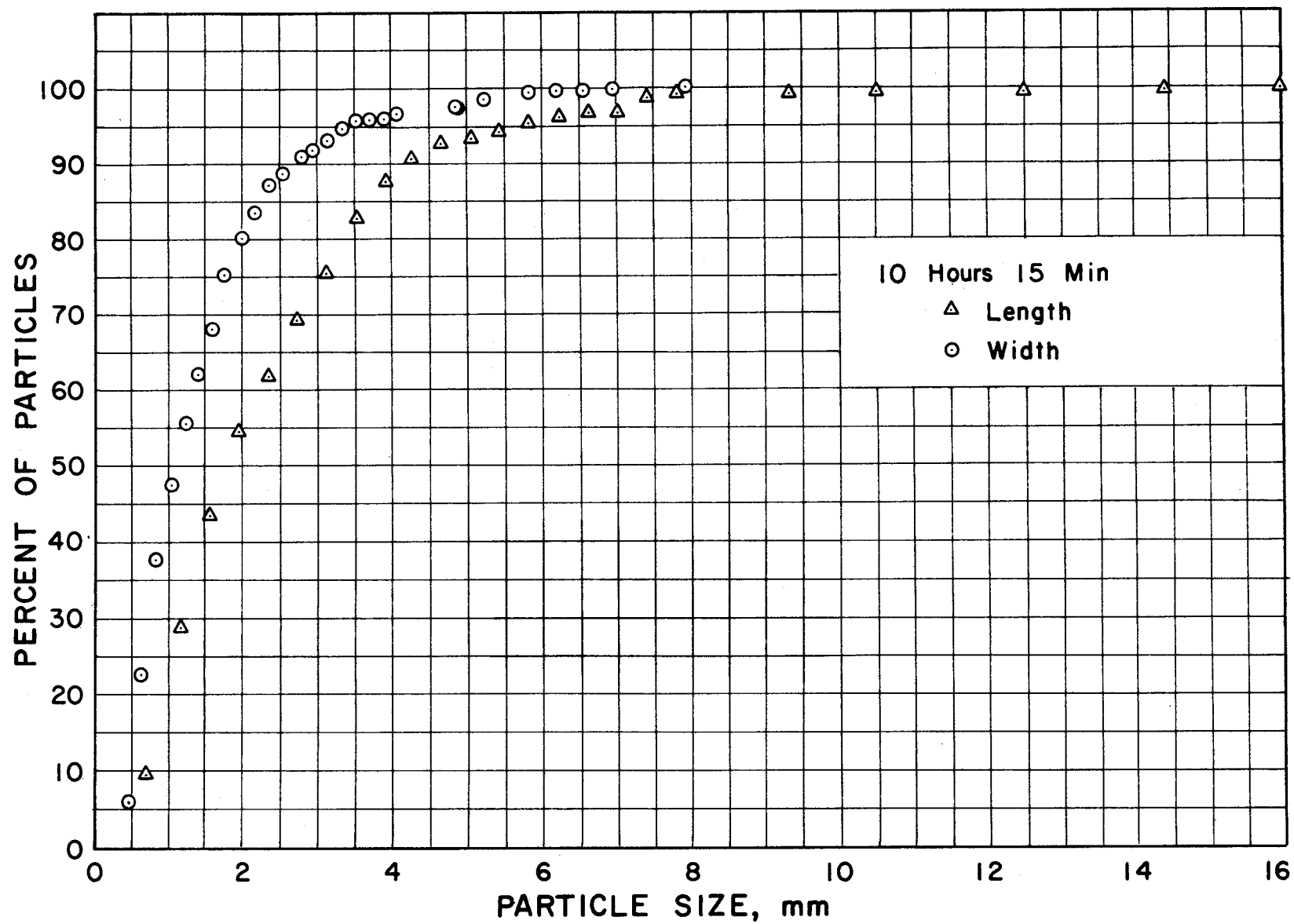


Figure 46. Particle Size, Age 10 1/4 Hours.

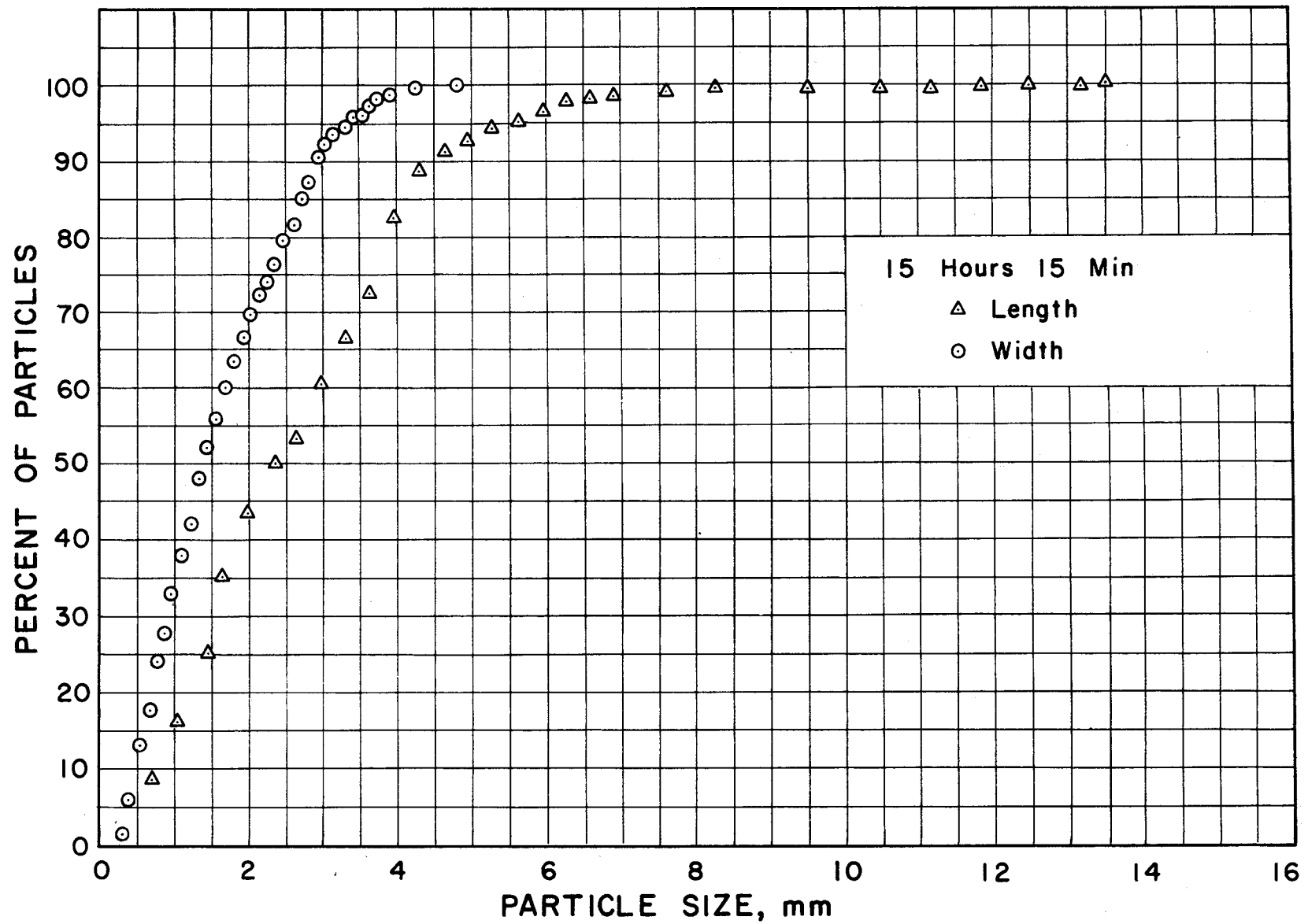


Figure 47. Particle Size, Age 15 1/4 Hours.

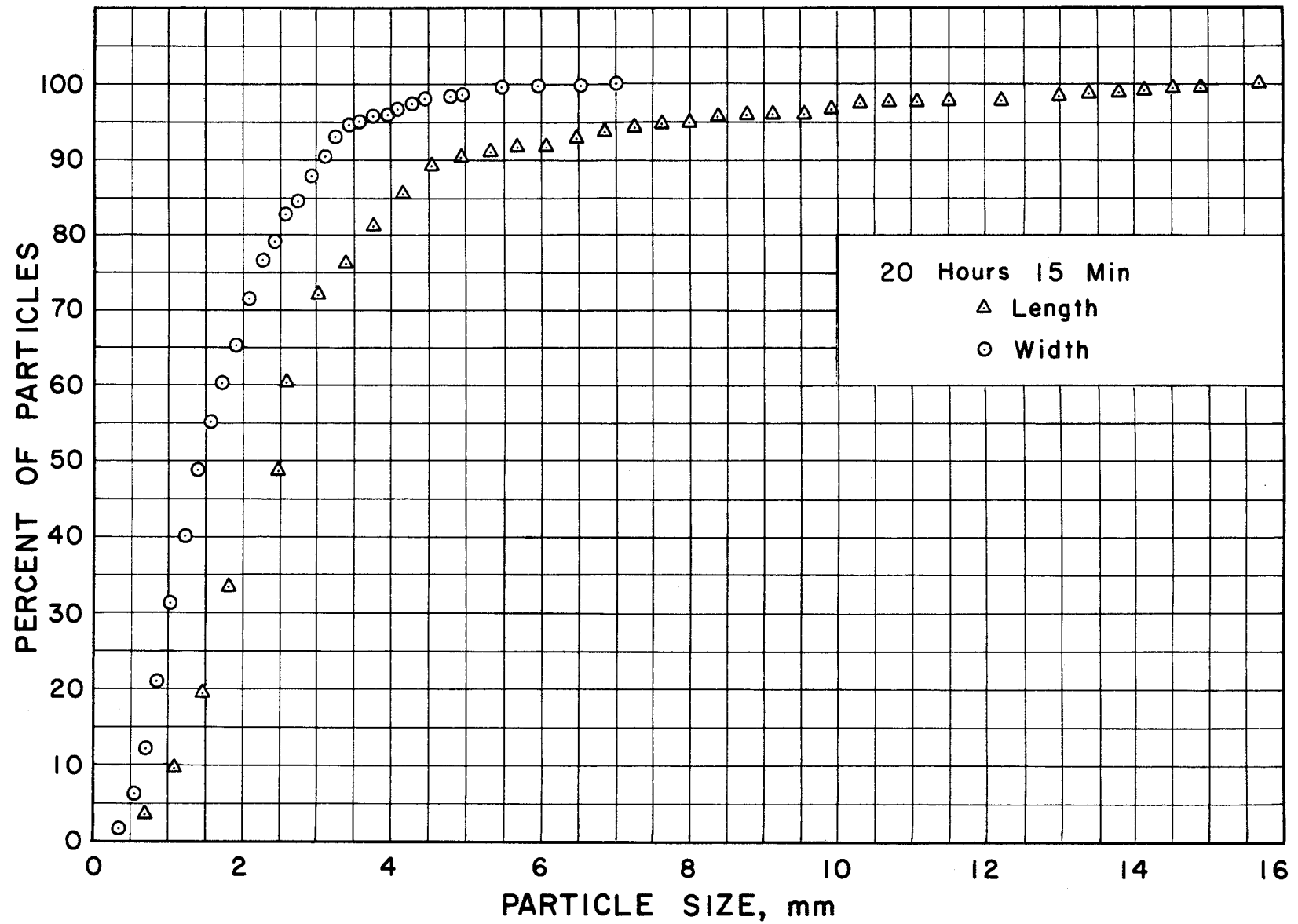


Figure 48. Particle Size, Age 20 1/4 Hours.

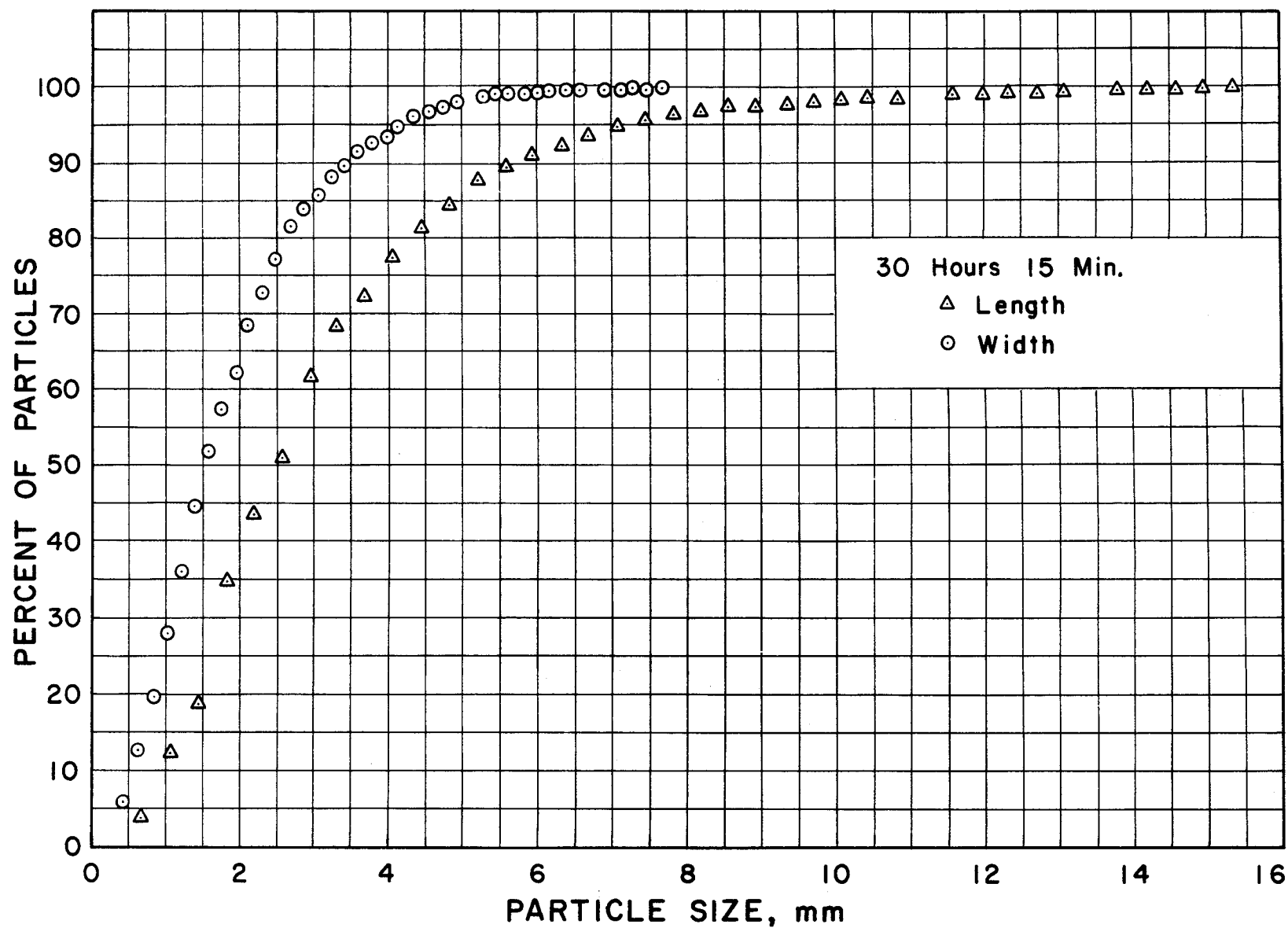


Figure 49. Particle Size, Age 30 1/4 Hours.

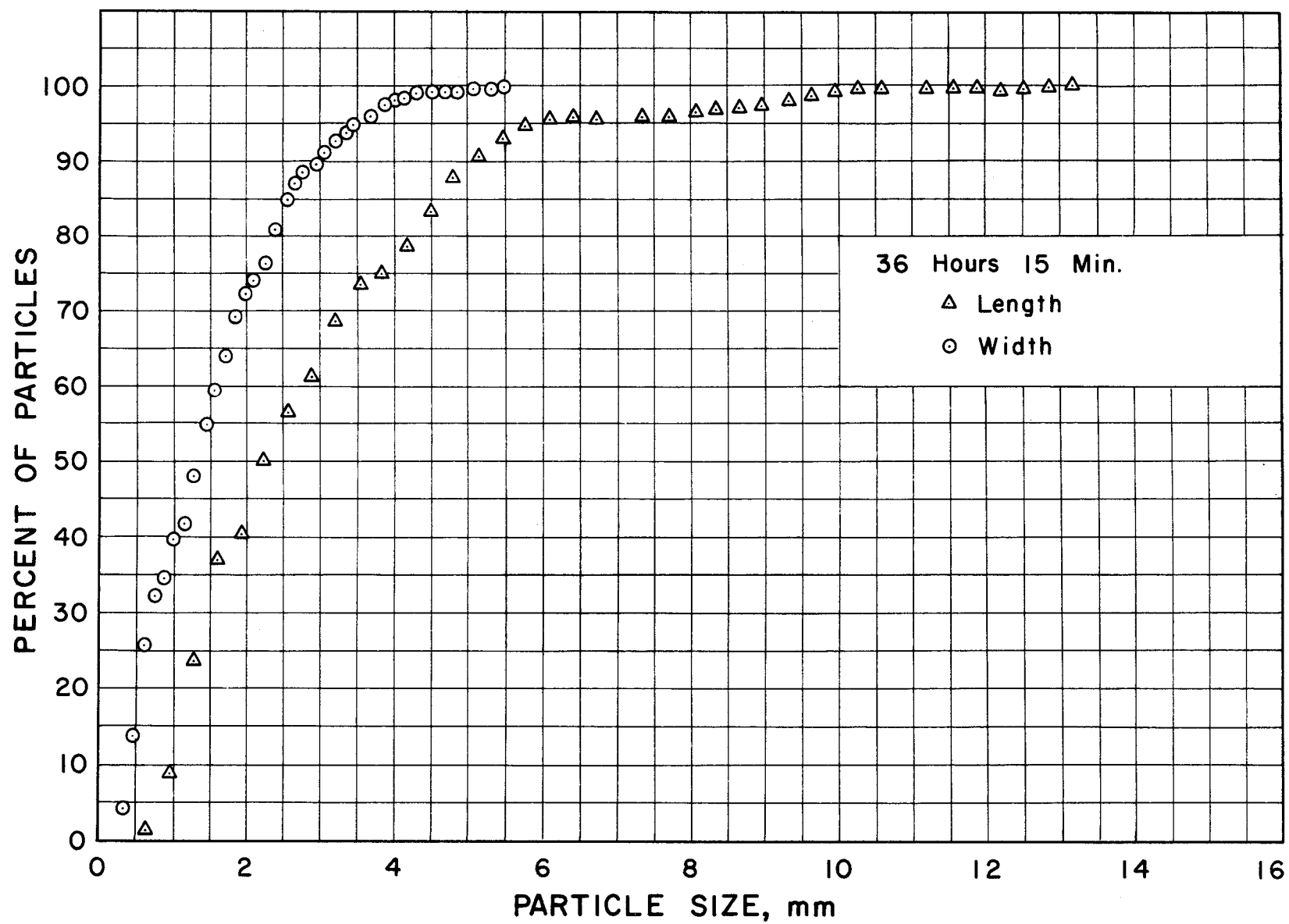


Figure 50. Particle Size, Age 36 1/4 Hours.

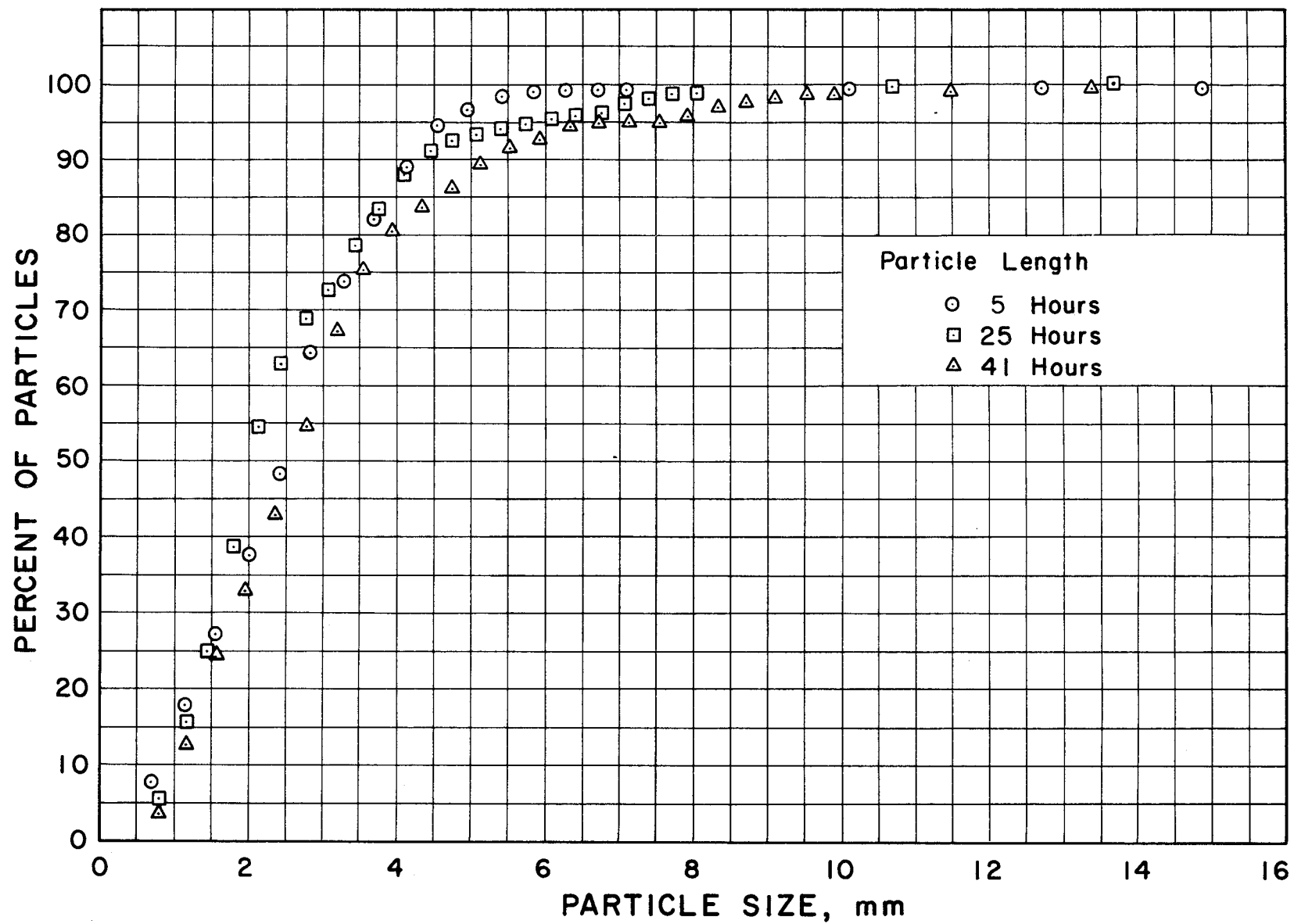


Figure 51. Particle Length - 5, 25 and 41 Hours.

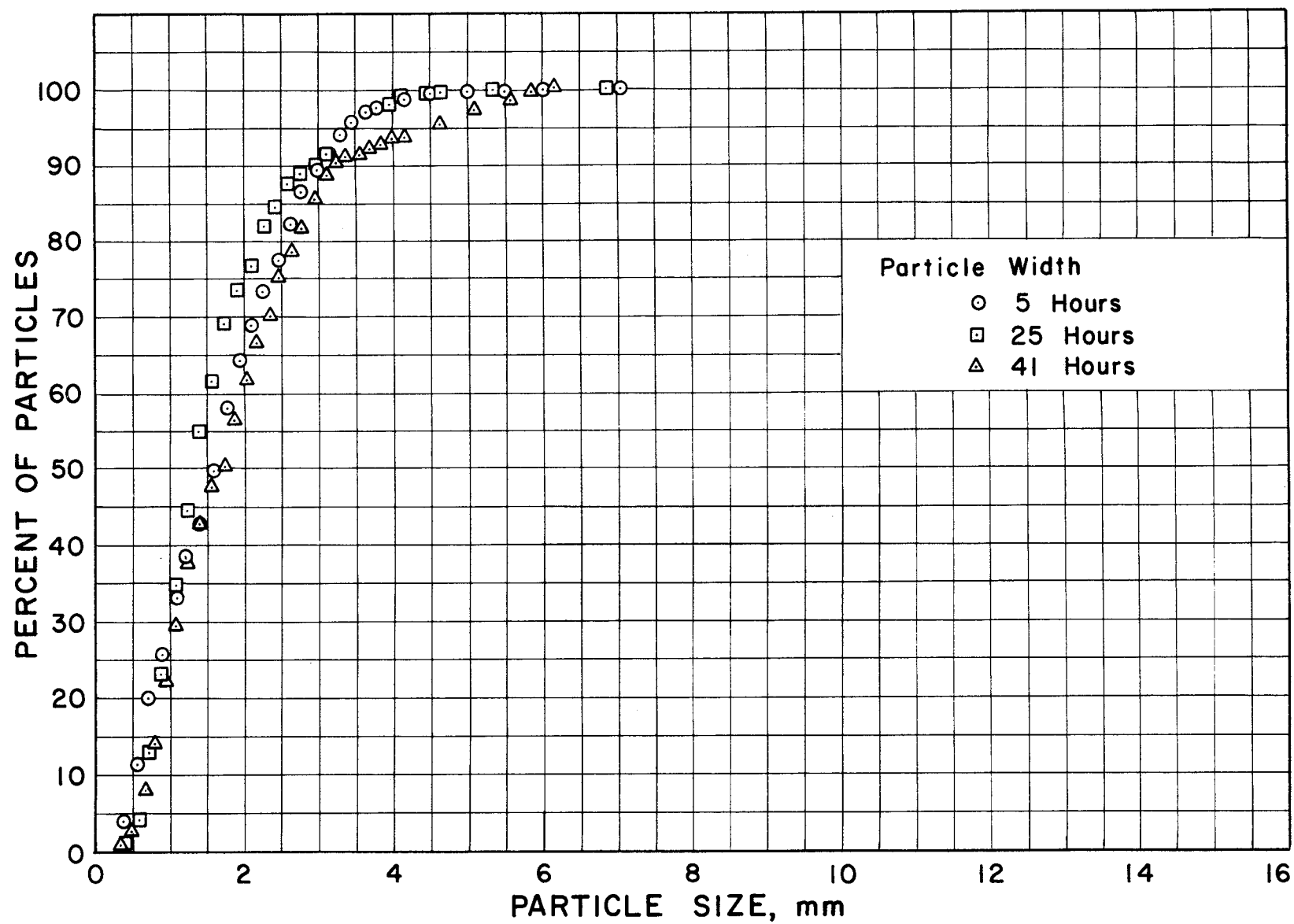


Figure 52. Particle Width - 5, 25 and 41 Hours.

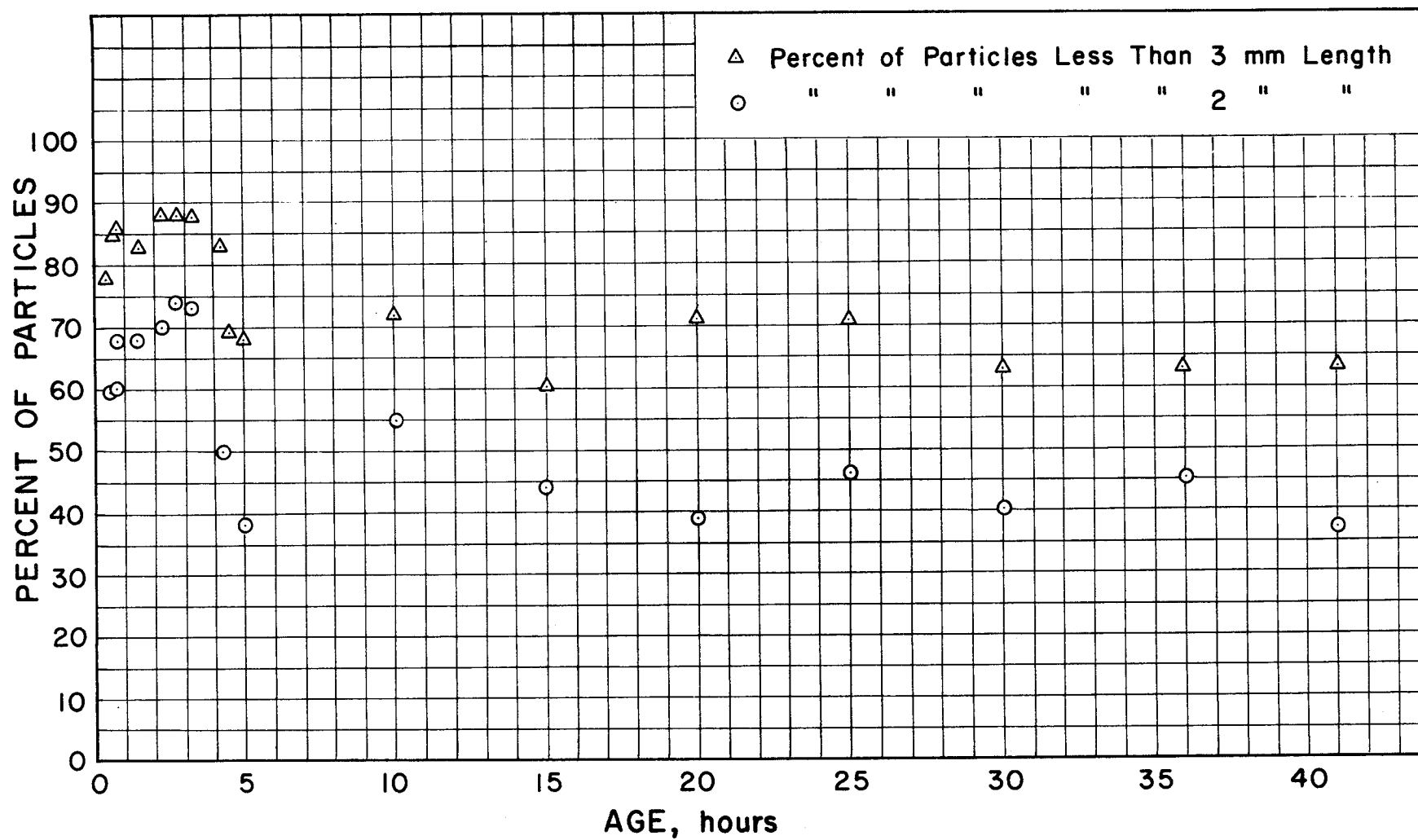


Figure 53. Percent of Particles Less Than 3 and 2 mm. Length.

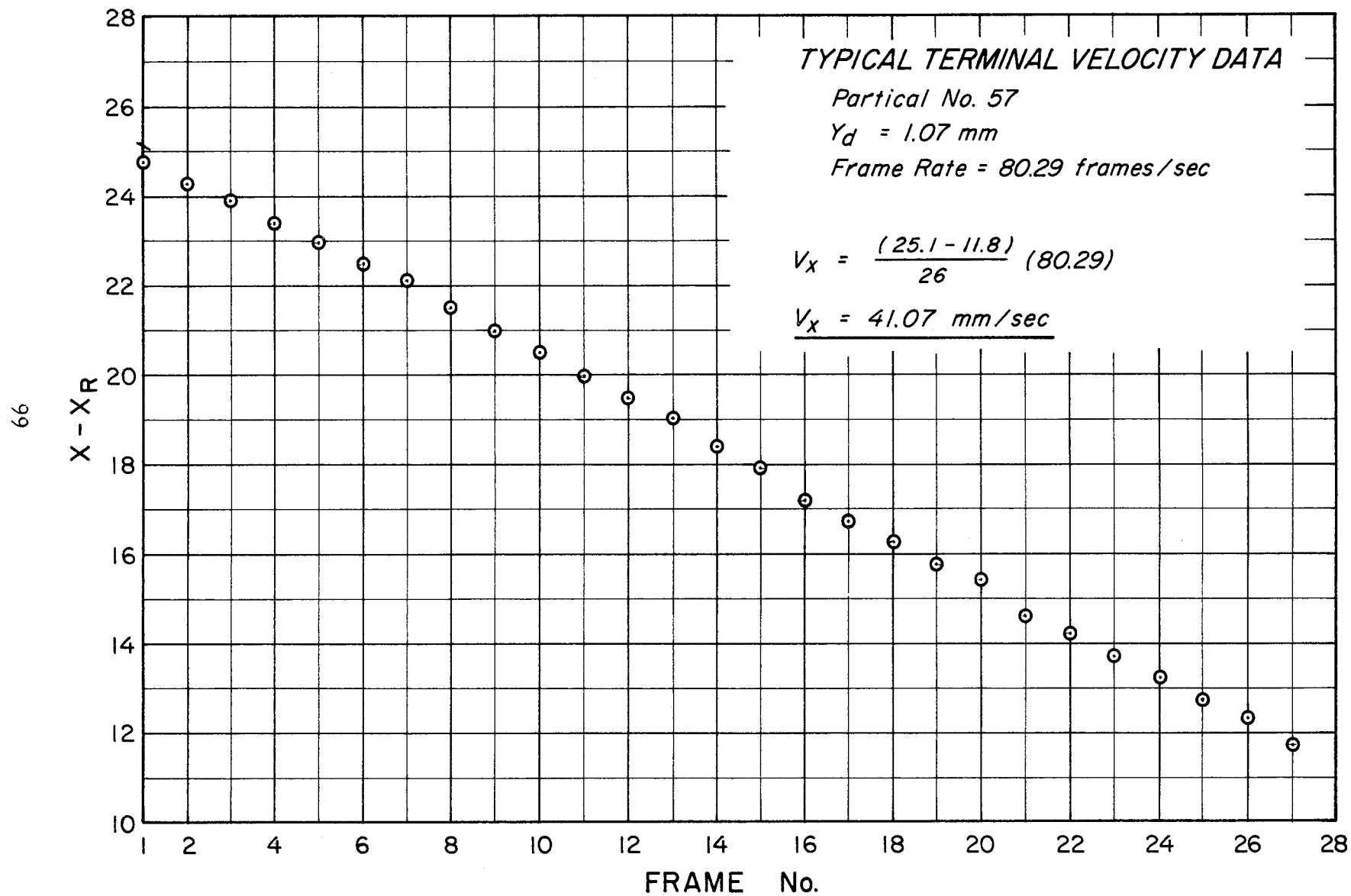


Figure 54. Typical Terminal Velocity Data

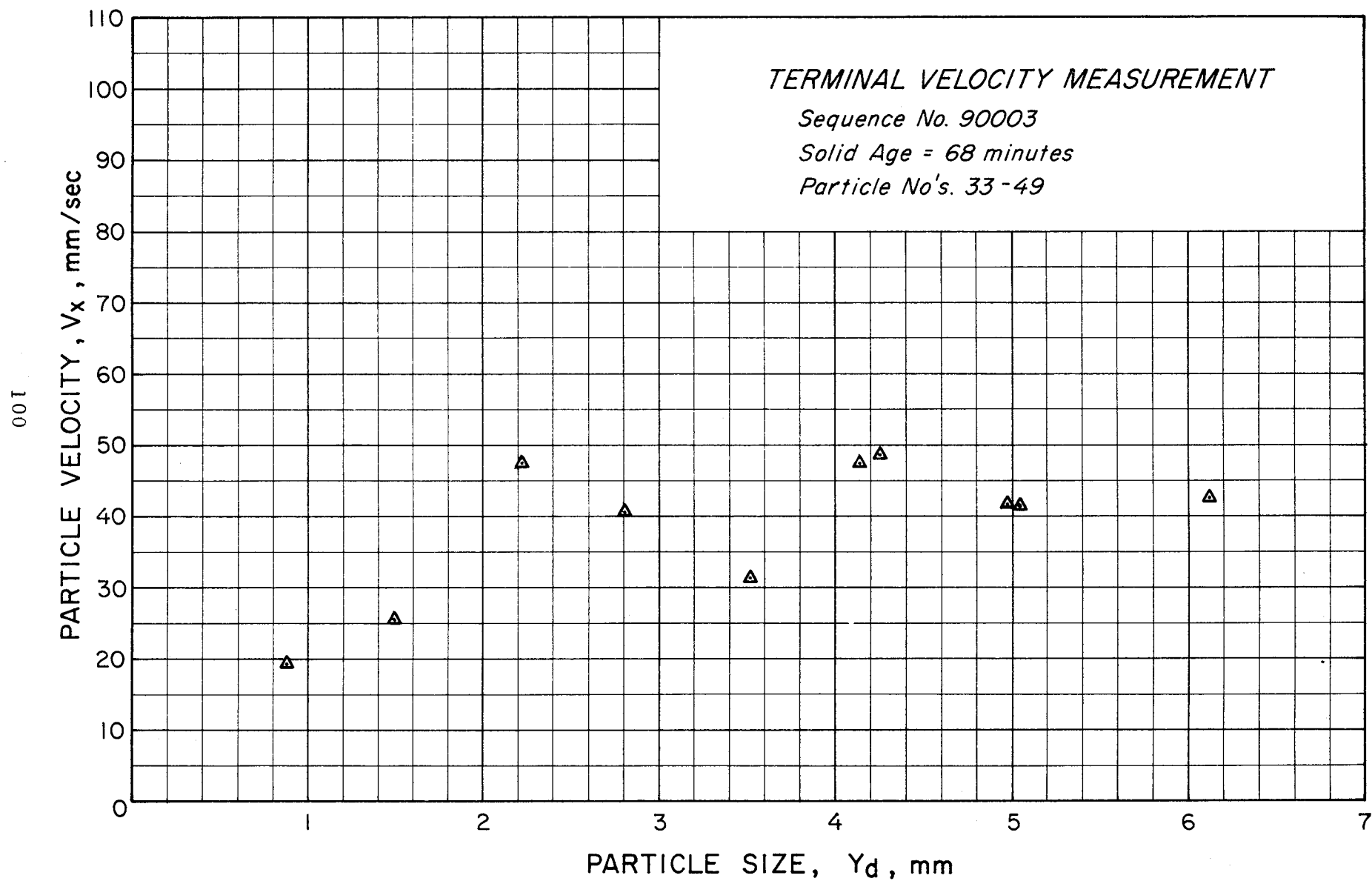


Figure 55. Terminal Velocity Measurement, Age 68 Minutes.

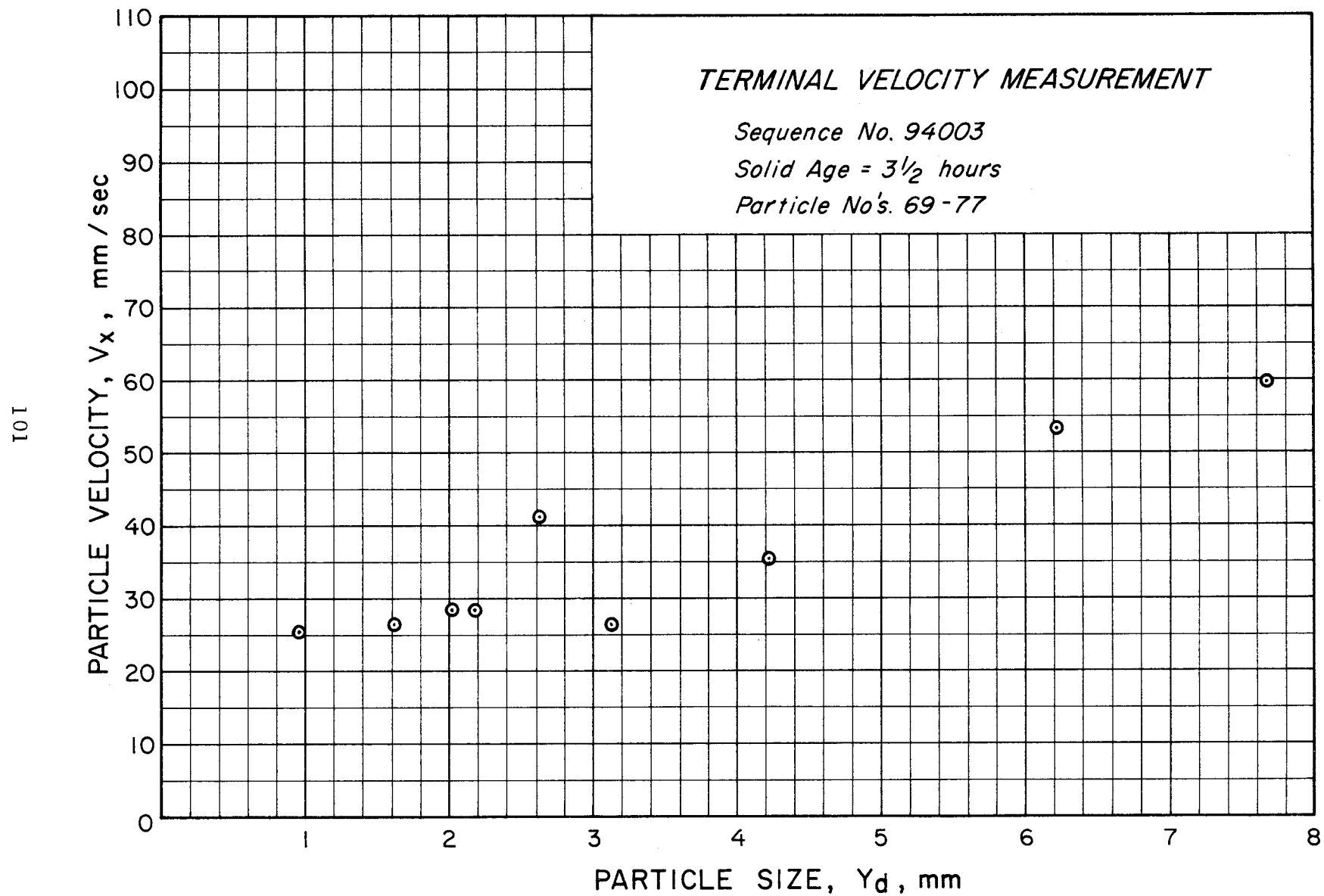


Figure 56. Terminal Velocity Measurement, Age 3 1/2 Hours.

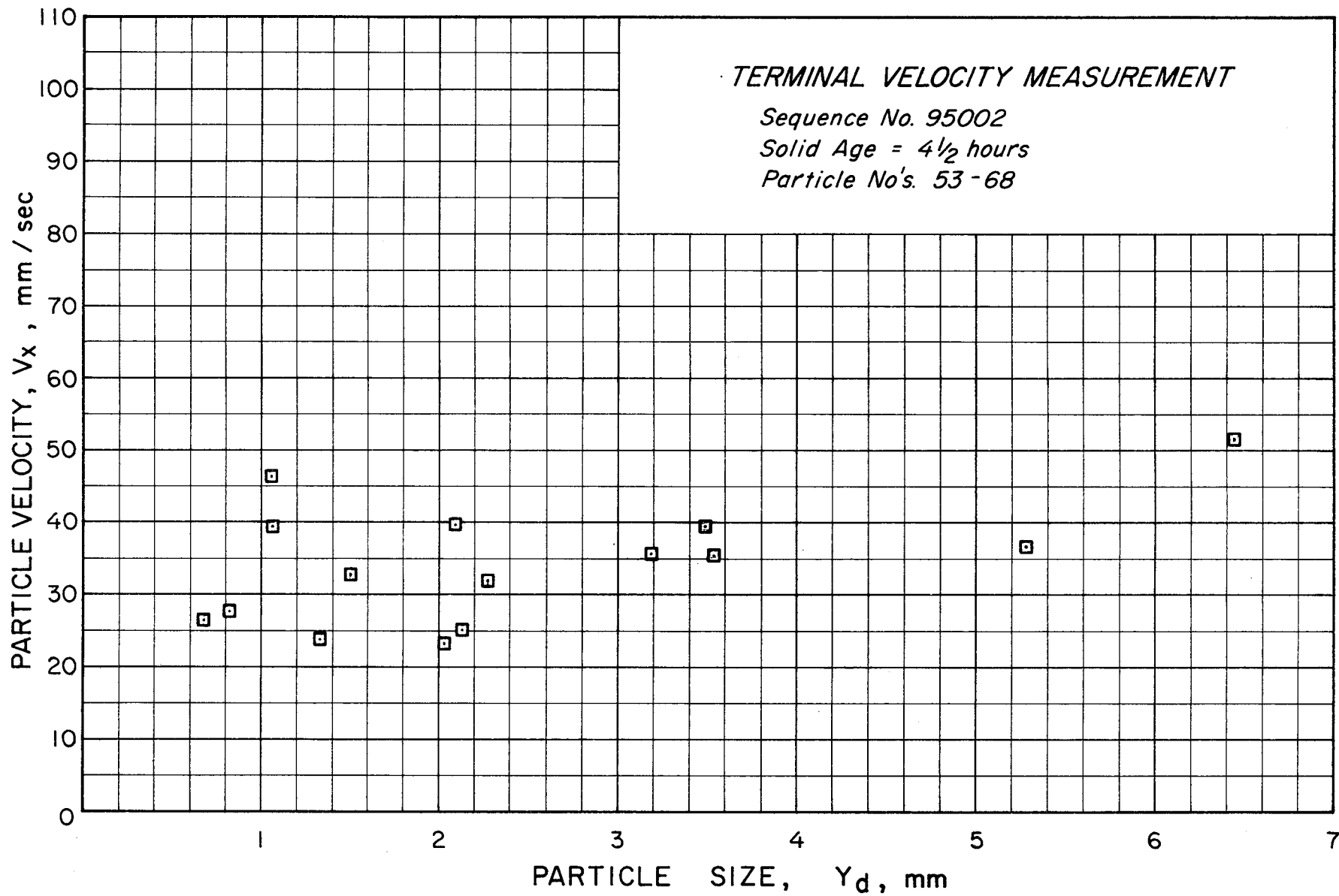


Figure 57. Terminal Velocity Measurement, Age 4 1/2 Hours.

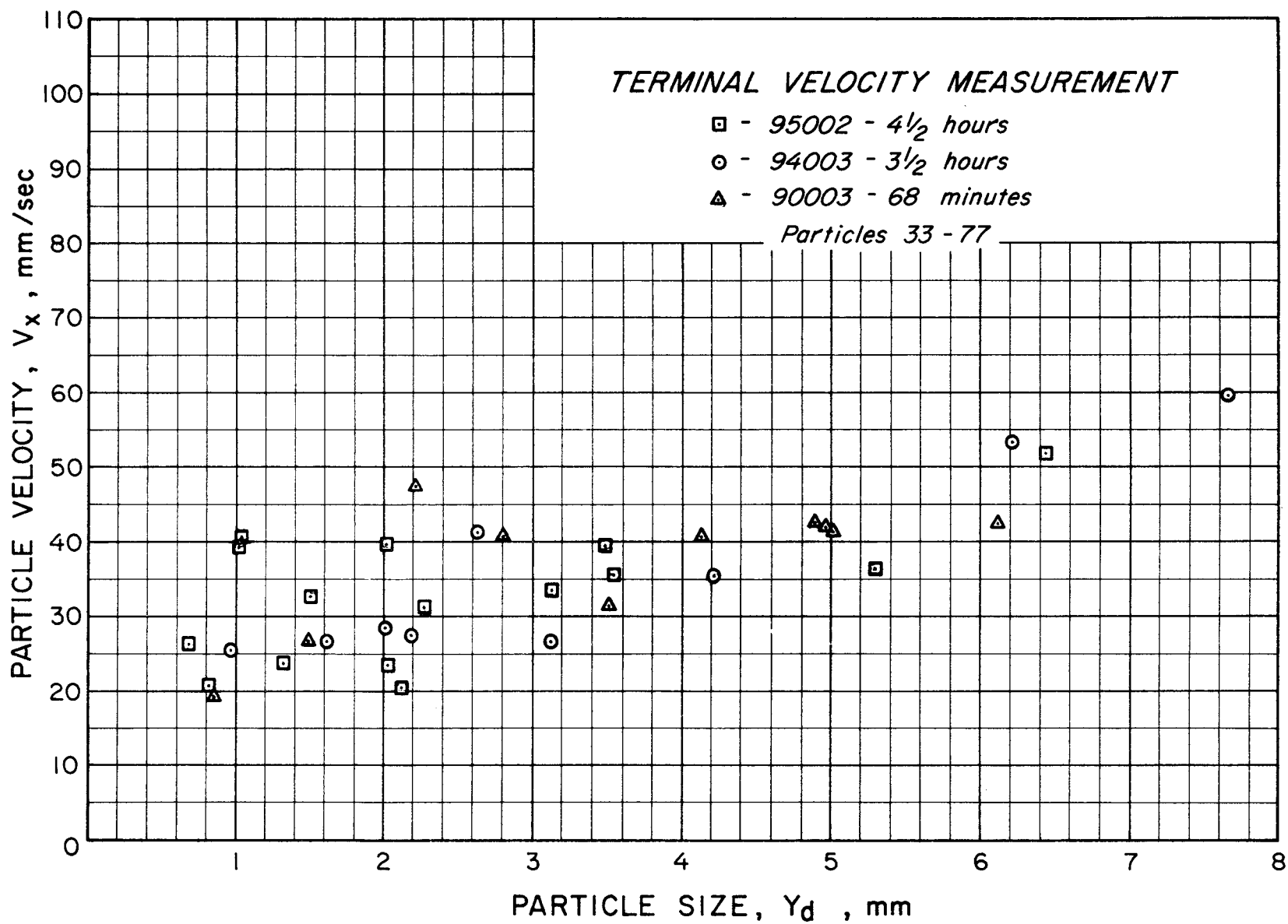


Figure 58. Terminal Velocity Measurement, Age 68 Minutes, 3 1/2 Hours and 4 1/2 Hours

PART C - TRANSPORT CHARACTERISTICS

1. Introduction

The following is a portion of the third progress review for the project "Slush Hydrogen Production and Instrumentation." The instrumentation portion of the program is reported separately. The work reported describes progress made from February 1965 to August 1965.

1.1 Activity Summary

Progress during the present reporting period was confined to problems associated with transport, storage, and handling of the liquid-solid mixture. A number of questions raised during the previous reporting periods were resolved.

The necessary experimental data required to predict transport characteristics, based on correlations developed for slurry flow, have been completed. Predictions of pressure drop and critical velocities have been made and will be compared to experimental results derived from a proposed transport loop.

Methods of storing the mixture at absolute pressures greater than one atmosphere have been developed and tested. Either helium or hydrogen may be used as the pressurizing gas. Stratification of a relatively thin layer of hydrogen liquid at the vapor-liquid interface provides the necessary condition for one atmosphere storage. The only restriction to the operation involves the location of the fill line connection on the storage container.

An analysis of the mass-energy balance method of determining slush quality in a storage container has been completed. The experimental method has been defined and will be tested under controlled conditions during the next reporting period.

Dewar-to-dewar transfer of the liquid-solid mixture through a

3/4-inch transfer line has been accomplished. A transparent glass transfer line section allows observation of the operation. Although only small total quantities of the mixture were transferred, the operational techniques have been established for larger scale experiments.

Confirmation of the events occurring during the freeze-thaw production process was made using high speed photography. The appearance of an initial thin solid layer prior to the violent boiling phase was documented. In addition, the slush produced by the spray technique (described in previous reports) was found to be similar in all respects, after aging, to that generated by the freeze-thaw method.

In addition to the above activity summary, a number of studies have been conducted during the present period to determine the mechanism of particle aging and the possibility of producing colloidal or homogeneous slush. These studies will be continued during the next reporting period.

2. Particle Size

Particle size measurements were made for four additional ages of particles to confirm or reject trends that were not sufficiently defined in the provisional data of the last reporting period. Four thousand additional particle sizes were determined for particles of 11, 38, 39, and 40 hours old. The trend for particles to increase in size from 25 to 42 hours was not verified by the additional particle measurements. In fact, some of the data was the reverse of the trend indicating that the particles do not continue to grow larger. The apparent higher percentage of smaller particles at 10 hours was also not verified. What appeared as trends in some of the provisional data are results of data scatter. Figure 59 is reproduced from the report of February 1965 with the additional data represented by ●, ▲ symbols.

2.1 Discussion

The aim and the result of the freeze-thaw technique is to provide solid hydrogen particles in the liquid hydrogen. In order to transfer the two-phase mixture efficiently with the techniques developed for pure liquid hydrogen, several conditions on the particle-size distribution must be satisfied. In general, flow is easy when the ratio of solid to liquid is small, when the individual solid particles are small, and when size distribution is broad. Since, for these applications, a large ratio of solid to liquid is needed, it is especially important to control and measure the size distribution of the solid. Results of recent investigations in this laboratory indicate that the particles may follow a logarithmic distribution.

Much work has already been reported on small-particle size distributions [Orr, 1959] and a well developed technology exists. Other than the work reported on the present project, the open literature contains very little information on small particles in cryogenic

systems. However, some of the room-temperature techniques may still be valuable when modified, i. e., particle measurement by sieves, by centrifugal sedimentation, and by light scattering and transmission. One of the well known results obtained by measuring small-particle sizes at ordinary temperatures is that the distribution is usually not symmetric about some mean, but is skewed in the direction of small particles. The most useful function for describing these distributions is the logarithmic distribution function,

$$y(x) = \exp \left[-(\ell n x)^2 / 2 \right], \quad (1)$$

in which x is some characteristic dimension of the particle. The probability that a particle has its dimension between x and $x + dx$ is proportional to $Y(x) dx$.

Equation (1) is plotted on figure 60. The important features are these: for real $y(x)$, only positive values of x are allowed; $y(0) = 0$ and $y(\infty) = 0$; and the (sharp compared to normal distribution) maximum occurs at $y(1) = 1$. These are all in accord, at least qualitatively, with the observed particle size distributions which also rise sharply from zero to a maximum and then fall off much more slowly for large sizes.

The observed particle distributions generally have maxima at sizes different from 1 mm and the distributions fall to zero for sizes larger than zero. In order that a logarithmic distribution fit the data, it is necessary to consider the more general distribution which may be conveniently written:

$$y(x) = \delta \exp \left[-\frac{\beta}{2} \{\ell n \gamma \alpha x - 1\}^2 \right]. \quad (2)$$

The parameters α , β , γ , and δ allow control of the logarithmic distribution in the following way:

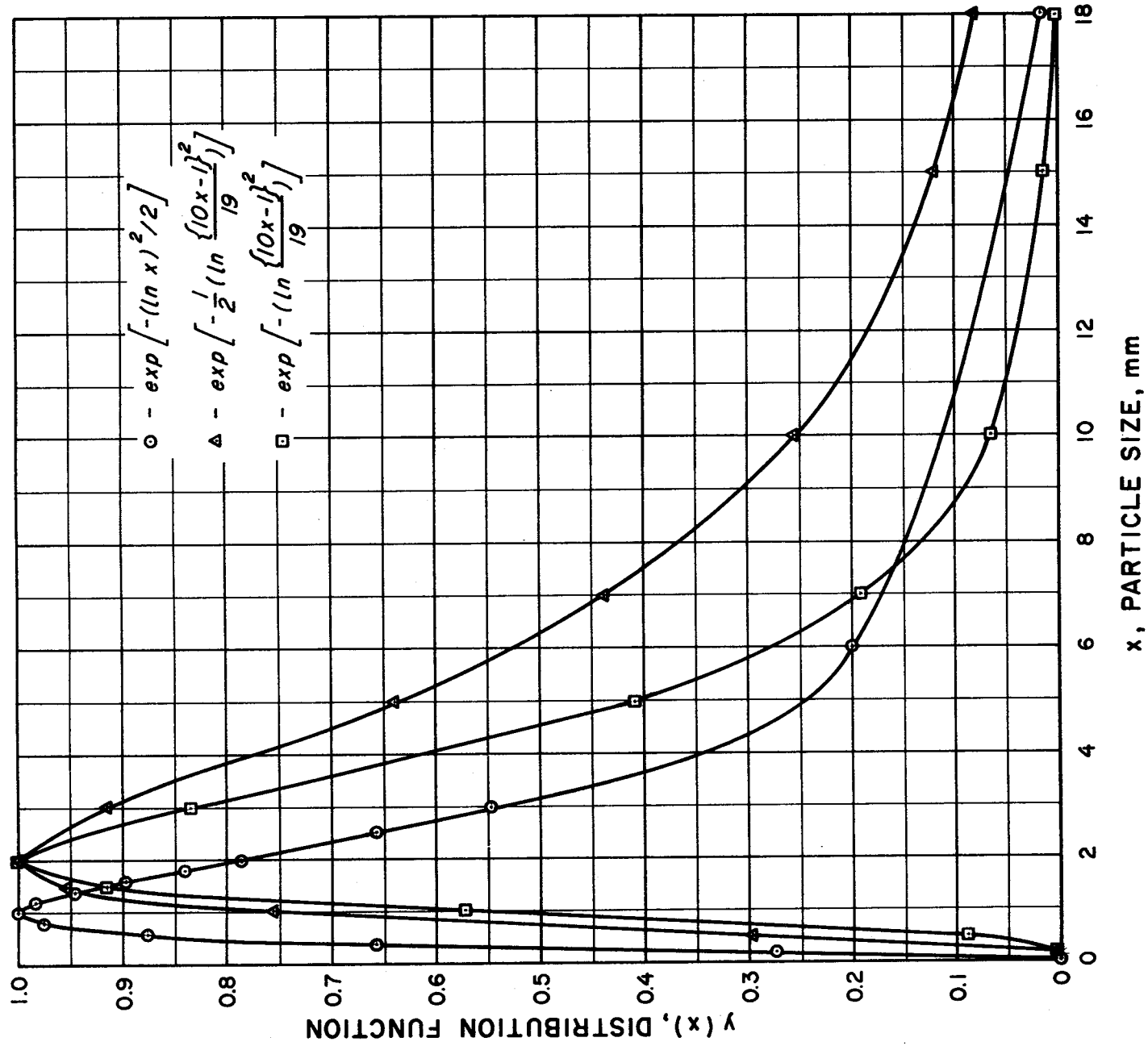


Figure 60. Selected Distribution Functions.

- a) $y(x)$ is zero to the left at $x = 1/\alpha$, instead of at $x = 0$ as in equation (1),
- b) $y(x)$ has its maxima at $\gamma\{\alpha x - 1\} = 1$, instead of at $x = 1$ as in equation (1),
- c) the slope of the distribution, $y'(x)$, is proportional to β (This means that, compared to equation (1), if $\beta > 1$ then the distribution falls to zero more rapidly on both sides of the maximum, and conversely.), and
- d) the maximum value of $y(x)$ is δ , instead of unity as in equation (1).

To determine whether size distribution data, obtained from analysis of the solid particles formed in the freeze-thaw technique, can be described by the distribution function of equation (2), a typical case has been analyzed in detail.

The data chosen were ID = 66001, age 20 hr. 15 min., $N = 995$ and the procedure was to first adjust α , γ , and δ to give a maximum of unity at $x = 2$ mm, and give $y(0.1 \text{ mm}) = 0$. This gives $\delta = 1$ and $\gamma\{\alpha x - 1\} = \frac{1}{19} \{10x - 1\}$; β is initially taken as 1. Then β was adjusted to give an approximate fit to the data. To illustrate the procedure, some of the curves have been included in figure 60; viz:

$$y(x) = \exp \left[-\frac{1}{2} \left(\ln \frac{\{10x - 1\}}{19} \right)^2 \right]; \text{ and}$$

$$y(x) = \exp \left[- \left(\ln \frac{\{10x - 1\}}{19} \right)^2 \right].$$

Figure 61 shows the data points along with the proposed fitting curve $y(x) = \exp \left[-2 \left(\ln \frac{\{10x - 1\}}{19} \right)^2 \right]$. The preliminary conclusion is that the data can be satisfactorily described by an empirically

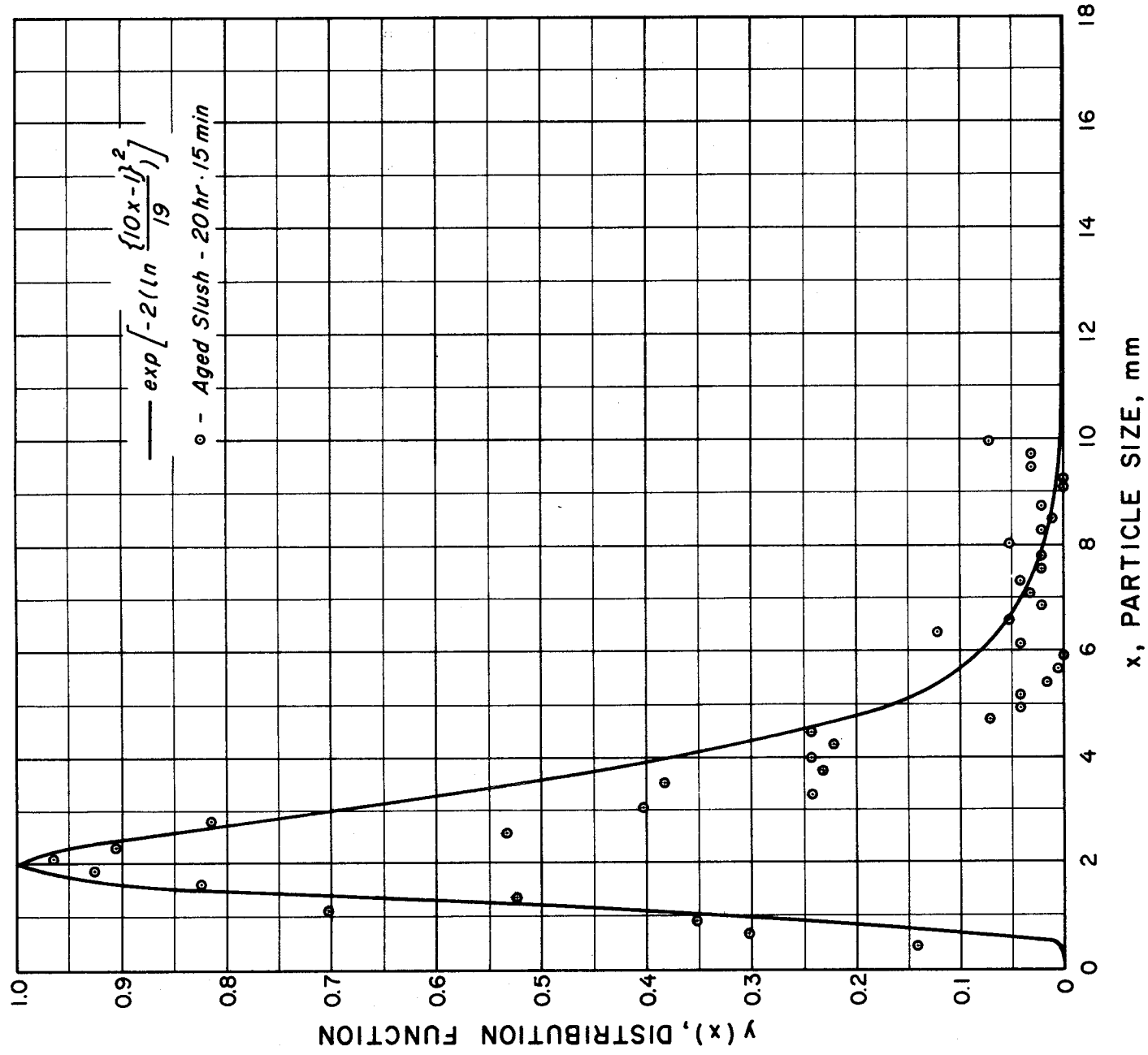


Figure 61. Data Comparison With Logarithmic Distribution

modified version of equation (2) and a computer program is being prepared. It should be emphasized that the fitting is merely empirical. A discussion, from first principles, of the logarithmic distribution and some modified versions of it has been given by Irani [1959].

3. Particle Terminal Velocity

The terminal velocities of 77 hydrogen particles were measured in the previous reporting period. There was considerable variation in the terminal velocities, probably because the solid was fresh, less than four hours old. Because of the scatter in the data, it was decided to take additional terminal velocity measurements with older solid. During the present reporting period, the terminal velocities of 117 additional particles of age 8 - 10 hours old were measured. These data show less scatter.

Most of the particles have terminal velocities in the range of 20 to 50 millimeters/second. The terminal velocities of the particles were plotted as a function of the product ($x y$). These are the two measured dimensions normal and perpendicular to velocity. The plot is shown in figure 62. A straight line was approximated through these points.

A plot was made showing the terminal velocities of solid hydrogen spheres in triple point liquid, using the appropriate analytical expressions for the laminar and turbulent regions. The experimental data were compared with these curves by plotting terminal velocity vs. nominal diameter of the particles on the same graph. The nominal diameter was assumed to be the square root of the two measured dimensions. The comparison is shown in figure 63. The broken line represents the experimental data. The curve for the irregular particles lies reasonably close to the curve for spheres falling in the turbulent region and has approximately the same slope. The difference in position of the two curves is most likely due to the irregular shape of the hydrogen particles. The difference in position may be used to determine an empirical particle shape factor or configuration factor necessary for analytical study. The terminal velocities of the irregular particles will be used

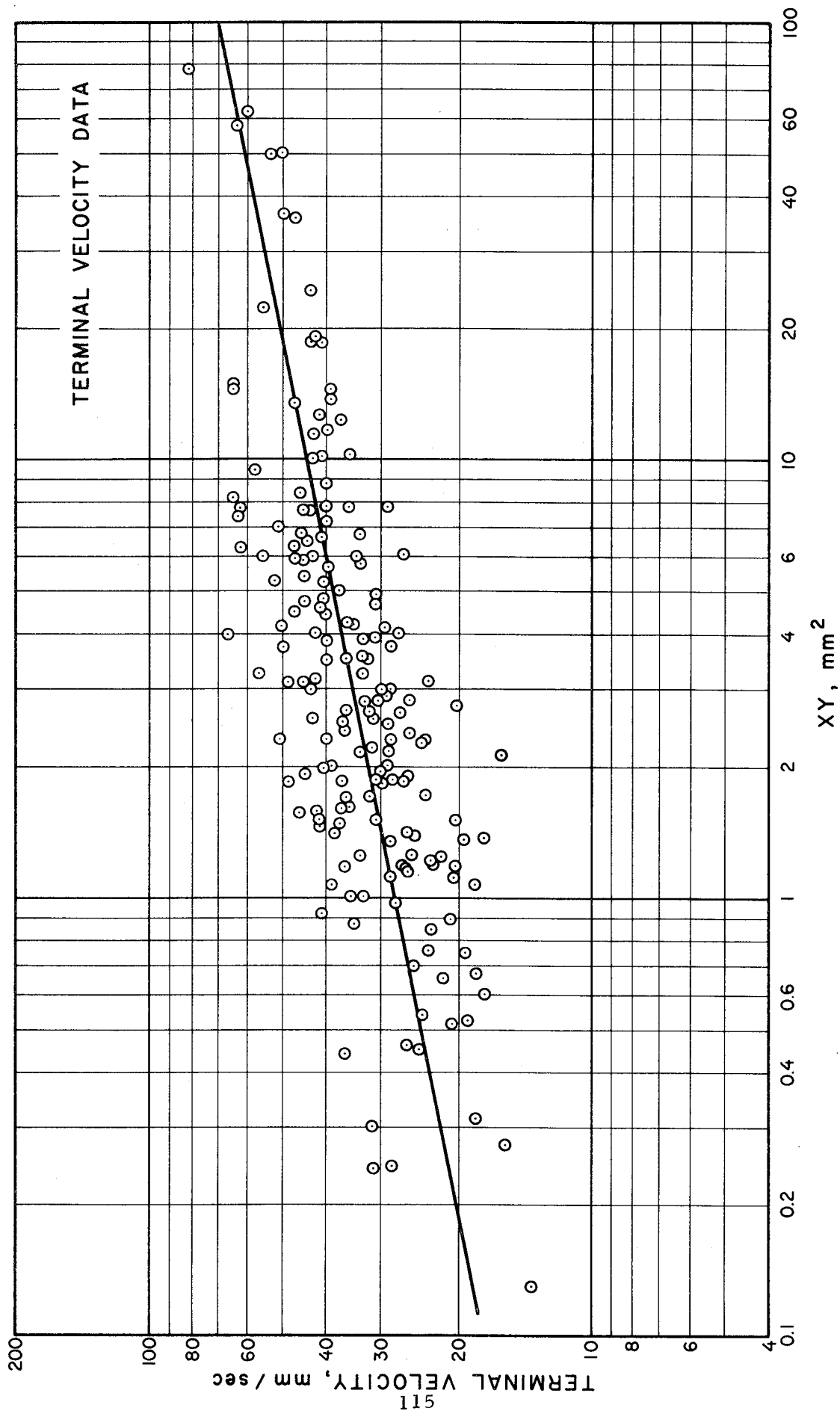


Figure 62. Terminal Velocity Data

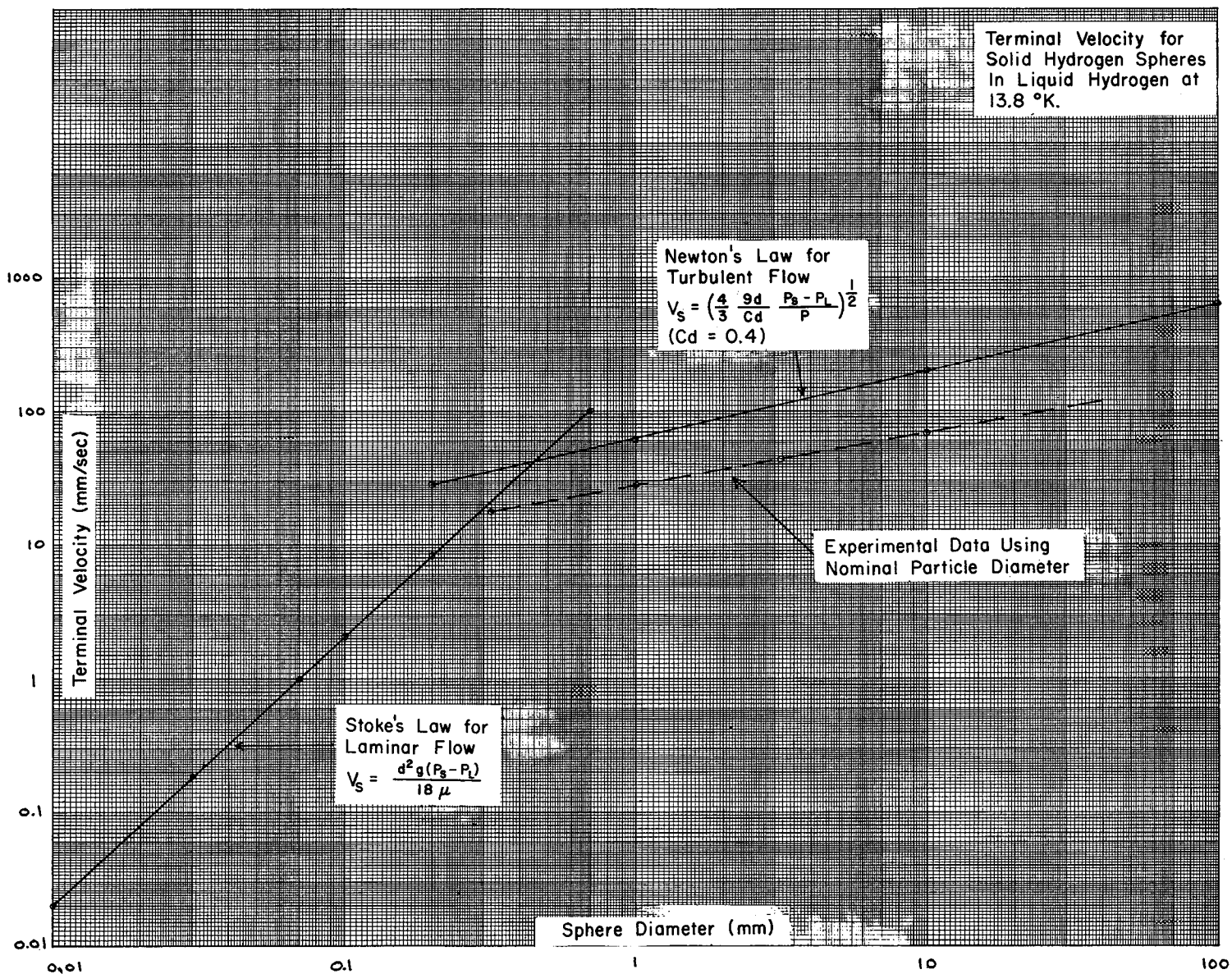


Figure 63. Terminal Velocity for Hydrogen Spheres and Experimental Data

to calculate the drag coefficients of the particles. From these coefficients, the apparent drag coefficient for the mixture will be calculated and used in the Condolious' expressions [1963] for slurry flow.

4. Dewar Pressurization Techniques

Transferring liquid-solid mixtures from one dewar to another requires some form of pumping. The most simple form applicable to our requirements is pressurization of the generating dewar with either hydrogen or helium gas. During periods of storage, it is desirable to maintain dewar total pressures above atmospheric pressure to prevent air leakage into the system. Either hydrogen or helium gas can be used for this purpose. An experiment was performed to establish the techniques necessary for pressurization with either of these gases.

The initial concept was to pressurize to slightly above atmospheric pressure with helium, maintaining the hydrogen liquid-vapor interface partial pressure at the triple point (52.9 Torr). With the surface at triple-point temperature, the liquid and solid levels can coincide and an additional quantity of solid can be stored.

4.1 Experimental Apparatus Modifications and Procedures

Modifications were made to the apparatus to measure the liquid surface temperature during and after the pressurization from the triple point to one atmosphere.

A radiation shield was attached to the control rod previously used to operate the lift. A gold-cobalt vs. copper thermocouple was placed approximately 0.5 inch above the radiation shield; another thermocouple was placed 0.5 inch below the shield. A third thermocouple was mounted near the bottom of the dewar and served as the reference cold junction (hydrogen triple point temperature). Figure 64 is a schematic of the apparatus. Solid was made by the freeze-thaw method and allowed to settle in the dewar. The upper thermocouple was positioned at the liquid-vapor interface by the control rod, placing the radiation shield in the liquid. The radiant energy from the apparatus, which is near ambient temperature, is reflected and absorbed by the shield. The

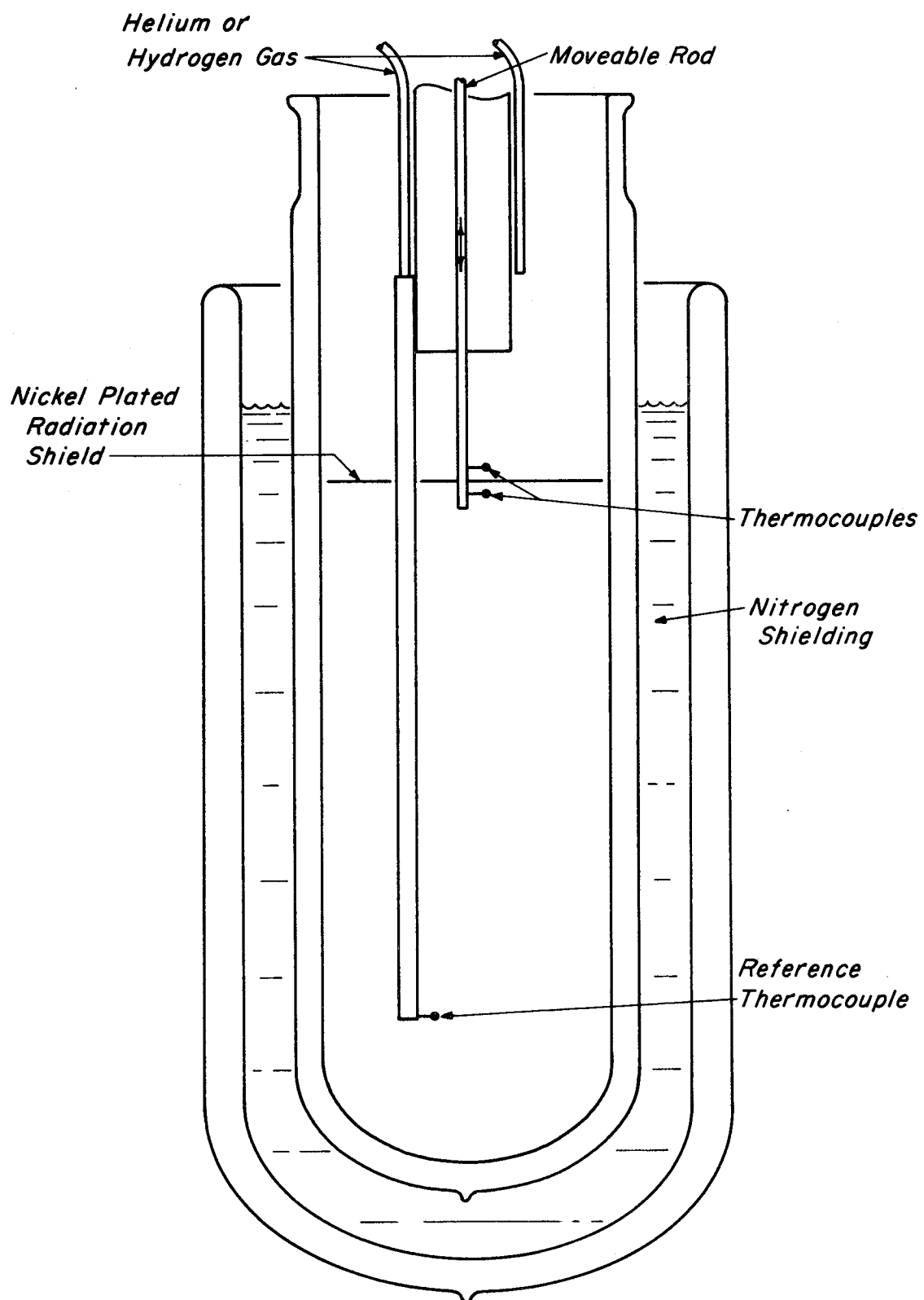


Figure 64. Dewar Pressurization Apparatus

heat absorbed in the shield is conducted to the surrounding liquid hydrogen. Pressurization gas was entered in the bottom of the dewar through the liquid or into the ullage in order to raise the pressure from the hydrogen triple point pressure to one atmosphere.

4.2 Experimental Results and Discussion

Introduction of warm helium gas into the ullage, to bring the total pressure from the hydrogen triple point pressure to the vent pressure, did not succeed in maintaining triple point temperature at the liquid-vapor interface. The liquid at the interface reached the normal boiling point temperature within 35 minutes. Precooled helium gas introduced into the ullage gave similar results.

Helium gas was then introduced near the bottom of the dewar and bubbled through the liquid hydrogen to assure cold helium gas at the liquid-vapor interface. When the helium first entered, the hydrogen partial pressure was reduced enough to form solid at the liquid surface; but the surface temperature again increased to the normal boiling point temperature within an hour after pressurization from the triple point pressure to one atmosphere.

Experiments were also conducted using hydrogen as the pressurant in the ullage. The temperature of the liquid at the liquid-vapor interface followed the vapor pressure curve as was expected.

Results of the helium pressurization tests indicate that the hydrogen mass transfer at the liquid-vapor interface predominated over diffusion of the helium gas down to the surface. Thus, a higher hydrogen partial pressure occurred at the liquid surface and the temperature followed the vapor pressure curve. Placing of the radiation shield near the liquid surface resulted in higher heat flux and, therefore, higher mass transfer at the surface than may be experienced without the radiation shield. The results of the tests may be applicable

to larger apparatus of different design.

4.3 Solid Hydrogen Tubes

While flowing helium gas into triple point liquid or a liquid-solid mixture at the bottom of the dewar, solid hydrogen was formed. A tube of solid hydrogen starts forming at the end of the tube, emitting helium gas, and grows vertically following the helium bubble path. The tube can be grown to the liquid hydrogen surface with the correct regulation of helium gas flow. The solid formed is clear, transparent, and of maximum density, having very few gas inclusions except at the inner walls of the tube. Formation of the solid hydrogen in the triple-point liquid results from the liquid hydrogen vaporizing into the helium gas bubbles. The refrigeration is supplied by liquid around the bubbles. The process continues even after a solid tube is formed. The solid sublimates into the helium gas, tending to further reduce the temperature of the solid tube. The walls of the solid tube continue to grow as more helium passes through. Clear, transparent, solid hydrogen tube walls of approximately 0.75-inch thickness were formed at the tube emitting helium gas.

The observed phenomenon has a direct bearing on the objectives of the program and could be used as a calibration method for the quality meter or a method of upgrading solid concentration.

5. Preliminary Transfer Studies

In previous work, liquid-solid hydrogen has been made by various methods, aged and studied very carefully; but there was no attempt to observe the liquid-solid mixture during transfer from one vessel to another. Two glass dewars and a glass section of insulated transfer line allowed the construction of a simple transfer loop to observe flowing slush. The loop was considered an intermediate step that would reveal some of the problems involved in cryogenic slurry transfer.

5.1 Flow Apparatus and Procedure

A schematic of the flow apparatus is shown in figure 65. The transfer tests are conducted in the following manner. Liquid hydrogen is transferred into a pretreatment chamber from the supply dewar. The bottom of the pretreatment chamber contains a three-way valve, composed of a stationary dual seat and two Teflon cones epoxied to a movable 1/4-inch control rod.

During the filling operation, the valve is placed in an intermediate position so the liquid can pass along the outside of the rod and fall into the glass dewar. Both glass dewars are approximately 15 liters capacity and the production dewar is liquid nitrogen shielded. Solid is then produced by the freeze-thaw method and allowed to settle.

The 13-foot transfer line and receiving dewar are precooled to reduce the heat present in the three couplings, one valve, the glass section and a six-foot flexible section. The control rod is raised until the lower Teflon cone seats, sealing the pretreatment chamber from the dewar. The transfer line valve is opened and reduced pressure is maintained in the receiving dewar. The supply valve is then opened and liquid hydrogen flows into the pretreatment chamber, out through a 3/8-inch copper line at the bottom, through the insulated transfer

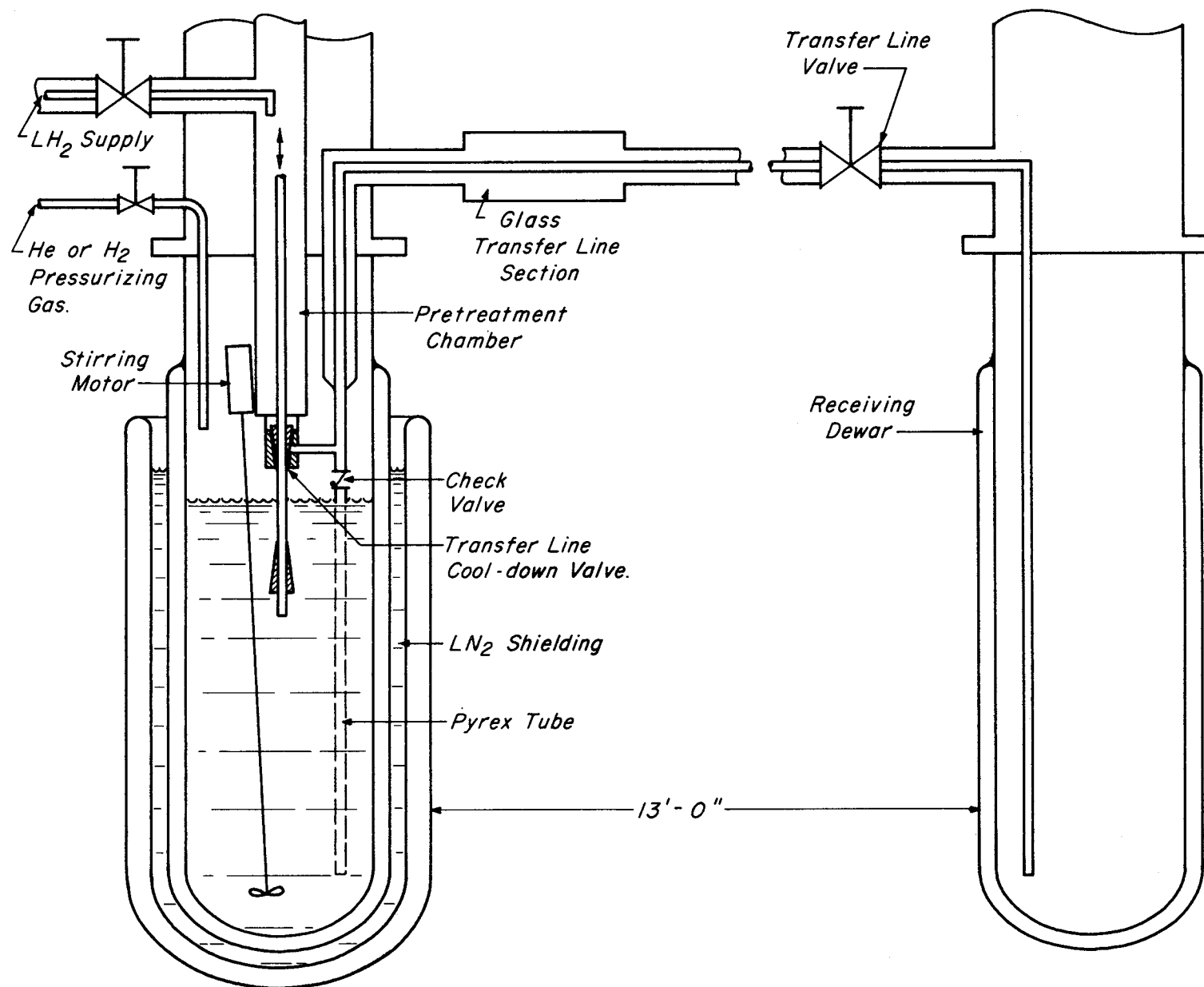


Figure 65. Preliminary Transfer Apparatus

line and into the receiving dewar. Liquid flows for approximately 2 to 3 minutes until about six inches of liquid appears in the receiving dewar. The supply line valve is then closed.

To transfer the liquid-solid mixture, the control rod is lowered, sealing the pretreatment chamber from the transfer line, the receiving dewar is vented through a 3 psi check valve, and the ullage space above the mixture is slightly pressurized (4 psi) with helium or hydrogen gas. The mixture is forced up the pyrex tube, through the small check valve and glass section into the receiving dewar. The mixture may be returned to the generator and the transfer repeated. A photograph of the transfer apparatus is shown in figure 66.

A photograph of the glass transfer line section is shown in figure 67. The inner line is a nominal 3/4-inch diameter pyrex tubing with kovar seals at each end. A flexible bellows near one end compensates for differential contraction. The outer 4-inch O.D. transparent section is made of acrylic plastic and is approximately 20 inches long. A pump-out valve is provided for evacuating the high-vacuum annulus between the inner and outer lines.

5.2 Transfer Characteristics

Several pertinent observations were made during the initial transfer operations. At first, the vertical tube inside the dewar extending into the bottom of the slush was not vacuum insulated. When hydrogen gas was used to pressurize the dewar, the relatively warm gas would rapidly condense on the exposed vertical transfer tube and melt the solid inside the line. The condensation was minimized by pressurizing with helium gas and vacuum insulating the vertical transfer line down to the check valve above the pyrex tube. There is strong evidence for the necessity of locating a discharge line on the bottom of the dewar or to vacuum insulate a discharge line extending down into the slush from

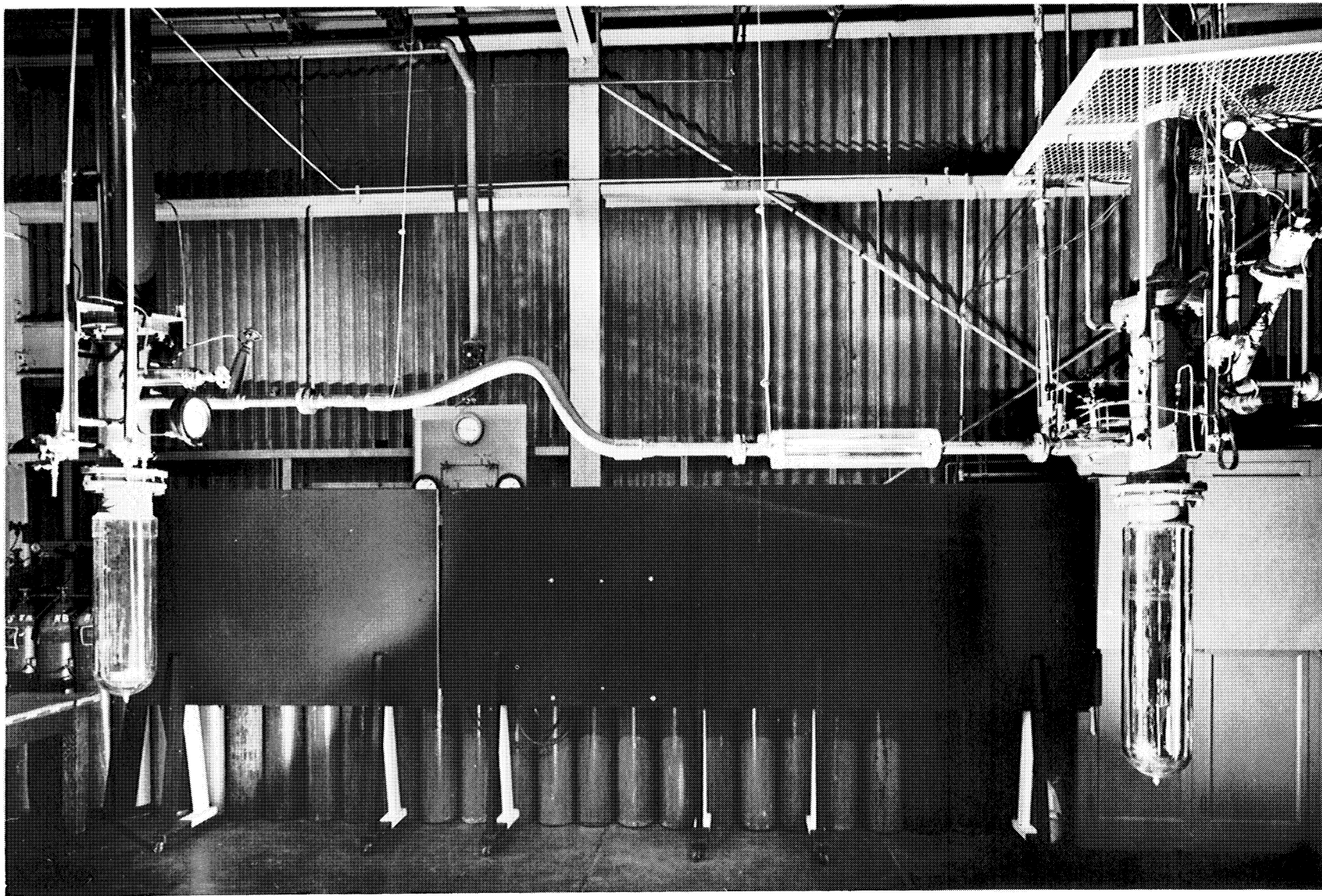


Figure 66. Transfer Apparatus, Photo

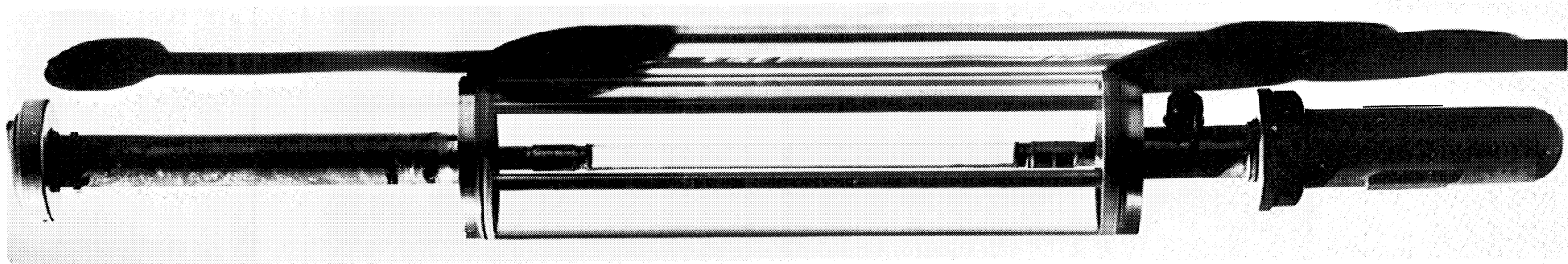


Figure 67. Glass Transfer Line

the top of the dewar. If a discharge line must be exposed to the pressurization gas, helium may be used to eliminate the condensation problem.

There was speculation about the solid flow pattern into and up the vertical pyrex tube. High speed motion pictures were taken of the solid entering the bottom of the 5/8-inch O.D. tube, the solid flow up the vertical tube, and the mixture in the dewar with and without stirring during transfer. The motion pictures showed no tendency for the solid to obstruct the entrance at the bottom of the tube with either slow or fast transfer. The entrance of the solid into the tube was uniform. Nitrogen and hydrogen liquid-solid mixtures flow very well up the vertical section of transfer line. Nitrogen and hydrogen mixtures also flowed out of the generating dewar with no apparent need for stirring.

High-speed motion pictures of liquid-solid nitrogen and hydrogen were taken at the glass section of transfer line. The camera was run at 1000 frames/second with an exposure time of 200 microseconds. A settling tendency and a moving solid bed were both observed when transferring nitrogen at low velocities. The motion pictures showed that hydrogen slurry transfers rapidly with very little pressure differential. The high velocity and turbulence present with hydrogen prevented settling or a moving bed. The viscosity of the liquid-solid hydrogen appeared to be nearly the same as that of the liquid. The motion picture film also showed intermittent, high frequency flow reversals when transferring hydrogen. These flow reversals did not occur with nitrogen mixtures and were probably inherent to the flow system and the transfer line. Two photographs, taken from the hydrogen transfer film, are shown in figures 68 and 69. These are pictures of fresh liquid-solid hydrogen made by the freeze-thaw method flowing through

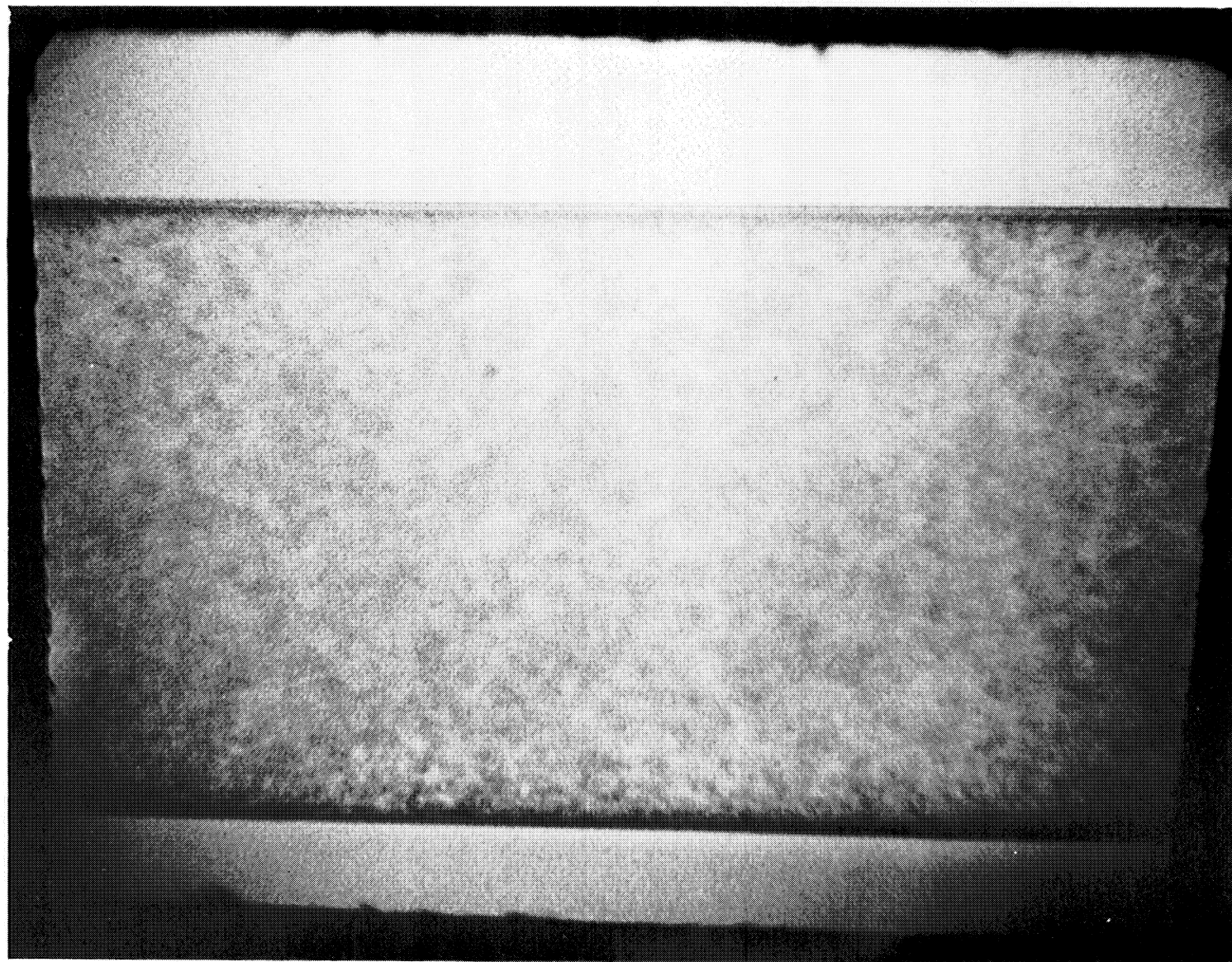


Figure 68. Thick Liquid-Solid Hydrogen In Transfer Line.



Figure 69. Thin Liquid-Solid Hydrogen In Transfer Line.

the glass section of transfer line. Figure 68 shows a thick mixture and the other is fairly thin.

No analytical data were taken during the initial transfer study, but useful information concerning some of the problems involved in cryogenic slurry transfer were revealed. The information will be useful in designing a large flow apparatus. No further work is planned with the small scale transfer system.

6. Line Pressure Drops From Classical Equations

A literature survey for information on pressure drop in circular pipes flowing a liquid-solid mixture has revealed several theoretical and empirical equations. The equations which were substantiated by the most experimental data were those of R. Durand [1952] and E. Condolios [1963]. The pressure drop predictions of these equations are based on particle size and particle terminal velocity instead of some measured pseudo viscosity as in most theoretical treatments. Because particle size and terminal velocity are more readily determined in liquid-solid mixtures of hydrogen, the methods of predicting pressure drop using these parameters were selected.

Durand and Condolios use two completely different equations to describe flow with homogeneous and heterogeneous mixtures. Since more than 90 percent of the particles observed are of the size that fall into the heterogeneous flow regime, flow in this regime is all that is being considered. The empirical equation for predicting line pressure losses in heterogeneous mixtures uses an apparent drag coefficient, which is determined from the terminal velocity and particle size. The drag coefficient for any particle can be determined from the following equations:

$$C_d = \frac{2F_d g_c}{AV^2 \rho_1} \quad , \quad \text{and} \quad (1)$$

$$F_d = \frac{v(\rho_s - \rho_1) g}{g_c} \quad , \quad (2)$$

where C_d is the drag coefficient, F_d is the force of drag, g_c is the gravitational constant, A is the particle cross sectional area normal to the velocity V , v is the volume of the particle, ρ_s and ρ_1 are the

densities of the solid particle and the liquid respectively, and g is the local acceleration of gravity. Equation (1) is the classical equation for drag of immersed bodies. In equation (2), the drag force is equated to the gravitational force less the buoyancy force, the condition for terminal velocity.

Durand and Condolios assume that the particles are spheres, and that the measured particle size is an approximation of a sphere diameter. From these assumptions, the equation for the drag coefficient of each size of particle reduces to the following:

$$C_d = \frac{K_1 g d \frac{(\rho_s - \rho_l)}{\rho_l}}{V^2}, \quad (3)$$

where d is the nominal diameter of the particle and K_1 is a constant. The apparent drag coefficient used in the line loss equation must include drag coefficients for the range of particle sizes involved. Durand and Condolios found that the apparent drag coefficient used for mixtures of particles of different sizes was dependent upon the drag coefficient for each size and the percent by weight of the size of particles. The actual relationship of drag coefficients and percent by weight of particles is given in equation (4). The square root of the apparent drag coefficient is given because it is required in the line loss equation,

$$\sqrt{C_d} = P_1 \sqrt{C_{d1}} + P_2 \sqrt{C_{d2}} + P_3 \sqrt{C_{d3}} - - - P_n \sqrt{C_{dn}}. \quad (4)$$

Subscripted P 's are percents by weight of the particles with drag coefficients of like subscripts.

The empirical equation for line loss gives the loss in head of the liquid, as follows:

$$J_m = J \left[1 + CK_2 \left\{ \frac{gD \frac{(\rho_s - \rho_l)}{\rho_l}}{V^2} \sqrt{\frac{1}{C_d}} \right\}^{1.5} \right], \quad (5)$$

where C is the percent of solid by volume, K_2 is an experimentally determined constant, J is the head loss for liquid under the same flow conditions, and D is the pipe diameter.

The curve of terminal velocity versus particle size as shown in figure 62 will be used to determine the drag coefficient for each size increment. The particle size distribution will be used to determine the percent by weight of the particles in each size increment. Sufficient particle size increments will be chosen to maintain the calculated C_d within the experimental accuracy.

The two constants in the equations have been evaluated by Condolios and Durand from data on particles of a wide range of sizes, shapes, and densities. The constant K_1 is a geometric shape factor--for spheres it is $4/3$. The experimental constant K_2 was determined to be 81 from the many data points taken by Condolios and Durand. Estimates for the design of experimental instrumentation can be made from these values. When experimental data for line pressure drops become available, they will be compared to those from the equations; and an analytical model will be developed to predict pressure drops in transfer lines. A computer program is being written for the analytical model.

7. Aged Solid Hydrogen - Spraying

Liquid-solid mixtures of hydrogen made by the spraying method were investigated to determine significant differences between aged solid particles made by the spray and by the freeze-thaw method. Early observation showed that fresh liquid-solid mixtures made by the spray method contained very large agglomerates of solid.

The apparatus used for the experiment was the same used for the particle aging studies of freeze-thaw formed solid. In the spray production method, the liquid was brought into the pretreatment chamber where the pressure is maintained above the triple point. The liquid was then sprayed from an orifice in the bottom of the chamber into the dewar where the pressure was maintained below the triple point. After the dewar was filled with solid, formed by the spray technique, the pressure was allowed to increase to 60 torr where it was maintained for approximately 5.5 hours. Samples of the solid were then taken from the bottom of the dewar and photographed as they settled across the grid as described previously. No visible differences were noted between the aged solid particles produced by the spray method and the aged solid particles produced by the freeze-thaw method.

8. Aged Solid Hydrogen - Continuous Pumping

Since aging of the solid made by the spray method and the freeze-thaw method resulted in the same particle characteristics, investigation of aged solid made by another production method was undertaken. The third production method investigated involved continuous pumping on the liquid in the dewar. The pressure over the liquid in the dewar was reduced to 52 torr and maintained for one-half hour. The pressure was then further reduced to 51 torr and held for one hour, at which time all of the liquid solidified. The pressure was then increased to 60 torr and maintained for 5.5 hours. Some liquid formed from the melting solid and some was added to cover the solid. Attempts to take solid particle samples at 5.5 hours were not possible since the solid remained in one large chunk in the liquid. The solid could not be broken up by stirring. It was concluded that the method of production of the solid does affect the aged particle size.

The results of the continuous pumping experiment may have application to the generation of smaller particles. The process of aging seems to lead to a more stable, dense and hard solid. If the particles could be broken up while fresh and friable, and held in suspension, it may be possible to generate stable particles of much smaller dimensions than previously reported. This possibility will be investigated during the current phase of the program.

9. Freeze-Thaw Solid Formation

There has been speculation and differences of opinion on the events taking place at the liquid-vapor interface when the pressure is lowered below the triple point at the start of the freeze-thaw cycle. To gain a better understanding of the interface behavior, high speed motion pictures were taken of a normal freeze-thaw production cycle using liquid hydrogen. The frame rate of the camera was 1000 frames/second and the exposure time was 100 microseconds.

The solid formation was carefully observed in slow motion. It appears that a very thin film of solid initially forms on top of the liquid, momentarily sealing the liquid from the vapor phase. Then, because of constant heat leak into the liquid and continued pumping above the solid film, pressure builds up immediately beneath the solid film and gas bubbles begin to form. Figure 70 is a photograph from the film strip showing this initial bubble formation. Figure 71 is a photograph of the bubbles taken \approx seven milliseconds later and showing the elongated bubbles forcing the solid film upward. The liquid immediately below appears to erupt and throw small droplets of liquid upward into the vapor space where the pressure is below the triple point pressure. Here the many droplets are partially vaporized and transformed into the solid phase. The high-speed motion pictures were extremely helpful in analyzing the solid production phase of the freeze-thaw cycle.

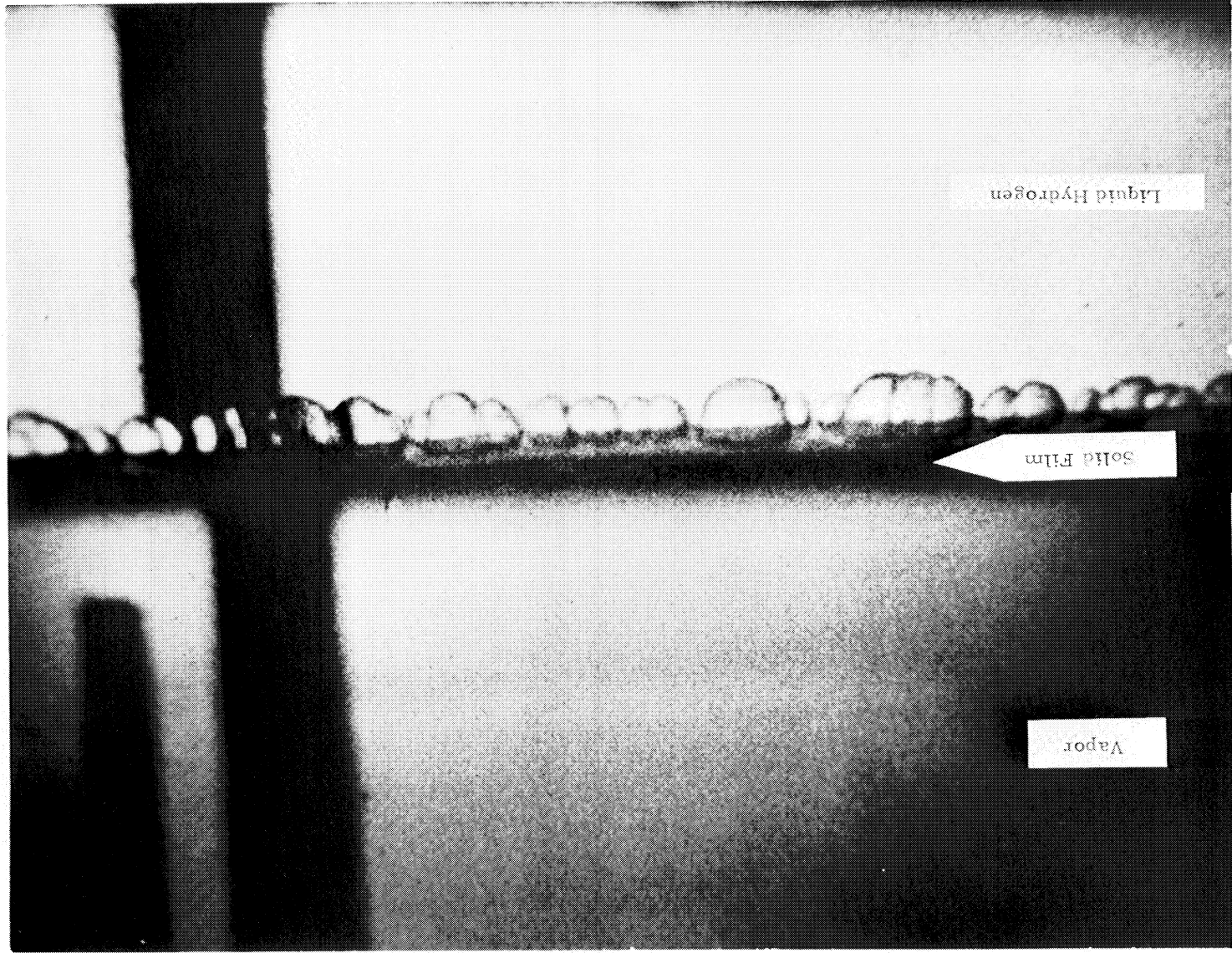


Figure 70. Freeze-Thaw Solid Formation, Time = 0



Figure 71. Freeze-Thaw Solid Formation, Time = 7 Milliseconds

10. Quality Determinations

In the freeze-thaw method of forming a triple-point mixture of hydrogen, a quantity of liquid hydrogen is partially evaporated under the reduced pressure maintained by a vacuum pump. A refrigeration effect, which is approximately equal to the latent heat of vaporization, is experienced by the remaining liquid or liquid-solid mixture. By specifying the initial state and the process or path followed, it is possible to predict the end state, i. e., the liquid-solid quality as a function of the mass of the vapor removed.

Figure 72 shows the path of the processes, on a temperature-entropy diagram, when the material in a constant volume container is considered. Saturated liquid at 1 atmosphere is cooled to the triple point, process 1 - 2, and then solid is formed, process 2 - 3".

10.1 Expansion to the Triple Point

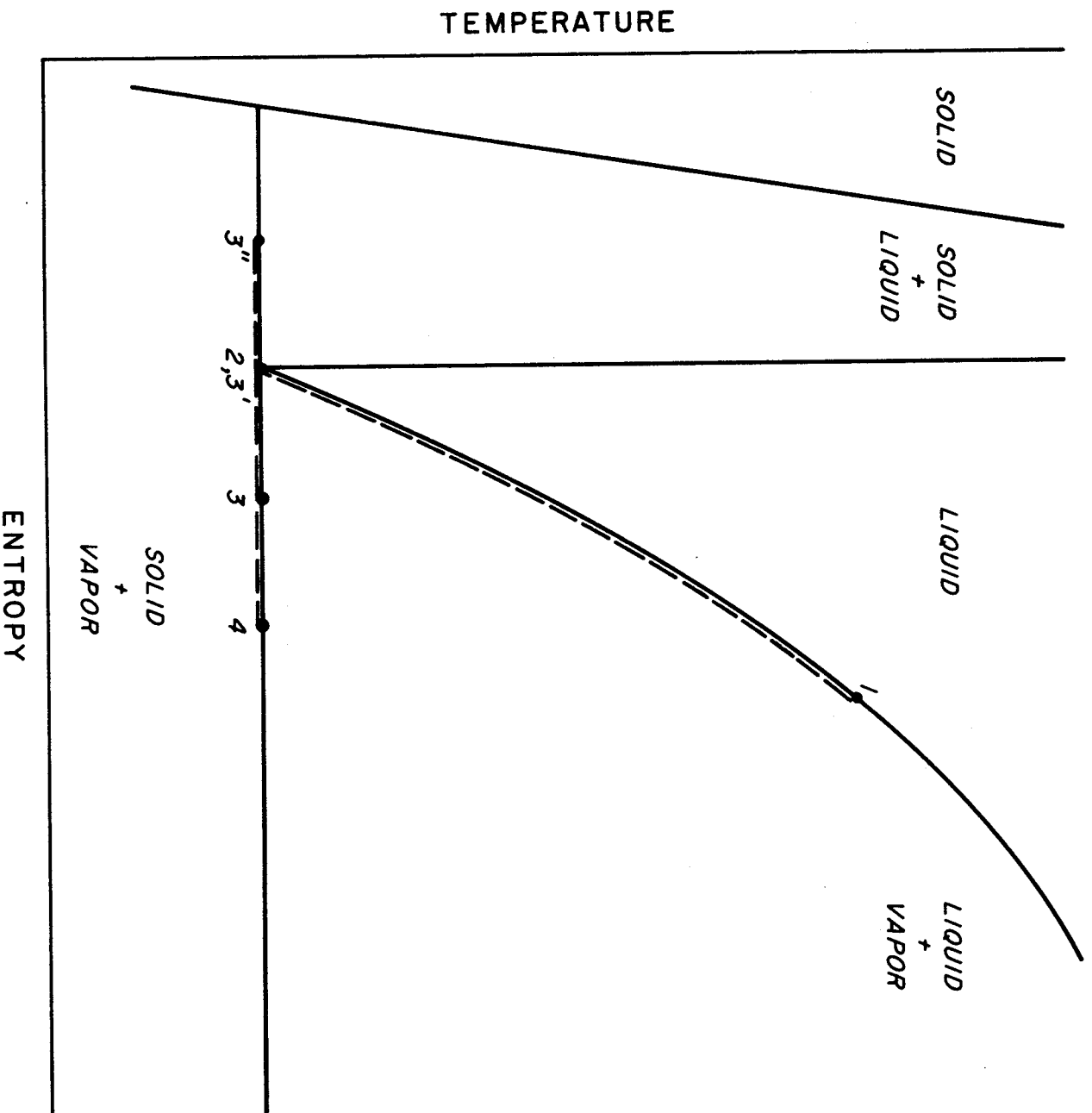
Process 1 - 2 may be analyzed by considering a control volume around a container initially filled with liquid hydrogen at one atmosphere. For a reversible process with heat transfer dq and mass leaving dm_i , the expression for the entropy in the control volume is:

$$S_1 + \int_1^2 \frac{dq}{T} = S_2 + \int_1^2 s_{vi} dm_i. \quad (1)$$

Since the evaluation of

$$\int_1^2 s_{vi} dm_i$$

requires solution of the problem at hand, it is necessary to consider a series of incremental expansions and replace the mass average entropy of the gas leaving by the arithmetic mean entropy. For such an incremental step, equation (1) may be rewritten as:



PROCESSES IN HYDROGEN SLUSH PRODUCTION AND QUALITY MEASUREMENT

Figure 72. T-S Diagram for Solid Production

$$\frac{dq}{T} + m_{l1} s_{l1} + m_{v1} s_{v1} = m_{l2} s_{l2} + m_{v2} s_{v2} + \Delta m_{1-2} s_{avg}, \quad (2)$$

where

$$s_{avg} = \frac{s_{v1} + s_{v2}}{2}.$$

With the specification of the conservation of mass,

$$m_{l1} + m_{v1} = m_{l2} + m_{v2} + \Delta m_{1-2}, \quad (3)$$

and the requirement of constant volume

$$v_{l1} m_{l1} + v_{v1} m_{v1} = m_o v_o, \text{ and} \quad (4)$$

$$m_{l2} v_{l2} + m_{v2} v_{v2} = m_o v_o, \quad (5)$$

the expansion process is defined and equations (2) through (5) may be

solved for $\frac{m_{l2}}{m_{l1}}$ and $\frac{\Delta m_{1-2}}{m_{l1}}$. The subscripts 1 and 2 refer to the

initial and final states for any incremental step, not the initial and final steps of the complete expansion. The subscript 0 refers to the initial conditions at 1 atm., state 1 on figure 72. The resulting expressions are

$$\frac{m_{l2}}{m_{l1}} = \frac{\left(s_{v1} + s_{v2} - 2s_{l1} - 2 \frac{dq}{m_{l1} T} \right) + R_1}{\left(s_{v1} + s_{v2} - 2s_{l2} \right) + \frac{v_{l2}}{v_{v2}} \left(s_{v2} - s_{v1} \right)}, \quad (6)$$

where

$$R_1 = (s_{v2} - s_{v1}) \left[\frac{m_o}{m_{l1}} - \frac{v_o}{v_{v2}} \left(1 + \frac{v_{v2}}{v_{v1}} \right) - \frac{v_{l1}}{v_{v1}} \right], \quad (7)$$

and

$$\frac{\Delta m_{1-2}}{m_{l1}} = 2 \frac{(s_{l1} - s_{l2}) + \left(1 - \frac{v_{l2}}{v_{v2}} \right) dq/m_{l1} T + R_2}{(s_{v1} + s_{v2} - 2s_{l2}) + \frac{v_{l2}}{v_{v2}} (s_{v2} - s_{v1})}, \quad (8)$$

where

$$\begin{aligned} R_2 = & \frac{m_o v_o}{m_{l1} v_{v2}} \left[\left(1 - \frac{v_{v2}}{v_{v1}} \right) s_{l2} - \left(1 - \frac{v_{l2}}{v_{v1}} \right) s_{v2} + \left(\frac{v_{v2}}{v_{v1}} - \frac{v_{l2}}{v_{v1}} \right) s_{v1} \right] \\ & + \frac{v_{l2}}{v_{v2}} \left[\left(1 - \frac{v_{l1}}{v_{v1}} \right) s_{v2} - s_{l1} \right] \\ & + \frac{v_{l1}}{v_{v2}} \left[\frac{v_{v2}}{v_{v1}} s_{l2} - s_{v1} \left(\frac{v_{v2}}{v_{v1}} - \frac{v_{l2}}{v_{v1}} \right) \right]. \end{aligned} \quad (9)$$

If only an approximate solution is desired, equations (6) through (9) may be simplified to:

$$\frac{m_{l2}}{m_{l1}} = \frac{(s_{v1} + s_{v2} - 2s_{l1} - 2 dq/m_{l1} T)}{(s_{v1} + s_{v2} - 2s_{l2})} \quad (10)$$

and

$$R_2 = 2 \frac{v_{l0}}{v_{v2}} (s_{l2} - s_{l1}). \quad (11)$$

Equations (8), (10), and (11) give a value of 0.106 for $\frac{\Delta m_{0-1}}{m_0}$,

the fraction of the initial mass vaporized in going from 1 atm. to the triple-point, for the case of zero heat leak. The error resulting from the simplification of the expressions is estimated at less than one percent. The parahydrogen properties used are those reported by Roder, Weber, and Goodwin [1963] and Roder [1964].

The specification of the heat leak dq could pose a problem if dq were sufficiently large. For the low rates of heat leak that are expected to be encountered, however, the assumption that Q is distributed evenly over the temperature range, i. e.

$$dq_{i \rightarrow (i+1)} = Q \frac{T_i - T_{i+1}}{T_0 - T_1} \quad (12)$$

will give sufficiently accurate results. The minimum change in entropy would occur if all the heat were added at temperature T_1 and the maximum entropy change would occur if it were added at temperature T_2 . If process 1 - 2 were to require one hour in a vessel having a heat leak equivalent to a loss of one percent of the liquid per day, Q would be 0.38 joules/gram mole and the maximum possible error introduced in the determination of m_v by using equation (12) would be 0.05 percent for hydrogen. The actual error would be considerably smaller. Larger rates of heat leak or larger times for the process would result in proportionately larger errors.

10.2 Formation of Solid at the Triple Point

Since the formation of solid at the triple-point, process 2 - 3", takes place at constant temperature and pressure, the process may be analyzed by considering a system contained by a piston and cylinder. If no heat is transferred to the system and the process takes place

reversibly, then as the piston is drawn out, the hydrogen expands with no change in entropy. For this closed system, the end of the expansion with some quality F is denoted by state 3' at the same entropy as state 2. If there is heat added to the system, the expansion takes place with an increase in entropy to state 3. The change in the specific entropy of the system, due to the addition of heat, is

$$\Delta s = \frac{Q}{mT} .$$

At state 3, the entropy of the individual phases is equal to the total entropy of the system and the total mass equal to the sum of the masses of the individual phases, so that

$$s_{\ell t} m_{\ell 3} + s_{vt} m_{v3} + s_{st} m_{s3} = ms_2 + \frac{Q}{T} , \quad (13)$$

$$m_{\ell 3} + m_{v3} + m_{s3} = m , \quad (14)$$

and the quality F is defined as

$$\frac{m_s}{m_s + m_{\ell}} = F . \quad (15)$$

In order to separate the calculations for process 2 - 3, from those for process 1 - 2, assume state 2 is pure liquid at the triple point. Then s_2 becomes $s_{\ell t}$ and

$$\frac{m_{v3}}{m} = \frac{F(s_{\ell t} - s_{st}) + \frac{Q}{mT}}{(1 - F)(s_{vt} - s_{\ell t}) + F(s_{vt} - s_{st})} . \quad (16)$$

Figure 73 gives the mass of vapor m_v/m vs. the quality F .

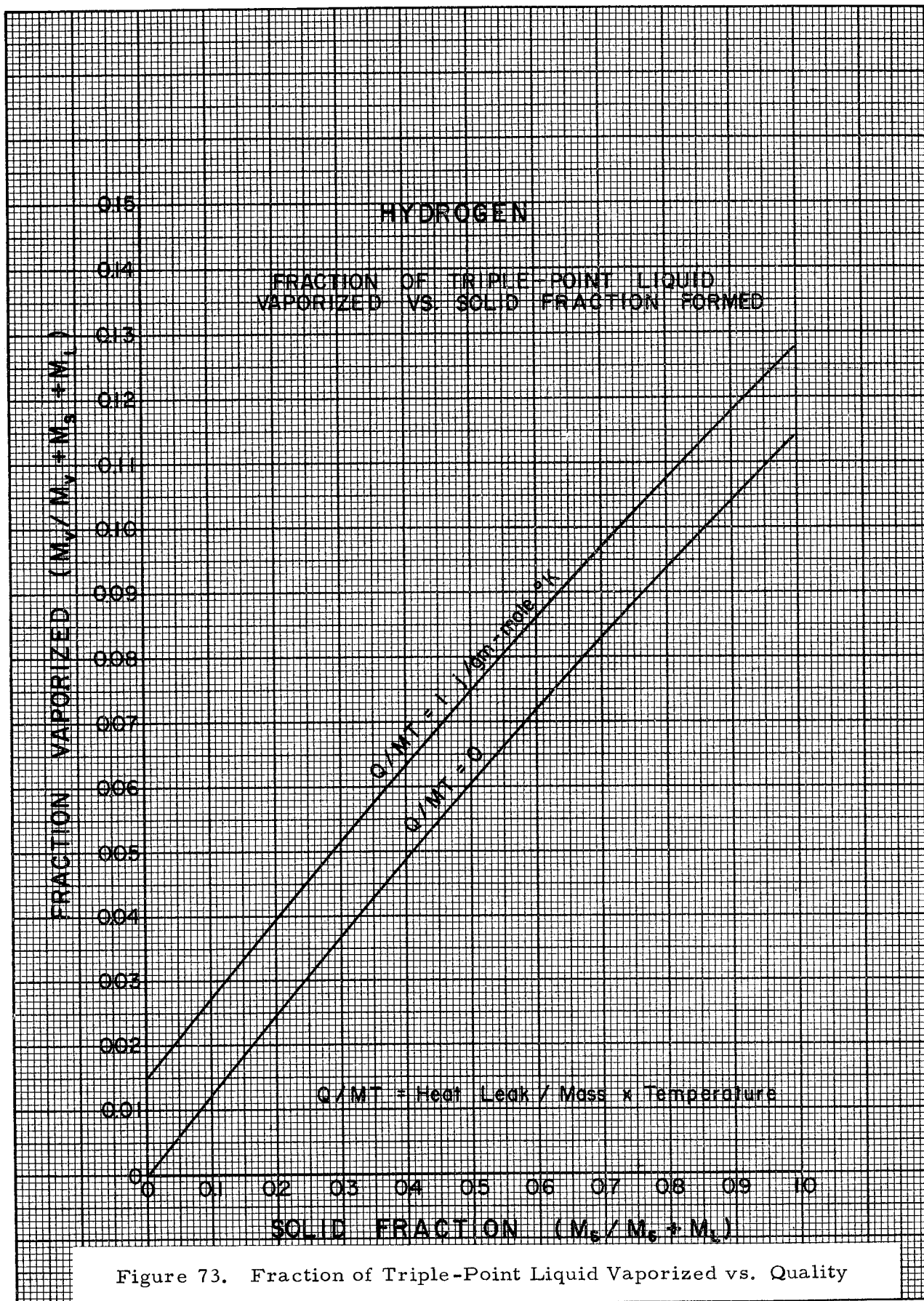


Figure 73. Fraction of Triple-Point Liquid Vaporized vs. Quality

The quantity of vapor calculated by equation (16) is the total amount of vapor formed, not the amount that would be removed from a container such as a dewar. A volume of vapor equal to the decrease in the volume of the liquid and solid phases remains in the container. The error resulting from the use of equation (16) is approximately equal to ratio of the specific volumes of the liquid to vapor phase

$\frac{v_{lt}}{v_{vt}}$. For hydrogen, $\frac{v_{lt}}{v_{vt}}$ is 1/608. Unless accuracies better than 1/2 percent are desired, equation (16) may be used without correction.

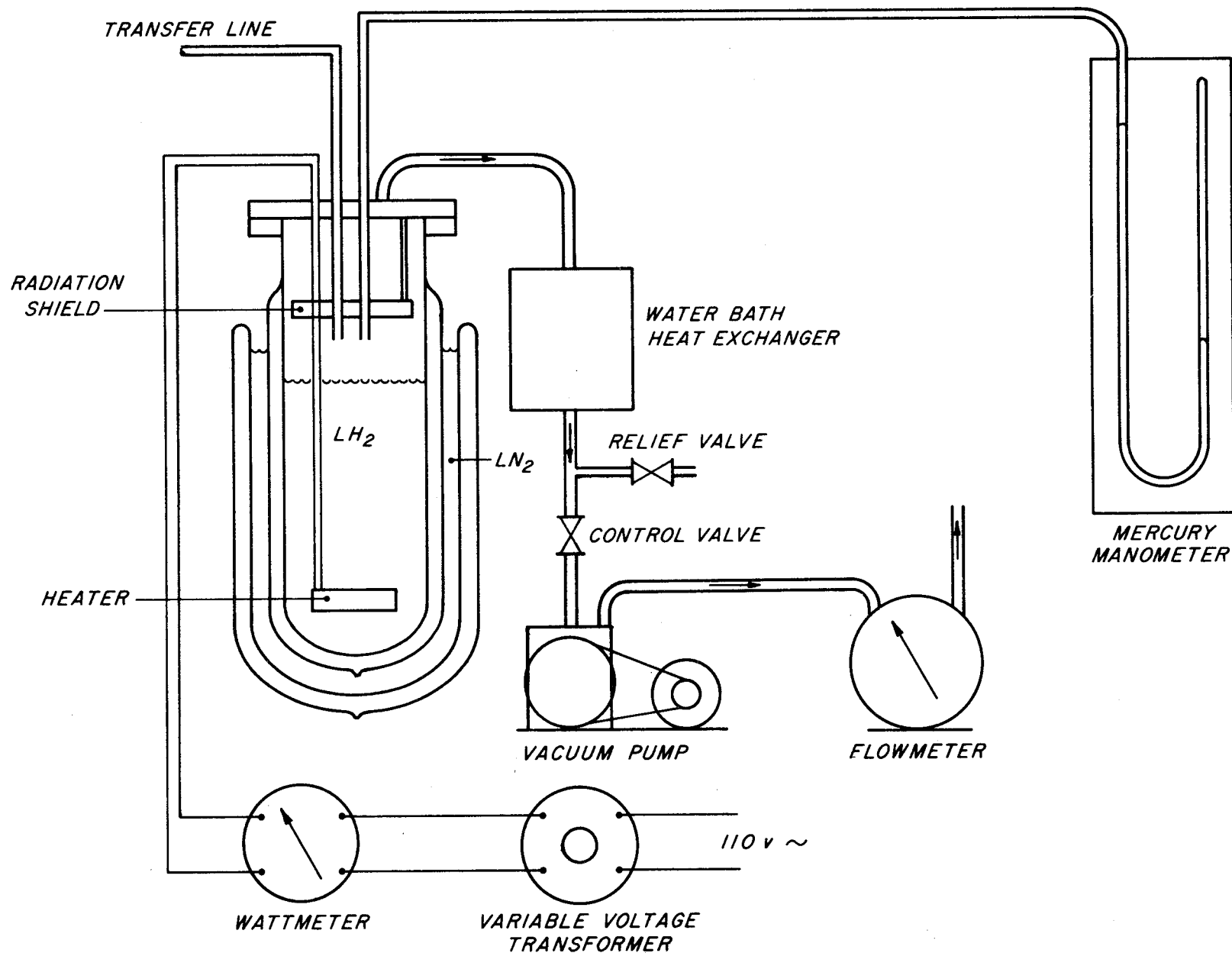
10.3 Experimental Determination of the Liquid-Solid Quality

Two methods will be used to experimentally determine the quality of a mixture of liquid and solid hydrogen. Both methods can be carried out as successive operations in the same apparatus. Figure 74 is a schematic diagram of the experimental arrangement.

10.3.1 Volumetric Method

When only the liquid and solid phases of a triple-point mixture are considered, the density of the two phases depends only on the quality. This provides a means for determining the quality which depends only on mass and volume measurements. The measurements required are as follows:

1. The mass of the liquid hydrogen at zero quality is determined by measuring the level of the liquid with a cathetometer after the dewar has been volume calibrated.
2. The decrease in the mass of the liquid-solid mixture is determined by measuring the volume of gas leaving the dewar with a flowmeter.



EXPERIMENTAL ARRANGEMENT

Figure 74. Quality Determination Apparatus

3. The change in volume of the mixture in going from zero quality to the quality F is determined by measuring the change in the level in the dewar with a cathetometer.

The quality F is then determined from the expression

$$F = \frac{\Delta V + v_l m_v}{(v_s - v_l)(m - m_v)} , \quad (17)$$

where m is the initial mass, m_v the mass of vapor removed, and ΔV the change in volume of the mixture.

10.3.2 Calorimetric Method

After the measurement of the quality by the volumetric method, the heater will be turned on until the solid just disappears, the heat being measured by a wattmeter. The process follows the path 3 - 4 on figure 72. The quality of the liquid-solid mixture at the state 3 can then be determined from the expression

$$F = \frac{\frac{Q}{mT} - \frac{m_{v4}}{m} (s_{vt} - s_{lt})}{s_{lt} - s_{st}} , \quad (18)$$

where m_{v4} is the mass of the vapor pumped off during the heating, m is the mass at state 3 and Q is the heat introduced by the heater plus the heat leak. It should not be necessary to pump on the dewar during the process, so m_{v4} would be zero and m would remain constant from 3 to 4.

Equation (16) evaluated for $F = 0$ gives

$$\frac{Q}{m_{v3} T} = s_{vt} - s_{lt} . \quad (19)$$

If Q is taken as the total heat introduced since the beginning of the solid formation, and m_{v3} is the total amount of vapor given off, then the equation (19) should hold. If values of $s_{vt} - s_{\ell t}$ obtained from equation (19) differ consistently from the accepted values, then the values obtained from equation (19) will probably give the best estimates of F when used in equation (16).

It is possible to estimate the liquid-solid quality by measuring the total mass of vapor removed from the system in going from state 1 to state 3 through the use of equations (8), (11), and (16). However, if the arrival at state 2, the edge of the triple-point region, is established by measuring the temperature of the liquid, and/or visual observation for the presence of solid, then the uncertainties in the estimation of the quality F should result. By measuring the vapor pressure in the dewar with a mercury manometer, the temperature may be determined from established values of vapor pressure vs. temperature at saturation.

10.4 Sources of Error

There are a number of possible sources of error in the determination of the liquid-solid quality by the methods discussed. Some of these are the listed below.

1. Errors may be made in determining the mass of vapor given off and the mass of liquid in the dewar at the beginning of process 2 - 3.
2. Errors may be made in the determination of the heat leak into the dewar. The heat leak will be experimentally determined by measuring the boil-off rate with liquid just above the triple-point.

3. There may be error in estimating the heat required to cool the dewar. This applies only for process 1 - 2 since 2 - 3 is at constant temperature.
4. Unless the surface of the liquid-solid mixture is completely quiescent during the formation of solid, minute particles of liquid and solid will be carried away and the entropy of the material leaving the surface will not be that of the pure vapor as assumed in the development of equation (16). Because of the large density difference between the liquid and vapor phases, only a small volume fraction of liquid or solid particles in the vapor could have a significant effect on the estimation of the quality. The use of values for $s_{vt} - s_{lt}$ obtained from equation (19) should at least partially compensate for this effect if it occurs. The volumetric method of determining the quality of the liquid-solid mixture makes no assumptions regarding the composition of the vapor being drawn off in process 2 - 3, so it should be possible to determine the magnitude of this effect.
5. The error equation (16) introduces, by giving the total amount of vapor formed rather than that removed from a constant volume container, has already been discussed and should be negligible compared to the other sources of error.

10.5 Summary

An expression for the fraction of vapor removed from a triple-point mixture to produce a given liquid-solid quality F has been

developed. Two independent experimental methods which can be successively carried out in the same apparatus are proposed for the purpose of checking the theoretically predicted values of F .

11. Cryogenic Colloids

The ideal mixture of liquid and solid hydrogen is a colloidal suspension of solid particles in the liquid. A colloid provides a homogeneous heat sink and a homogeneous fluid for transfer. If such a suspension could be prepared, studies of its properties could be investigated by techniques described in the abundant literature on colloids [Krulyt, 1952]. The fraction of the mixture which is solid could be determined by light absorption experiments, the size of the colloidal particles could be determined by light scattering experiments and the morphology of the solid could be studied with ultramicroscopy.

The following is a preliminary discussion of some aspects of the feasibility of production and application of cryogenic colloids for the present purposes. Unfortunately, very little attention has been given to these substances until now, and therefore very little is known about their properties. In our judgment, support of basic research into the properties of cryogenic colloids would yield increased understanding which would have wide application.

Colloidal solid particles are usually defined as particles between one millimicron and one micron in diameter or, alternatively, as particles containing between 10^3 and 10^9 molecules. A spherical solid hydrogen particle which contains 10^9 molecules has a diameter of about 0.5 microns. For use as a fuel, however, there is no need to keep the solid particles this small. Flow properties will probably remain largely indistinguishable from pure liquid flow properties even if the particles are 200 times larger than this, i. e., with diameters of 0.1 millimeters. The central problems are (a) Production: How may such suspensions be prepared? and (b) Stability: How can the solid particles sizes be maintained and particles kept in suspension?

In the most common case, the colloidal solid component is different from the liquid component and not soluble in the usual sense. The solid component is prepared separately and mixed into the liquid. In a one component system, such as solid hydrogen in liquid hydrogen, this technique can be modified. In the most practical method being considered, the solid formed in the freeze-thaw technique could be initially broken up into particles of colloidal size by an impeller.

Another means of producing a one component colloid of solid in liquid is to cool the liquid and concurrently control the nucleation probability of crystals so that crystallites result in a liquid bath which are of colloidal size. A similar technique is used in rubber manufacture where crystal growth processes are slow because of the complicated geometry of the macromolecules. In hydrogen crystallization, the molecules are small and condense onto a lattice almost independent of the relative geometry. In addition, the parameters which control crystal growth, i. e., thermal gradients, purity, cooling rates, and seeding, are much more difficult to control in cryogenic systems. The concept is potentially very useful although, for the present, only empirical experimentation can be projected.

The most serious problems are associated with stability. Unless some force acts to keep the colloidal particles suspended, they will gradually settle in their container. In biocolloids, the stability is usually supplied by hydration. Some other colloidal particles are charged and the mutual coulombic repulsion keeps them in suspension. Other more complicated mechanisms are probably not relevant. The most straightforward means of keeping cryogenic colloids stable is to continually stir the mixture; however, this is inconvenient for large volumes and also introduces extra energy.

It may be possible to adapt the charge stability conditions to

the hydrogen system. The solid hydrogen particles could be charged, i. e., by spraying with low-energy electrons in the spray technique or by overall energy irradiation of the liquid-solid mixture in the freeze-thaw technique. Because of their higher density, the solid particles will pick up greater charge density than the liquid. The charge will eventually leak off from the solid onto the walls and into the liquid. Until this happens, the colloid may be stable. Preliminary calculations are underway to determine the relaxation time of the system and the optimum radiation to use for producing the charged particles. Other feasibility problems are being studied. The technique seems to be good in principle, but may be difficult in practice.

12. Conclusions

The progress of the liquid-solid hydrogen investigation over the past seventeen months can be divided into two general categories: (1) characteristics that bear directly on production and transport and (2) associated properties and handling techniques necessary for a more basic understanding of the fluidized mixture. Both categories are essential to the development of the liquid-solid mixture as a possible upgraded fuel.

Generation, storage, and transport characteristics of a particular type of mixture have been established and will be tested on a larger scale in future reporting periods. The continuing study of the basic properties of the solid particle in the liquid should lead to changes in production techniques, which may result in a mixture of more homogeneous nature; one that may be more easily adapted to existing transport and instrumentation techniques.

13. Future Work

During the next reporting period, emphasis will be placed in two major areas.

13.1 Liquid-Solid Flow

Experimental parameters necessary for the development of the slurry flow model are based on relationships derived during phase 1 of the program. The experimental verification of the mathematical model for slurry flow will be performed. In particular, pressure drop will be determined as a function of pertinent, predictable flow parameters and of mixture quality. These studies will primarily be conducted in a straight tube, but will include a determination of behavior at the pipe entrance and exit and at other flow restrictions. Line sizes will be varied as much as possible, consistent with the apparatus, but will be in the range of 0.50 to 1.25 inches. If smaller particles can be produced, the lower limit of the line size will be decreased. Critical flow velocities will be determined. The flow apparatus will be designed to allow both visual and photographic observation of the above characteristics. The quantities of hydrogen handled will be of the order of 100-200 liters. It is important to keep in mind that it must be possible to extrapolate the results to the anticipated size of vehicle systems and launch facilities.

13.2 Homogeneous Mixtures

Future applications of liquid-solid mixtures of hydrogen to space vehicles will, in most instances, be enhanced if the mixture is of a homogeneous nature. This specific property is important because density (quality) measurement will be more simple and accurate, flow rates more predictable, and the increased heat sink potential can be more efficiently utilized. Therefore, a continuing study of the crystallography of hydrogen will be performed. This phase of the study will

include, but not be limited to, the following areas.

- (A) Production - Attention will be given to the formation of smaller particles using additional production controls and seeding (addition of foreign particles to form a greater number of nucleation centers). Pumping pressures may be varied in time, absolute value, and frequency in order to inhibit particle agglomeration.
- (B) Mechanical - Attention will be given to reducing the size of the particles after their formation by mechanical means. These methods would include vigorous stirring of the solid in the area of crust formation and actual physical crushing of the fresh and aged solid.
- (C) Gel - Attention will be given to combining techniques of gel formation, recently investigated by others, [Kartluke, 1964] with the present program. Experiments will be performed to determine any advantage to the gelling of a mixture of liquid-solid hydrogen over that of liquid hydrogen at one atmosphere vapor pressure.

REFERENCES

- Condolios, E. and E. Chapus (June 1963), Solids Pipelines, Chemical Engineering, No. 13, 93-98, No. 14, 131-138, No. 15, 145-150.
- Cook, G. A. and R. F. Dwyer (Dec. - March, 1964), Research on Rheologic and Thermodynamic Properties of Solid and Slush Hydrogen, Quarterly Report No. 3, Project No. 3048, Task No. 304802, Contract No. AF 33(657)-11098.
- Durand, R. and E. Condolios (Nov. 1952), The Hydraulic Transport of Coal and Solid Material in Pipes, Proc. Colloq. on Hydraulic Transportation, London.
- Dwyer, R. F. (June - Sept., 1964), Research on Rheologic and Thermodynamic Properties of Solid and Slush Hydrogen, Quarterly Report No. 5, Project No. 3048, Task No. 304802, Control No. AF 33(657)-11098.
- Irani, R. R. (1959), The Interpretation of Abnormalities in the Log-Normal Distribution of Particle Size, J. Phys. Chem. 63, 1903-1907.
- Kartluke, H., C. D. McKinney, R. Pheasant and W. B. Tarpley (July 1964), Gelling of Liquid Hydrogen, Final Report, NASA Contract No. 3-2568, NASA CR-54055.
- Kruyt, H. R. (1952), Colloid Science, Vol's. I and II, (Elsevier Publishing Co., Amsterdam).
- Mullins, J. C., W. T. Ziegler and B. S. Kirk (Nov. 1961), Technical Report No. 1, Project No. A-593, Engineering Experiment Station, Georgia Institute of Technology, NBS Contract CST-7339.
- Orr, Clyde Jr. and J. M. Dallavalle (1959), Fine Particle Measurement (Macmillan Book Co., New York, N. Y.).
- Roder, H. M., L. A. Weber and R. D. Goodwin (Nov. 1963), Thermodynamic and Related Properties of Parahydrogen From the Triple Point to 100° K at Pressures to 340 Atmospheres, NBS Report No. 7987 (unpublished).

REFERENCES (Continued)

Roder, H. M. (1964), Parahydrogen . . . Supplemental Tables, NBS Report 7987, Lab Note, File No. 64-22 (unpublished).

Woolley, H. W., R. B. Scott and F. G. Brickwedde (1932), Compilation of Thermal Properties of Hydrogen in its Various Isotopic and Ortho-Para Modifications, NBS J. Research RP.